Open Research Online

The Open University's repository of research publications
and other research outputs

A Role of Unfolded Protein Response in the Cellular Response to Flavivirus Infection

Thesis

How to cite:

Kazungu, Yvette (2020). A Role of Unfolded Protein Response in the Cellular Response to Flavivirus Infection. PhD thesis The Open University.

For guidance on citations see FAQs.

© 2019 The Author

https://creativecommons.org/licenses/by-nc-nd/4.0/

Version: Version of Record

Link(s) to article on publisher's website:
http://dx.doi.org/doi:10.21954/ou.ro.00010f93

Copyright and Moral Rights for the articles on this site are retained by the individual authors and/or other copyright owners. For more information on Open Research Online's data policy on reuse of materials please consult the policies page.

oro.open.ac.uk

A role of Unfolded Protein Response in the cellular response to Flavivirus infection

PhD candidate: Yvette Kazungu

A thesis submitted in fulfillment of the requirements of the Faculty of Life Sciences of the Open University for the degree of Doctor of Philosophy

International Centre for Genetic Engineering and Biotechnology (ICGEB)

Trieste, Italy

Director of Studies: Alessandro Marcello (Ph.D)

External Supervisor: Licio Collavin (Ph.D)

September, 2019

ABSTRACT

Flaviviruses are responsible for a myriad of epidemics globally. Factors like movement and climate change perpetuate their spread making control rather challenging. The understanding of host-virus interactions is therefore cornerstone in attempts to produce efficient vaccines and/or therapies.

The host immune system is indispensable in fighting infections but viruses have developed evasion strategies which abrogate the response that would otherwise function in virus clearance.

The unfolded protein response (UPR), an intrinsic cellular proteostasis pathway is increasingly associated with innate immunity in response to cellular insults including viral infection. UPR activation by external stimuli elicits an earlier induction of IFNβ and antiviral ISGs suggesting UPR as a priming event that potentiates a more robust response against flaviviruses.

Prerequisite to the core of this study, an analysis of the effects of TM and TG (UPR chemical inducers) as used in our current experimental settings show that they are only cytostatic but not cytotoxic.

Afterwards, I delve into the search for alternative UPR inducers as potential alternatives for the ones currently in use. I show that E, NS1 and NS2B proteins of TBEV can induce UPR and several antiviral ISGs when ectopically expressed, an effect that inhibits TBEV in infection.

Of the three proteins studied, NS2B seems to be the most potent inducer of UPR and antiviral ISGs. Furthermore, expression of NS2B together with RIG-I augments the IFNβ promoter activity suggesting a possible role in innate signaling independent of infection.

The findings of this work open up possible avenues that require further investigation particularly in the case of NS2B, which is not a well-documented flavivirus protein apart from the context of its function as a protease cofactor. The mechanism by which it induces ER stress is especially intriguing because unlike E and NS1 proteins, it is not a glycoprotein.

-

DEDICATION

In loving memory of the late Mrs. Musanna. Thank you for shining a light and planting a seed of belief in my academic path. May your soul find eternal peace.

ACKNOWLEDGEMENTS

My three-year journey would not have been possible without many people I've met along the way. Firstly, I thank God for the strength and courage when I needed it the most especially in the few months just before my PhD defense when both my parents fought serious medical battles so far away from me.

I am deeply indebted to my supervisor, Dr. Alessandro Marcello for taking a chance on me and accepting me in the laboratory. Having come from a completely different scientific background and environment, his mentorship, patience and encouragement as I got to know the field and find my bearings in this journey have been incredibly appreciated. Many thanks to Dr. Licio Collavin, my external supervisor for the regular discussions and supervision. Prof. Ariberto Fassati and Dr. Emmanuele Buratti for my PhD viva discussion and inputs to make my write-up and future work better.

My utmost gratitude goes to my past and present colleagues and friends in the Molecular Virology laboratory, it has been an incredible journey with all of you, thank you for helping me grow as a person and as a scientist. Special thanks to Tea and Khalid who assisted me as I got acquainted to the project and learned various techniques during my first year and continuous support and discussions throughout my time in the laboratory. Erick, it was an honor and my pleasure to do this journey beside you. Ambra and Sree, you became my family, my home away from home, I cannot thank you enough.

I'm grateful to my parents, my brother Prince and sister Yvonne for their prayers, encouragement, moral and material support especially at times when I felt like I was falling apart, I am lucky and grateful to have you in my life. Prince, thank you for always cheering me on, you are more than just my brother, you are my confidante and a trusted ally.

Prof. Paul Gwakisa, thank you for being my mentor both in academics and in life.

Emmanuel, thank you for being the very best friend a girl could ever ask for, thank you for always being one of my biggest fans and for seeing me through some of the lowest moments during this journey even from thousands of miles away. Your words of courage always give me a boost...you are the best.

And last but not least, Krisztián, thank you for holding my hand, for encouraging me especially during the writing and defense of my thesis, I've never felt alone ever since you came into my life. I am grateful to have met you when I did.

TABLE OF CONTENTS

LIST OF FIGURES

LIST OF TABLES

LIST OF APPENDICES

LIST OF ABBREVIATIONS & ACRONYMS

AAT/α1AT: Alpha-1-antitrypsin

AMP: Ampicillin

ANOVA: Analysis of Variance

AP-1: Activator protein 1

ATF4: Activating transcription factor 4

ATF6: Activating transcription factor 6

ATP: Adenosine triphosphate

BiP: Binding Immunoglobulin protein

bZIP: Basic Leucine Zipper Domain

CARD: Caspase activation and recruitment domain

CD: Cluster of differentiation

cGAS: cyclic GMP-AMP Synthase

ChIP-Seq: Chromatin Immunoprecipitation DNA Sequencing

CHOP: C/EBP homologous protein

CMC: Carboxymethyl cellulose

CPE: Cytopathic effects

CRISPR-Cas9: clustered regularly interspaced short palindromic repeats-CRISPR-associated protein 9

DDIT3: DNA damage inducible transcript 3

DENV: Dengue virus

DHX58: DExH-Box Helicase 58

DMEM: Dulbecco's Modified Eagle Medium

DMSO: Dimethylsulfoxide

DNA: Deoxyribonucleic acid

dsRNA: double-stranded RNA

DTT: Dithiothreitol

E (protein)/Env: Envelope protein

EDEM1: ER Degradation Enhancing Alpha-Mannosidase Like Protein 1

EDTA: Ethylenediaminetetraacetic acid

eIF2α: Eukaryotic translation initiation factor 2 alpha

ER: Endoplasmic Reticulum

ERAD: ER-associated degradation

ERK: Extracellular signal–regulated kinases

FACS: Fluorescence-activated cell sorting

FBS: Fetal bovine serum

FC: Flow cytometry

GADD34: Growth arrest and DNA damage-inducible protein

GAPDH: Glyceraldehyde 3-phosphate dehydrogenase

GRP78: Glucose-Regulated Protein, 78kDa

GRP94: Glucose-Regulated Protein, 94 KDa

h.p.i/t: hours post infection/transfection

HA: Hemagglutinin

HAV: Hepatitis A virus

HSPA5: Heat Shock Protein Family A (Hsp70) Member 5

HCMV: Human cytomegalovirus

HCV: Hepatitis C virus

HEK cells: Human embryonic kidney cells

HIV: Human Immunodeficiency virus

HRP: Horseradish peroxidase conjugate

HSV: Herpes simplex virus

IAV: Influenza A virus

ICAM3: Intercellular Adhesion Molecule 3

ICTV: The International Committee on Taxonomy of Viruses

IFI44: Interferon Induced Protein 44

IFI44L: Interferon Induced Protein 44 Like

IFI6: Interferon Alpha Inducible Protein 6

IFIH1: Interferon Induced with Helicase C Domain 1

IFIT1: Interferon Induced Protein with Tetratricopeptide Repeats 1

IFITM: Interferon-induced transmembrane protein

IFNα/β: Interferon alpha/beta

IFNAR: Interferon-α/β receptor

IFNLR: Interferon Lambda Receptor

IKKε: Inhibitor of nuclear factor kappa-B kinase subunit epsilon

IPS-1: IFNβ promoter stimulator

IRE1: Inositol-requiring enzyme 1

IRES: internal ribosome entry site

IRFs: Interferon regulatory factors

ISG: Interferon-stimulated gene

ISGF3: Interferon-stimulated gene factor 3

JAK: Janus Kinase

JEV: Japanese encephalitis virus

JNK: c-Jun N-terminal kinase

Kana: Kanamycin

kDa: kilo Dalton

KUNV: Kunjin virus (West-Nile subtype)

LB: Lysogeny broth/ Luria broth/ Lennox broth/ Luria-Bertani medium

LGP2: Laboratory of Genetics and Physiology 2

LPS: Lipopolysaccharides

LTR: Long terminal repeats

MAM: Mitochondria-associated membrane

MAPK: Mitogen-activated protein kinase

MAVS: Mitochondrial antiviral-signaling protein

MDA5: Melanoma Differentiation-Associated protein 5

mRNA: messenger RNA

MyD88: Myeloid differentiation primary response 88

NCR: Non-coding region

NF-κB: Nuclear factor kappa-light-chain-enhancer of activated B cells

NHK: Null Hong Kong

NLRs: Nod-like receptors

NS: Non-structural

NY99: New York 1999 (West-Nile virus subtype)

O/N: Overnight

OASL: 2'-5'-Oligoadenylate Synthetase Like

PAMPs: Pathogen-associated molecular patterns

PBS: Phosphate-Buffered Saline

PCR: Polymerase chain reaction

PDI: Protein disulfide isomerase

PERK: Protein kinase R (PKR)-like endoplasmic reticulum kinase

PFA: Paraformaldehyde

PI3K: Phosphoinositide 3-kinase

prM: premembrane

PMSF: Phenylmethylsulfonyl fluoride

PRRs: Pattern recognition receptors

qRT-PCR: Real-Time Quantitative Reverse Transcription PCR

RIG-I: Retinoic acid-inducible gene I

RIP1: Receptor interacting protein 1

RIPA: Radioimmunoprecipitation assay

RLRs: RIG-I like receptors

RNA: Ribonucleic acid

RT-PCR: Reverse Transcription PCR

SDS-PAGE: sodium dodecyl sulphate-polyacrylamide gel electrophoresis

siRNA: small interfering RNA

S1/2P: site 1/2 protease

ssRNA: single-stranded RNA

STAT1/2: Signal transducer and activator of transcription ½

STING: Stimulator of interferon genes

SV40: Simian VIRUS 40

TBEV: Tick-borne encephalitis virus

TBK1: TANK Binding Kinase 1

TG: Tharpsigargin

TGN: Trans-Golgi Network

TLRs: Toll-like receptors

TM: Tunicamycin

TRAF3: TNF receptor-associated factor

TRIF: TIR-domain-containing adapter-inducing interferon-β

TRIM56: Tripartite Motif Containing 56

TYK2: Tyrosine-protein kinase

U20S: Human Bone Osteosarcoma

UPR: Unfolded Protein Response

UTR: Untranslated region

VISA: Virus- induced signaling adapter

WB: Western blot

WNV: West-Nile virus

WT: Wild type

XBP1(s): X-Box Binding Protein 1 (spliced)

YFV: Yellow fever virus

ZIKV: Zika virus

1.INTRODUCTION

1.1 Family Flaviviridae

Flaviviridae is a large family of small (40 to 60 nm diameter), enveloped viruses with a linear, non-segmented, single-stranded RNA of positive polarity. The genome of members in this family ranges from 9 to 13kbp and their surface proteins are arranged in an icosahedral-like symmetry (Lindenbach and Rice, 2001; Wengler *et al*., 1978; Zhang *et al*., 2003). The word Flaviviridae is derived from "Flavus" which is Latin for "yellow", this came due to the importance of the Yellow Fever virus, the prototype virus in this family and the genus Flavivirus; that was the first proven human pathogen, isolated in 1927 in the Rhesus monkey (*Macaca mulatta*), through the inoculation of blood from an African patient (Stock *et al*., 2013, Strode G. 1951)

There currently exist four genera in this family (Fig. 1).

1.1.1 Flavivirus

This genus is largely made up of arboviruses, that is, their transmission to vertebrate hosts is through arthropod vectors mainly mosquitoes and ticks. However, there also exist viruses in this genus with no known vectors. The 5' end of the genome possesses a type I cap (m^7GpppAmp) not seen in the other genera and the 3' end lacks terminal polyadenylation (Simmonds *et al*., (ICTV), 2017). The genus Flavivirus will be discussed in more detail in the following paragraphs.

1.1.2 Hepacivirus

This genus contains both primate (Hepacivirus C) and non-primate viruses. Non-primate viruses have been described in horses, donkeys, colobus monkeys as well as in rodents and bats. Hepacivirus C has been widely characterized virologically and clinically more than all its counterparts in the genus. A general distinctive feature of members of this genus as compared to other members in the family is the limited propagative ability of Hepaciviruses in cell culture. The 5' UTR of Hepacivirus C contains a type IV IRES structural element that directs cap-independent translation. (Simmonds *et al*., (ICTV), 2017)

1.1.3 Pegivirus

This genus in contrast to the Hepaciviruses does not encode a core protein and instead of the type IV IRES structural element, it employs a type III IRES in the cap independent translation of the genomic RNA. Pegiviruses can be found in a wide variety of humans, non-human primates, pigs, horses as well as rodents and bats (Simmonds *et al*., (ICTV), 2017).

1.1.4 Pestivirus

Translation of the Pestivirus genomic RNA is cap-independent and initiated by a type IV internal ribosomal entry site of about 370-385 nucleotides within the 5'-non- coding region of the virus genomic RNA and the 3'-NCR, with about 185–273 nucleotides, is complex and contains a region with variable sequences and a highly conserved terminal region. The genome encodes for four structural and 8 non-structural proteins. Pestiviruses infect pigs and ruminants but have also been detected in wild ruminants and wild boar (Smith *et al*., 2017, Simmonds *et al*., (ICTV), 2017)

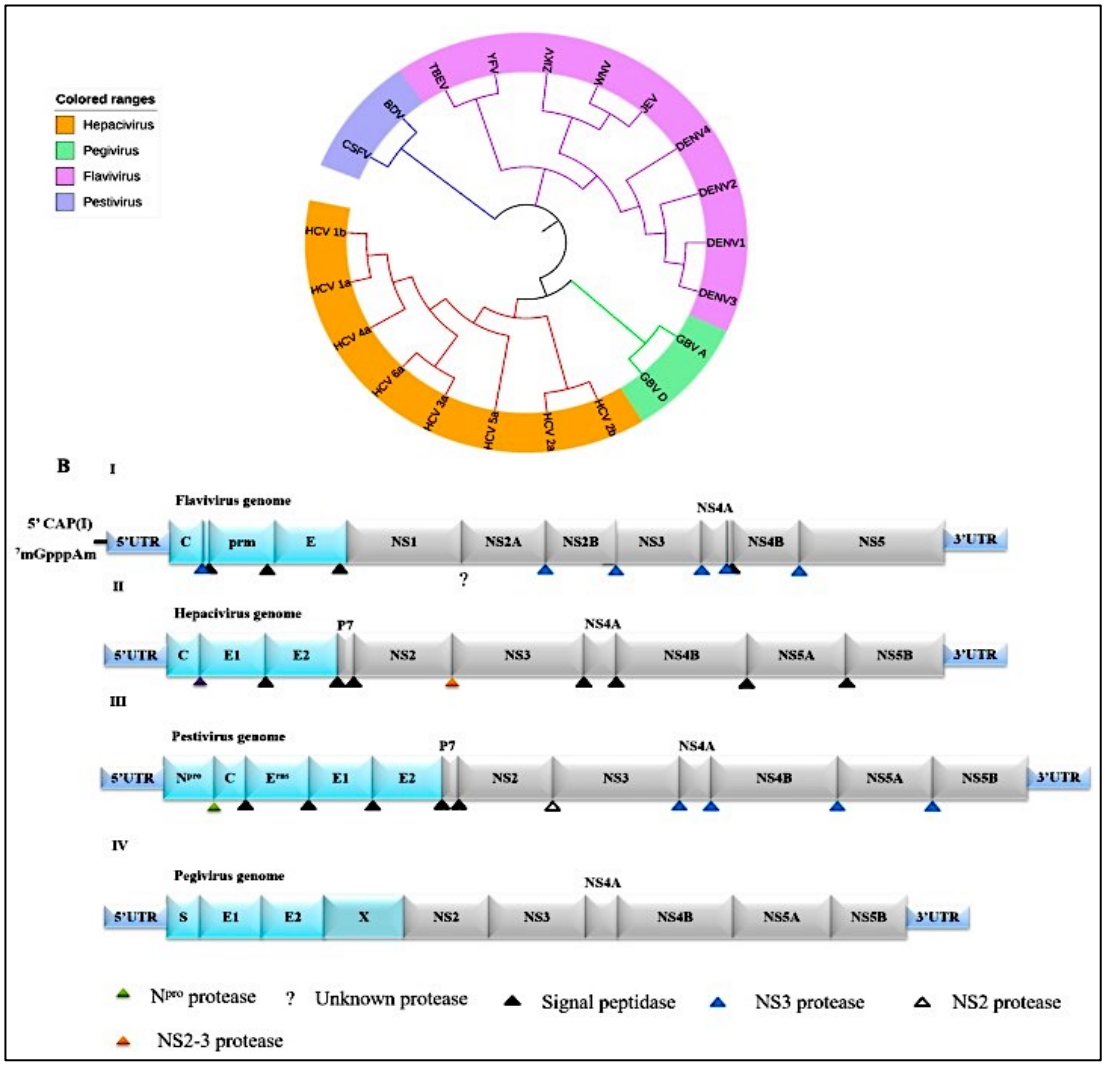

Figure 1: Flaviviridae phylogenetic characteristics and basic features of reference genomes (Chen S. *et al*., 2017)

1.2 Flaviviruses

Majority of viruses in the genus flavivirus are arthropod-borne pathogens that is, transmitted between arthropods (mainly ticks and mosquitoes) and vertebrates also referred to as dual-host viruses (Blitvich and Firth, 2015). With over 40 human-tropic viruses most of which are mosquito-borne, Flavivirus is an important genus in the family Flaviviridae because of its members' global distribution, most of them considered important human and veterinary pathogens responsible for a myriad of haemorrhagic fevers and encephalitides that have been considered global public health threats. One example is the dengue virus (DENV), reported to cause approximately 390 million cases globally

per year (Bhatt *et al*., 2013). In addition to ticks and mosquito-borne viruses, there exists viruses with no-known vectors also termed vertebrate-specific viruses, these are isolated from rodents and bats, as well as insect-specific flaviviruses which have only been known to infect insect cells but not mammalian cells (Kenney *et al*., 2014; Blitvich and Firth, 2015; Bolling *et al*., 2015). Some of the most important flaviviruses include Yellow fever virus (YFV), dengue virus (DENV 1-4), Japanese encephalitis virus (JEV), West Nile virus (WNV), Zika virus (ZIKV) and Tick-borne encephalitis virus (TBEV), which is endemic in Europe and parts of Asia.

There is a constant spread of flaviviruses to new geographical areas where they never existed before such as the recent re-emergence of WNV and Zika virus in the Americas in 1999 and 2015, respectively (Asnis *et al*., 2000; Nash *et al*., 2001; Fauci *et al*., 2016; Petersen *et al*., 2016).

Despite wide deployment of the YFV-17D vaccine in many African countries since 2006, in 2016, new YFV epidemics occurred in Angola and DR Congo resulting to about 965 confirmed cases and 400 mortalities. According to WHO, about 27 countries in Africa remain at risk of epidemics despite the current efforts (https://www.afro.who.int/health-topics/yellow-fever)

This like many other epidemics are highly contributed by factors such as urbanization, transportation, poor public health infrastructure especially in the developing world, land use changes as well as natural factors, such as genetic changes in the viruses, host-vector relationships, bird migration and global climate changes (Mackenzie *et al*., 2004).

Due to the close relationships among flaviviruses and the general rapid mutation rates of RNA viruses, there is a general problem in specific diagnosis, as well as a general lack of approved and/or efficient treatments and/or vaccines.

There exist effective, licensed vaccines against JEV, TBEV and the 17D vaccine against Yellow fever virus (YFV), which is the "gold standard" of successful vaccines and has severally been declared as the most efficient live attenuated vaccines ever generated to date (Fernandez-Garcia *et al*., 2016)

1.2.1 Flavivirus life cycle (Fig. 3)

Most of the flavivirus life cycle is largely inferred to from collective studies done on multiple flaviviruses especially Dengue virus

1.2.1.1 Attachment and entry

Binding of the virus is mediated by the viral large surface E glycoprotein and putative receptors on target cells. Additionally, some attachment factors such as the heparin sulphate, a factor present in many cell types have been shown to be involved in the initial stages of virus attachment in several flaviviruses. TIM and TAM proteins are coreceptor families identified to function as entry factors in DENV (Meertens *et al*., 2012).

Other attachment factors documented to be utilized by flaviviruses include the ER chaperone protein GRP78/BiP which facilitates entry of JEV (Nain *et al*., 2017), heat shock proteins 70 and 90, laminin, ICAM-3 and CD14 (Smit *et al*., 2011). The virus is then taken up by receptor-mediated endocytosis via clathrin-coated pits and then virions are trafficked to prelysosomal endocytic compartments of the host cell. The acidic pH in these vesicles induces a conformational change and reorganization of the viral envelope protein E from dimers, dissociation into monomers and then reformation into trimers (Allison *et al*., 1995). Some identified receptors and entry strategies of DENV, YFV, ZIKV and JEV have been reviewed by Laureti *et al*., 2018

While not much is known about the uncoating process, it is thought that the conformational change at this stage is key in the fusion of the viral proteins and endosomal membrane, a process that results in the uncoating and release of the viral nucleocapsid into the host cytoplasm (Heinz and Allison, 2003).

1.2.1.2 Translation and polyprotein processing

Translation is cap-dependent, occurs in the ER, is coupled with replication and initiates by ribosomal scanning. After uncoating, the positive, capped RNA viral genome (being an mRNA) allows for direct translation of the single open reading frame in the Endoplasmic reticulum to produce a single precursor polyprotein of approximately 3400 amino acids that is further co- and post-translationally processed by both virus-encoded NS2B/3 protease and host signalases into 3 structural (Capsid, Envelope and the pre-Membrane which matures into the Membrane) and 7 non-structural proteins (NS1, NS2A, NS2B, NS3, NS4A, NS4B, NS5) (Fig.2).

The 5’ end contains the structural proteins followed by the non-structural proteins stretching out until the 3’ end. It has been previously suggested that translation competency may determine infectivity in flaviviruses and they therefore use several mechanisms to facilitate that with some specialized structures within the 5’ and 3’ non-coding regions, mutations the 3’UTR in DENV2 has been shown to influence the RNA structure and changes the translation efficiency and the ultimate infectivity phenotype (Edgil *et al*., 2003)

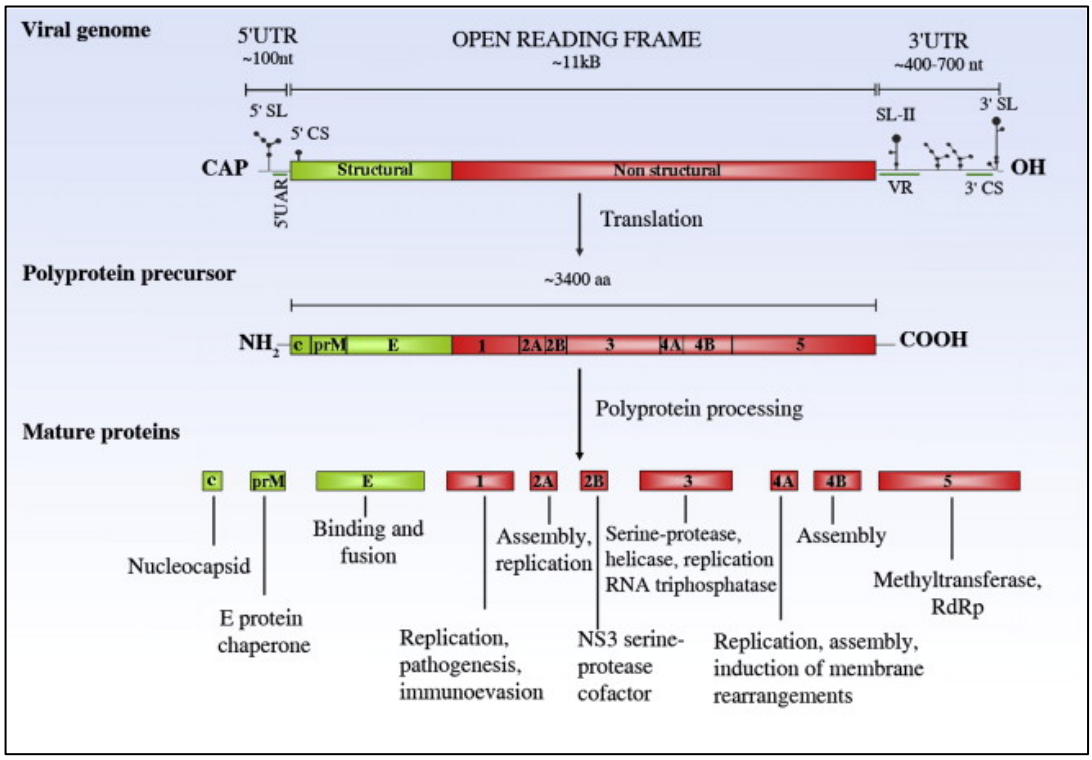

Figure 2: Schematic representation of the flavivirus polyprotein and its cleavage products (Fernandez-Garcia *et al*., 2009)

1.2.1.3 Replication

The process of replication occurs within invaginations of the ER membrane called replication vesicles. Replication is catalyzed by the virus-encoded RNA dependent RNA polymerase activity of NS5 and is typically benchmarked by the production and accumulation of double-stranded RNA (dsRNA) intermediates that are classical markers of flaviviral replication (Paul and Bartenschlager, 2015). The process begins with the production of first negative strand copies that are further used as templates in proceeding rounds of replication yielding new positive strands that serve as the genome packaged into newly formed viral particles but also for more rounds of replication. During polyprotein synthesis, the surface proteins prM and E are translocated into the ER lumen and released by host cell signalase (Mandl, 2005).

NS1 also translocates into the ER lumen once cleaved from the polypeptide and undergoes dimerization there, this dimeric form is ER-associated while the hexameric form, whose synthesis mechanism is unclear moves further along the

Golgi secretory pathway and is the circulating form.(as reviewed by Yap *et al*.,2017)

1.2.1.4 Assembly and Budding

The process of replication is closely related and somewhat intertwined with that of virus assembly both spatially and temporally. Additionally, it has been suggested that only actively replicated RNA gets packaged and this plays a role in the infectivity of the virus (Khromykh *et al*., 2001) The RNA genome is packaged by the Capsid protein in nucleocapsids on the cytoplasmic side of the ER membrane, a process coordinated with the viral envelope assembly that is acquired by budding of the nucleocapsid into the ER. Nucleocapsids are then transported into the lumen of the endoplasmic reticulum at the replication vesicle pore during formation of the prM-E lipid envelope (Roby *et al*., 2012).

1.2.1.5 Maturation and virion release

Assembled, immature virions are trafficked to the Trans-Golgi Network (TGN) where they undergo reversible conformational changes due to the low pH rendering them accessible to furin, a cellular protease abundant in the TGN and responsible for the proteolytic cleavage of the prM and the ultimate dissociation of its pr peptide. This event is the hallmark of virion maturation and marker for infection-competent virions. Mature virions finally bud out of the cell by exocytosis (Yu *et al*., 2008).

Only properly cleaved progeny virions, with a nucleocapsid containing a full genome copy can successfully infect other cells in proceeding rounds of infection (Chambers *et al*., 2003)

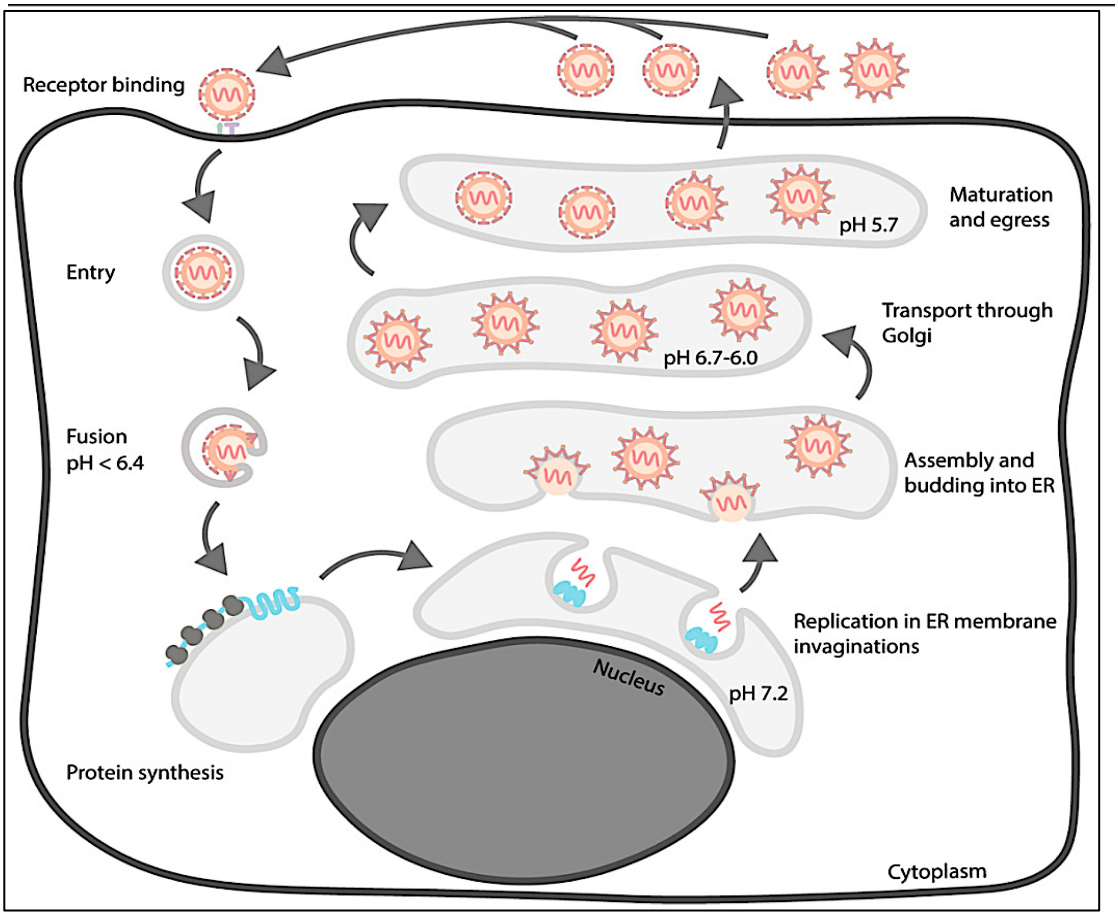

Figure 3: An overview of the TBEV life cycle (Pulliknen *et al*., 2018)

1.2.2 Flavivirus structural Proteins

Throughout replication, post-translational control of flaviviral structural proteins is strictly controlled to regulate efficient virion assembly, secretion and infectivity. These proteins and some of their known functions are highlighted in Figure 2.

Capsid protein

This is a small (approximately 11kDa), highly basic, dimeric cytosolic flaviviral protein that is translated at the N-terminus of the polyprotein. It has four structurally conserved α-helices and an internal hydrophobic domain that presumably interacts with viral membranes while the other side interacts with the viral RNA. Maturation to a soluble protein happens after cleavage from the prM signal sequence by the viral encoded NS2B/3 protease (Lindenbach *et al*., 2007; Chambers *et al*., 2003)

prM glycoprotein

This is an approximately 26kDa glycoprotein which is the precursor of the membrane protein. It folds quite rapidly and acts as the chaperone of the Envelope that is, it assists in the proper folding and secretion of the E protein. The N-terminal region of the prM contains one or three N-linked glycosylation sites and six conserved cysteine residues all of which are disulfide linked. The prM protein has been implicated together with several host factors in the flavivivirus life cycle specifically in virus entry, secretion and egress from the cell. The prM prevents the Envelope from undergoing rearrangements to a fusogenic form during transit in the secretory pathway and the dissociation of its pr peptide by furin yields mature virions (Duan *et al*., 2008; Lindenbach *et al*., 2007)

Envelope glycoprotein

The envelope (E) is a protein of approximately 53kDa and the major surface glycoprotein in flaviviruses. It contains 12 conserved cysteins forming disulphide bonds. The E protein is the viral hemagglutinin and induces a protective immune response and the domain III of this protein is the target of neutralizing antibodies.

Its major function in the flaviviral life cycle is mediating binding of the virus to the host receptors and the fusion of the virus onto the host cell membrane. The proper folding and secretion as well as its stability in low pH conditions depend on its co-expression with the prM protein (Heinz *et al*., 1991; Lindenbach *et al*., 2007).

1.2.3 Flavivirus non-structural proteins

NS1 glycoprotein

The flavivirus NS1 is a highly conserved glycoprotein, approximately 46 to 55kDa depending on its glycosylation status. It is localized in the ER lumen by a signal sequence located at the C-terminus of the E protein. This glycoprotein contains two or three N-linked glycosylation sites and 12 conserved cysteines that form disulfide bonds. NS1 is thought to be involved in the viral RNA replication.

process and the development of disease. NS1 is considered a major viral immunogen and found in the blood during early stages of infection as a viral marker of infection (Avirutnan *et al*., 2007; Lindenbach *et al*., 2007)

NS2A

This is an approximately 22kDa, hydrophobic membrane non-structural protein that is a product of the processing of the NS2 portion of the flaviviral polyprotein. The actual function of NS2A is not entirely known but has been suggested to function as a scaffold protein that organizes the replication complex (Barrows *et al*., 2018). It has been suggested that NS2A, alone or in complex with NS3, may be involved in genome transport (reviewed by Apte-Sengupta *et al*., 2014).

NS2B

This is a small membrane associated protein of approximately 14kDa. Its main known function is to serve as a cofactor of the viral protease NS3 forming the NS2B3 complex. This interaction between the two proteins is absolutely essential for optimal protease activity during infection. The cofactor activity of NS2B is encoded in a conserved hydrophilic region of 40 residues flanked by hydrophobic regions that mediate membrane association, suggesting a possible role of the protein in modulation of membrane permeability during infection (Lindenbach *et al*., 2007). NS2B of JEV and DENV have been shown to be associated with lipid rafts, a feature which makes them possess membrane-destabilizing properties (Cordero et al., 2014; Gopala Reddy *et al*., 2018). NS2B of JEV has been shown to contribute to replication and virion assembly through interaction with NS2A, and its transmembrane domains playing a fundamental role in both (Li *et al*., 2016).

NS3

This is a multifunctional, modular protein of approximately 70kDa involved in processing of the polyprotein and also in viral RNA replication. NS3 serves as the viral protease in the complex NS2B3 by processing the precursor polyprotein and therefore in the maturation of viral proteins. However, it harbors an NTPase-dependent RNA helicase activity in its C-terminus that functions may play a role

in genome replication and vRNA synthesis. (Barrows *et al*., 2018; Li *et al*., 2014; Lindenbach *et al*., 2007).

NS4A

This is a small (≈16kDa), hydrophobic transmembrane protein and one of the products of the processing and cleavage of the NS4 portion of the polyprotein that yields NS4A and NS4B proteins. The two proteins are linked by a fragment of approximately 23 amino acids that form the 2K-linker peptide. NS4A has been suggested to be a major driver of ER rearrangements in DENV infection (Miller *et al*., 2007) where the replication factories are assembled, and has a role in replication (Lindenbach *et al*., 1991). NS4A may also help in the organization of luminal, transmembrane and cytoplasmic components of replication complexes (Barrows *et al*., 2018)

NS4B

This is a transmembrane protein of approximately 27kDa linked to NS4A by the 2K-linker peptide. The linker specifically leads NS4B into the ER membrane where it has been shown to localize at sites of replication as well as in the nucleus (Barrows *et al*., 2018). It has also been shown to interact with NS3 suggesting an interaction with the replication complexes, and probably its role in replication. NS4B has also been implicated in ER rearrangements (Kaufusi *et al*., 2014).

NS5

This is the largest (≈ 103kDa), most conserved multifunctional protein that is indispensable in viral replication. It contains at its C-terminal the RNA dependent RNA polymerase and a methyltransferase at its N-terminus that catalyzes the methylation in the genome capping process (Lindenbach *et al*., 2007). These processes are vital for viral genome replication (suggested to occur in complex with NS3 by Barrows *et al*., 2018) as well as viral genome stability and are therefore central to the regulation and coupling of RNA synthesis and virion morphogenesis (Murray *et al.,* 2008)

1.2.4 Virus–induced membrane rearrangements

A vast majority of viruses from different families have been shown to induce extensive membrane rearrangements in the cells they infect and more specifically in the endoplasmic reticulum that has been described as a favorite niche for most viruses including flaviviruses as the site of replication and assembly of viral particles. This is of a particular interest due to different families of viruses converging at this particular organelle in the course of infection and even incorporating some of the ER intrinsic functions to exert a promotive role in almost every step of the life cycle (reviewed by Ravindran *et al*., 2016).

The morphological changes are nonetheless quite distinct among DNA and RNA viruses as well as among virus families (Fig 4). Studies done in flaviviruses have shown dramatic morphology changes of ER membranes in infected cells and mor***e*** importantly the formation of ER-derived invaginations or vesicle packets or replication vesicles. This vesiculation of the ER lumen results in the membrane sheets become dilated giving rise to swollen ER sacs. The vesicles serve as physical support where the replication factories/complexes are anchored for the coordinated accumulation of viral and cellular components required for efficient replication. Moreover, membranes ensure minimal or no exposure of viral nucleic acids to the host immune system by shielding the viral genome from cellular pattern-recognition receptors and nucleases (Mackenzie *et al*., 1999, 2005; Miorin *et al*., 2012, 2013; Overby *et al*., 2010).

These invaginations of ER membranes retain an open connection to the surrounding cytoplasm via a pore that may be involved in the import of host factors and nucleotides required for efficient RNA replication and the export of the newly synthesized viral genomes (Welsch *et al*., 2009; Miorin *et al*., 2013).

While the actual mechanism of membrane remodeling is unknown, it is thought to be a collective output of modulation of host lipid metabolism, influence of integral membrane proteins, activity of cytoskeleton components and microtubule motors, scaffolding by peripheral and integral membrane proteins (McMahon and Gallop, 2005). More importantly is the primal involvement of

some viral proteins such as the NS4A and NS4B proteins that have been implicated in remodeling of membranes, in DENV and the Kunjin strain of WNV infections (Miller *et al*., 2007; Kaufusi *et al*., 2014). NS4A and NS4B of DENV contain central helices assumed to lie in plane on the ER-luminal membrane leaflet, this arrangement is thought to locally increase the membrane surface area and induce invaginated vesicles. The oligomerization of NS4A and its interaction with NS4B may be the sustenance force to membrane rearrangements (Miller *et al*., 2006, 2007; Stern *et al*., 2013; Zou *et al*., 2015).

However, it has been suggested that additional viral proteins may also play a role in the rearrangements that are induced in the morphogenesis of replication factories as expression of these proteins alone did not resemble those observed in infected cells. One such protein may be NS1 that has been shown to dimerize and bind to and remodel membranes in vitro (Akey *et al*., 2014) and likely interacts with the NS4A-NS4B complex (Lindenbach and Rice, 1999; Youn *et al*., 2012). In addition, there is a possibility that NS2A might also be involved in the induction of flavivirus replication organelles (Chang *et al*., 1999; Xie *et al*., 2013; Kummerer and Rice, 2002)

ER invaginations result in vesicle packets, elongated vesicles or tubular structures that arise in the ER during DENV and TBEV infection of mammalian cells. The abundance of these structures differs between acute and persistent infections, with the latter showing more remodeling. These tubules have been suggested to be replication factories that are products of anomalous remodeling or represent an antiviral cellular defense mechanism restricting infection (Welsch *et al*., 2009; Offerdhl *et al*., 2012).

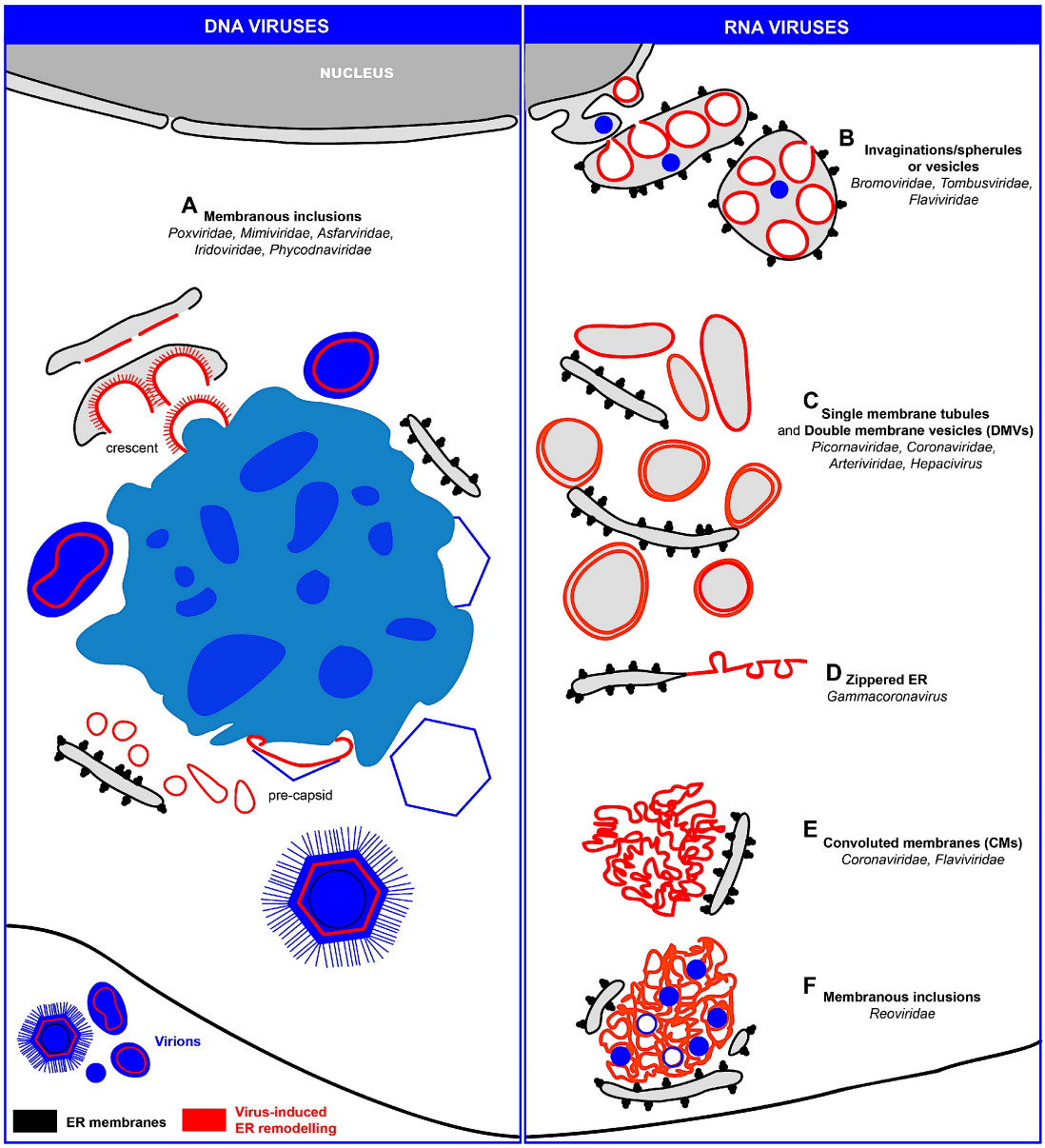

Figure 4: Different ER morphological changes owed to different families of DNA and RNA viruses (Romero-Brey and Bartenschlager, 2016) A) Membrane Inclusions; viral genome replication occurs in the cytoplasm in close-association with ER-derived membranes B) ER-derived invaginations/vesicles or spherules curving towards the ER lumen, what is referred to as negative curvature C) Single membrane tubules and Double Membrane Vesicles (DMVs); 'exvaginations' derived outwardly from the ER (positive curvature manner) D) Zippered ER; tethered spherules lacking luminal space due to zippering of ER cisternae E) ER-derived convoluted membranes, devoid of ribosomes, probably derived from smooth ER membranes F)Membranous inclusions; also called viroplasm, of cellular origin and closely surrounded by rough ER cisternae, both ER elements and virus particles are in contact with the cytosolic face of the plasma membrane that are part of the replication and assembly factory**.**

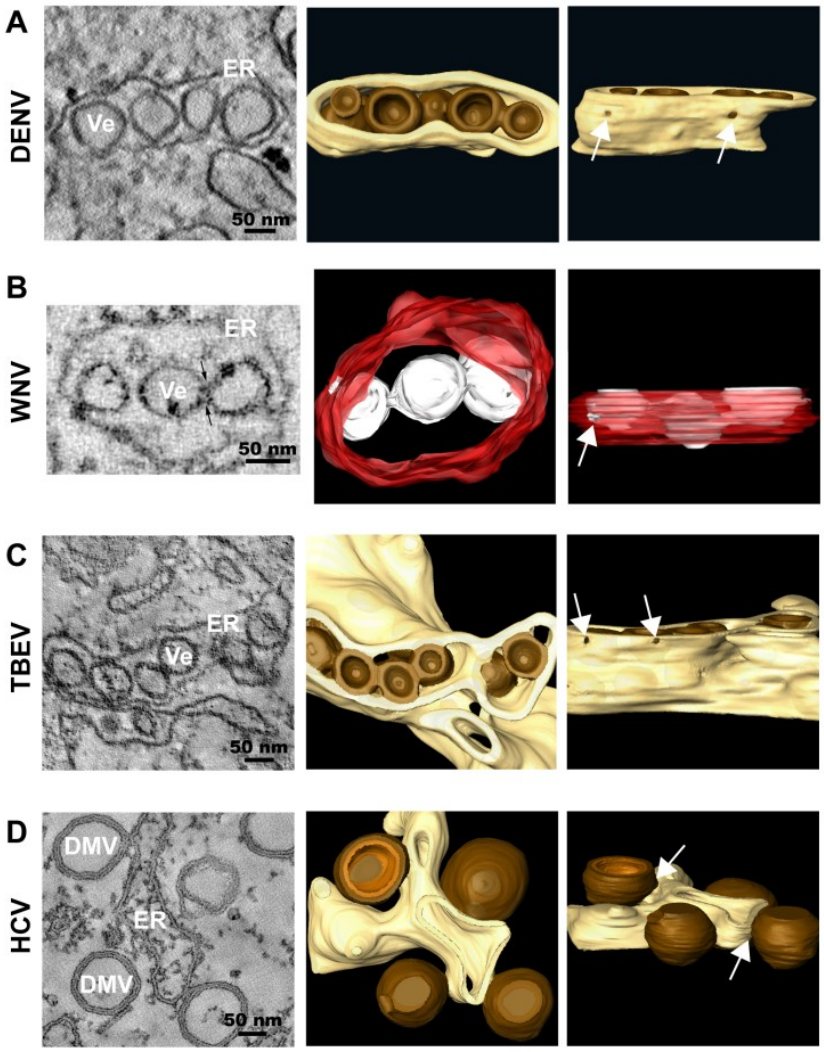

Figure 5. **Representative images of membrane rearrangements induced by different members of the family Flaviviridae** (Romero-brey and Bartenschlager, 2014). Slices through tomograms of cells infected with A) Dengue Virus (DENV); B) West Nile Virus (WNV); C) Tick-borne Encephalitis Virus (TBEV); D) Hepatitis C Virus (HCV) showing characteristic virus-induced structures.

1.3 Host innate sensing and resistance to flaviviral infection

1.3.1 Pattern Recognition Receptors

To establish a potent antiviral state upon infection, target cells possess germ-line encoded receptors that recognize distinct signatures from invading pathogens known as pathogen-associated molecular patterns (PAMPs), these are conserved molecular motifs unique to specific pathogens that are essential for survival, and cannot be altered by the pathogen (Nazmi *et al*., 2014), the PRR-PAMP interactions are therefore specific depending on PRR localization and PAMP specificity, this is also how the host cells that respond to viral invasion differentiate self from “non-self “molecules.

The identification of these signatures is the core event in the initiation of the antiviral signaling cascade which culminates in the production of numerous host cell defense molecules including type I and type III interferons that promote an antiviral state. These receptors are known as pattern recognition receptors (PRRs) and they are located on both the cytoplasm and the cell surface (Cumberworth *et al*., 2017). There are different classes of PRRs but the most important as far as flaviviral infections are concerned are the Toll-like receptors (TLRs) and the cytoplasmic sensors, retinoid acid- Inducible gene I (RIG-I) like receptors (RLRs) and Node-like receptors (NLRs) (Munoz‐Jordan and Fredericksen, 2010; Takeuchi and Akira, 2010; Suthar *et al*., 2013).

1.3.2 Toll-like Receptors

These are membrane-bound sensors, a family of about 11-12 members that detect specific PAMPs. Specific in flavivirus infections, TLR7 and TLR8 identify single-stranded RNA (ssRNA) and TLR3 identifies double-stranded RNA (dsRNA) produced during viral infection. TLRs sense invading pathogens from both outside the cell and in intracellular endosomal compartments, they do so through their leucine-rich ectodomains that mediate PAMP recognition. Signaling

of all TLRs except TLR3 is mediated by the adaptor protein MyD88 whereas TLR3 does so through the adaptor protein TIR-domain containing adaptor Inducing Interferon β (TRIF) (Kawai and Akira, 2010). The recruitment of these intermediate proteins in the course of the cascade leads to activation of the NF-κB, MAPK, ERK, and JNK pathways. TLR3 through TRIF signals through the TRAF3 and RIP1 signaling pathways to activate the transcription factors IFN‐regulatory factor, IRF3, NF-κB, and AP-1 to stimulate the IFN-I pathway (Akira *et al*., 2006).

1.3.3 RIG-I like receptors

The RLR family of receptors is made up of three members namely; retinoic acid-Inducible gene I (RIG-I), melanoma differentiation-associated gene 5 (MDA5) and Laboratory of genetics and physiology 2 (LGP2; also known as DHX58). These sensors are localized in the cytoplasm and trigger antiviral responses including type I interferon (IFN) production and pro-inflammatory signaling following viral invasion (reviewed by Pichlmair and Caetano e Sousa, 2007, Rehwinkel and Caetano e Sousa, 2010). RIG-I and MDA5 contain a DExD/H box RNA helicase domain that hydrolize ATP and binds and possibly unwind the dsRNA in the cytoplasm, two caspase-recruitment domains (CARDS) important in signaling and carboxyl-terminal repressor domain, which in RIG-I is involved in autoregulation (Takeuchi and Akira, 2010; Kato and Fujita, 2015). LGP2 lacks the CARD domains and is thought to positively regulate RIG-I and MDA5 (Satoh *et al*., 2010)

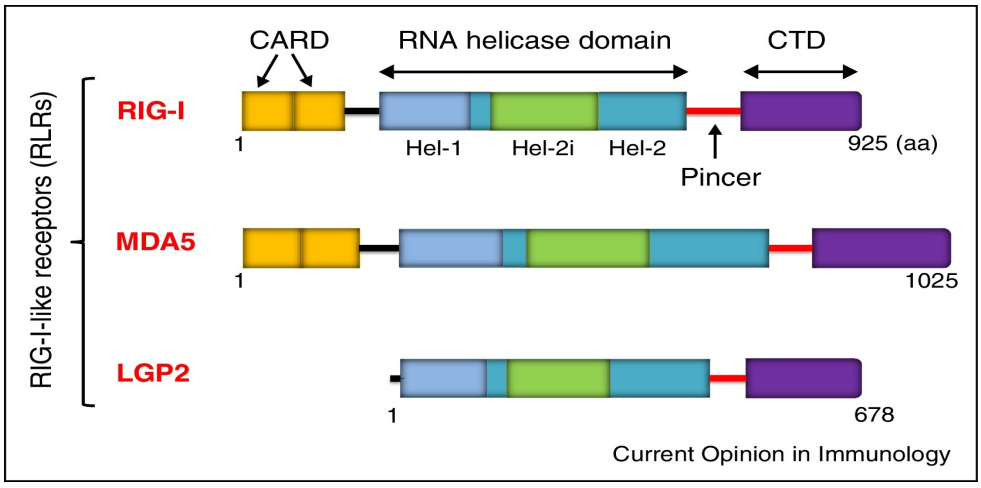

Figure 6: RIG-I like receptors RIG-I, MDA5 and LGP2 highlighting the distinctive features of each receptor (Kato and Fujita, 2015)

1.3.4 RIG-I signaling in flaviviral infection

The RIG-I cytosolic sensor specifically recognizes ssRNA molecules containing free 5'triphosphate (5'ppp) moieties (Cui *et al*., 2008; Hornung *et al*., 2006; Spiegel *et al*., 2005; Takahasi *et al*., 2008), 5' diphosphate (5'pp) such as those found in genomes of some viruses (Pichlmair *et al*., 2006; Goubau *et al*., 2014). Reportedly, RIG-I has been triggered experimentally by a variety of double-stranded RNAs (dsRNA) in a length-dependent manner, regardless of the 5' end modifications (Kato *et al*., 2008).

In non-infected cells where RIG-I is in a resting state, the CARD domains are folded over one another and the Repressor domain is folded over the helicase and RNA binding domains (Saito *et al*., 2007)

In the course of infection, when the pathogenic signature is recognized, RIG-I hydrolyzes ATP and undergoes a conformational change that triggers the interaction between the RNA binding domain with the pathogenic RNA. At the same time, the CARDs are released for interaction with the adaptor protein mitochondrial antiviral signaling (MAVS, also known as IPS-1, VISA, and Cardif), located in the mitochondrial-associated membrane (MAM) (Liu *et al*., 2012). MAVS relays the signal to kinases such as TANK-binding kinase 1 (TBK1) and IκB kinase (IKKε), which phosphorylate interferon regulatory factors (IRF3, IRF7) and nuclear factor-kappa beta (NF-κB), to initiate downstream signaling (Hou *et al*., 2011) through the translocation to the nucleus to evoke the transcription and secretion of Type I interferon, pro-inflammatory cytokines and the establishment of an antiviral state within the cell.

1.3.5 Type I IFN signaling

The cell intrinsic immunity against cellular insults including viral invasion is a conserved entity in nucleated vertebrate cells. It is primarily mediated through a signaling cascade that culminates in the production of IFN, virus-induced cytokines that are produced by both immune and non-immune cells (de Weerd *et al*., 2013; Chen K. *et al*., 2017). The first part of this cascade involves the PRR-PAMP interaction that has been previously explained (Fig. 6A), while the

secondary signaling involves the use of the secreted interferon molecules that bind to specific receptors on target cells (Fig. 6B).

The initial production of interferon serves as a "warning/alarm signal" of infection but the secondary signaling is what is indispensable in the antiviral activity because, IFNs themselves are not antiviral effectors. Rather, they are secreted by virally infected cells and act in an autocrine and paracrine amplification loop, binding to IFN receptors that signal to induce interferon-stimulated genes (ISGs) (Caetano Reis e Sousa, 2017).

The type one interferons IFNα and IFNβ bind to an ubiquitously expressed receptor(s) known as IFNAR1/2 which associates with Janus kinase 1(JAK1) and Tyrosine kinase 2(TYK2) kinases which phosphorylate Signal transducer and activators of transcription 1 and 2(STAT1 and STAT2) transducer proteins which then associate with IRF9 to form the ISGF3 complex that culminates in the expression of ISGs, which are the actual antiviral effectors (Stark and Darnell, Jr., 2012; Ivashkiv and Donlin., 2014). ISGs encode a variety of effector proteins that restrict virus propagation by shutting down cell translation, cleaving cellular and viral RNAs and blocking virion replication, assembly and/or release (Caetano Reis e Sousa, 2017). In addition to antiviral functions, ISGs play a role in the modulation of the IFN (Kumar *et al*., 2003). Several ISGs desensitize cells to IFN stimulation, and the ability of the IFN subtypes to signal can be differentially affected.

The type I and type III interferons are both known as the antiviral cytokines but the type III interferons signal through a heterodimeric receptor complex IFNLR1 and is largely restricted to epithelial cells. Even though they bind different receptors, both type I and type III interferons regulate similar sets of genes and display similar activities (Sommereyns *et al*., 2008)

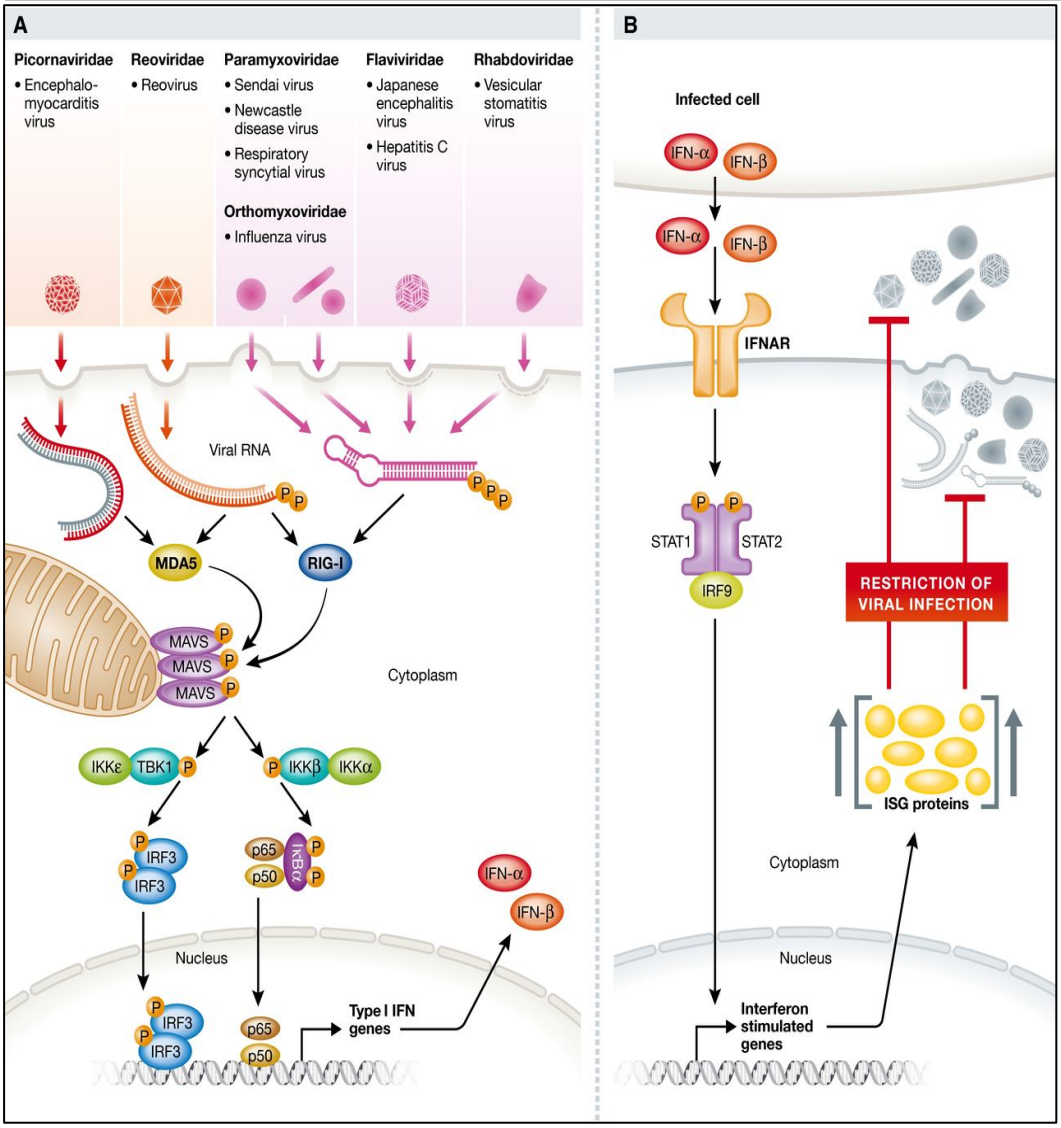

Figure 7: The IFN pathway of cell intrinsic antiviral Immunity (Caetano Reis e Sousa, 2017). Depiction of A) primary and B) secondary type I interferon signaling highlighting the various viral PAMPs, their respective PRRs/sensors (e.g. RIGI, MDA5), adaptor proteins (e.g. MAVS) and several kinases (e.g. IKKε, TBK1) that phosphorylate regulatory proteins (e.g. IRF3 in the case of TBEV), the translocation of which culminates in the secretion of type I IFN genes that facilitate the secondary cascade which involves the IFNAR receptors which bind the IFN molecules, followed by the phosphorylation of STAT transducer proteins and nucleus translocation. These events culminate in the production of ISGs in the nucleus which are in essence the actual antiviral effectors.

1.3.5.1 Interferon Stimulated genes

Following initial discoveries of IFN and its role in cell-intrinsic antiviral immunity, the role of ISGs became more apparent with their function as the actual effectors of antiviral signaling. Simply defined, an Interferon-Stimulated Gene is any gene that is induced during the IFN response. However, some of these genes are direct targets of Interferon regulatory factors (IRFs), NF-κB and can thus be induced even in the absence of IFN signaling. Additionally, some ISGs exist basally but are also IFN- inducible. Factors such as these make the classification of ISGs not as simplistic as one would hope (as reviewed by Schoggins, 2019). Other ISGs are themselves IFN signaling promoters while others are negative regulators targeting PRRs and IRFs. A set of ISGs have also been characterized to be pro-viral in some infections (Fig. 8, Chen *et al*., 2010, Randall *et al*., 2006)

Initially, ISGs were identified by the approach of associating their expression with virus suppression during infections and functional testing usually followed this. Ectopic ISG expression as a gain-of-function approach has also been used.

However, more recently there has been large-scale screening of ISGs credit to development of techniques such as RNA-Seq, CHIP-Seq and Microarray technologies as well as the revolutionary gene editing technology, CRISPR-Cas9.

Some of the mostly characterized antiviral ISGs include those of the Interferon-induced proteins with tetratricopeptide repeats (IFIT) family, RSAD2 commonly known as Viperin, Interferon-inducible transmembrane (IFITM) family and the IFI-6-16 family. Some analyses have also been done to identify further the steps in the virus life cycle that these ISGs target as well as their mechanism of action (as reviewed by Schoggins, 2019)

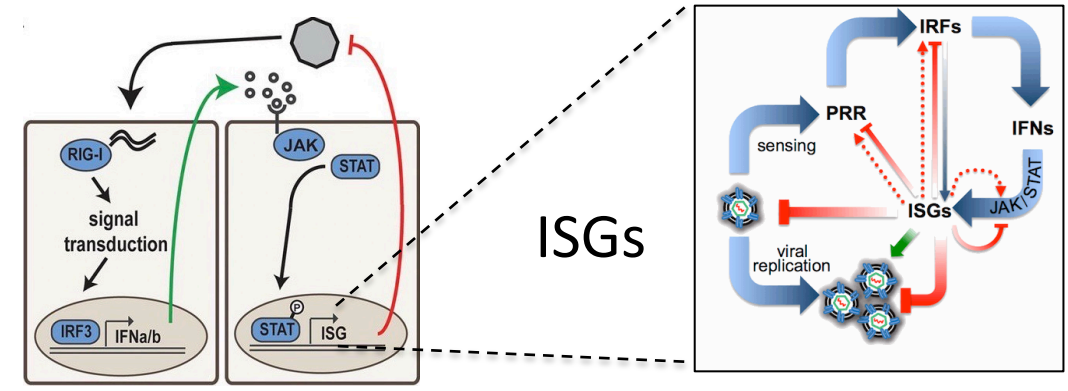

Figure 8: Interferon Stimulated Genes. A simplified depiction of the primary and secondary IFN signaling (left panel, Tanguy *et al*., 2017) and a general categorization of ISGs (right panel). Most characterized ISGs are antiviral (red blocked lines), some IRFs are induced independently of IFN (Thin blue line), some are themselves IFN signaling promoters (dotted red lines), Others are negative regulators targeting PRRs, IRFs (thin, red blocked lines) and some are proviral (green lines) (Schoggons' lab, UT SouthWestern web page)

1.3.6 Virus innate immunity evasion strategies

To ensure productive, potent infection cycles, viruses have evolved some strategies through which they use to evade the host cell innate immunity. They do so by hijacking some of the intrinsic cellular functions and using them to their advantages and/or using their proteins to inhibit different parts of the innate immune signaling cascade thereby defeating the host cell in eliciting an antiviral response.

Flaviviruses are no exception and some members have been shown to successfully subvert the innate antiviral signaling and promoting their replication. As described earlier, some flaviviruses such as TBEV, DENV and WNV replicate in modified ER membranes, which not only serve as replication sites but a way to evade PRR-sensing by delaying the host cell immunity (Frederickson and Gale, 2006; Mackenzie *et al*., 1999, 2005; Miorin *et al*., 2012, 2013) which offers a replication advantage during early stages of replication.

DENV suppresses the IFN signaling cascade by blocking TYK phosphorylation, impairing STAT1 phosphorylation, and it targets STAT2 by its NS5 protein for proteosomal degradation (Ashour *et al*., 2009; Mazzon *et al*., 2009; Green *et al*., 2014). NS2A of DENV has also been shown to be important in the RNA synthesis and plays a role in the viral evasion of innate immunity by inhibiting the RIG-I/MAVS signaling by inhibiting TBKI/IRF3 phosphorylation in DENV and HCV

infections (Kaukinen *et al*., 2013; Dalrymple *et al*., 2015) and the NS1 of WNV has been shown to target RIG-I and MDA5 to antagonize IFNβ production (Liu *et al*., 2004, 2005; Zhang *et al*., 2017). Additionally, the NS2B3 complex of DENV2 has been shown to target the human cGAS-STING pathway and thus impeding type 1 interferon signaling (Aguirre *et al*., 2012, 2017) same as the NS2B3 of WNV subtypes NY99 and KUN that prevent the translocation of STAT proteins to the nucleus in response to IFN-α treatment (Liu *et al*., 2005). The roles of NS5 proteins of different flaviviruses in the antagonism of type I Interferon signaling have been reviewed by Best, 2017.

Even when the primary IFN signaling has been activated, some viruses are able to inhibit some ISG effectors from eliciting their antiviral activity for example the methylation and capping of WNV RNA, there may be some modulation of the activity of the ISG IFIT1 (Daffis *et al*., 2010; Szretter *et al*., 2012)

DENV and JEV block caspase-dependent apoptotic cell death by activating PI3K signaling at early stages of infection, which initiates survival signaling to maintain the cells in a favorable condition for sustained virus production (Lee *et al*., 2005)

1.4 ER stress and the Unfolded protein response (Fig. 9)

1.4.1 ER stress

The ER is the designated cellular organelle for protein folding and maturation of nascent secretory and transmembrane proteins. To ensure that these functions are carried out effectively, the ER lumen maintains a homeostasis in balancing the protein load entering the ER and its capacity to handle this load.

In case of ER perturbations by physiological and pathological insults such as high protein demand, viral infections, environmental toxins, inflammatory cytokines, and mutant protein expression resulting to an accumulation of misfolded and unfolded proteins in the ER lumen, ER stress occurs (Oslowski and Urano, 2011).

The chronic induction of ER stress by accumulation of misfolded and unfolded proteins without the activation of the proceeding remedial pathway is characteristic of some disease pathogeneses (as reviewed by Lin *et al*., 2008)

1.4.2 Unfolded Protein response

The unfolded protein response (Figs. 9, 10) is a cellular response to ER stress, a remedial process to restore protein synthesis regulation that is highly conserved in vertebrates (Schrodder and Kaufmann, 2005)

The activation of UPR is mediated by three transmembrane proteins Inositol Requiring kinase I (IREI), Activating transcription factor 6 (ATF6) and PKR-like endoplasmic reticulum kinase (PERK) that are held in place by the chaperone protein BiP/HSPA5/GRP78 in their inactive form. Upon ER perturbation and the induction of ER stress, BiP dissociates from these proteins rendering them active (Lee, 2005).

The UPR involves up regulation of chaperone proteins such as BiP, GRP94 and PDI to promote protein folding, translational attenuation to reduce the load of proteins within the ER, preventing further accumulation of misfolded proteins, and up-regulation of ER-associated protein degradation (ERAD) as well as autophagy to promote degradation of misfolded proteins (Zhu and Lee, 2015). In circumstances of prolonged ER stress, however, the UPR becomes pro-apoptotic and triggers cell death (Perri *et al*., 2015)

The unfolded protein response as the name suggests is almost always assumed to be in response to the presence of unfolded proteins that create ER stress. However, it has been shown in yeast to also be due to changes in the ER lipid composition, in essence a more specific stress on the membranes with little or no involvement of unfolded proteins. This was performed in IRE1 mutants that were deficient in their ability to bind unfolded proteins. Other forms of stress stimuli culminating in membrane and/or lipid composition changes may be detected by the UPR sensors (in this case IRE1) in a different manner (Promlek *et al*., 2011). The mechanism that IRE1 employs has been further expounded on that the sensing mechanism relies on a juxta-membrane amphipathic helix that causes local membrane compression and acyl chain disordering. This way, the amphipathic helix can sense aberrant physical membrane properties. IRE1 is therefore able to combine both stress due to unfolded proteins as well as lipid

bilayer stress (Halbleib *et al*., 2017). In mouse cells, both IRE1α and PERK can be activated by luminal-independent signals in cells with enhanced lipid saturation, this is to say lipid perturbation may also be such a stimulus that can invoke UPR in the absence of unfolded proteins Volmer *et al*., 2013.

The plasticity nature of the ER allows for its dilation in conditions of stress. This is true for both ER stress due to external stimuli but also due to different cellular requirements such as B-cell differentiation that is typically accompanied by expansion of the ER (van Anken *et al*., 2003).

ER expansion/dilation can be measured by estimating the amount of phospholipid biosynthesis that occurs during UPR in response to ER stress. This is done by labelling cells with fluorescent dyes that can bind to lipid droplets and then analysed by flow cytometry and/or fluorescent microscopy (Yu *et al*., 2006)

More elaborate morphological changes occur during viral infection as a result of emergence of replication vesicles where viruses exploit the ER during the different steps of their life cycle. The morphology of these vesicles is due to changes in ER shaping proteins such as a family of Rab GTPases (Mateus *et al*., 2018) and tubule formation proteins such as the Reticulon family of proteins. ER membrane rearrangements appear to be specific among viruses as discussed in section 1.2.4 and summarised in Figure 4. ER dilation and/or remodelling in this context, i.e. during virus infection can be visualized by electron microscopy which has been extensively used to study replication vesicles in multiple viruses (Oslowski *et al*., 2011, Romero-Brey and Bartenschlager,2016).

1.4.2.1 ATF6

ATF6 is a type II transmembrane protein with two isoforms ATF6α and ATF6β. ATF6 has its carboxyl terminus on the luminal side and a basic leucine zipper (bZIP) transcription factor in its amino terminus (Yoshida *et al*., 1998; Haze *et al*., 1999). In response to ER stress, ATF6 is trafficked to the Golgi apparatus, where it undergoes regulated intramembrane proteolysis by sequential cleavage by site 1 and site 2 proteases (S1P and S2P, respectively) (Hetz *et al*., 2011). This releases a 50kDa fragment that translocates to the nucleus and there it functions

as a transcriptional activator that upregulates many UPR genes related to protein folding. (Haze *et al*., 1999; Lee *et al*., 2002; Yamamoto *et al*., 2007).

1.4.2.2 IREI

IREI is an approximately 110kDa type I transmembrane protein with a serine-threonine kinase domain and a RNase domain. There exist two isoforms of the protein: IREIα and IREIβ but the earlier is the ubiquitously expressed form. Upon activation, IRE I oligomerizes and subsequently allowing transphosphorylation of juxtaposed kinase domains. This activates the RNase domain, which cleaves XBP1 mRNA (encoding 'X-box-binding protein 1', a transcription factor of the bZIP family) at two discrete stem-loop structures through an unusual cytoplasmic splicing reaction. The resulting fragments are ligated by an RNA ligase, yielding the active transcription factor XBP1s (Cox *et al*., 1996; Yoshida *et al*., 2001). XBP1s translocates to the nucleus and induces the expression of chaperones, molecules involved in lipid biosynthesis and ERAD.

IREI is the most conserved arm of the UPR and appears to respond to a vast majority of UPR inducers, possibly an evolutionary consequence as a sole ER stress sensor (DuRose *et al*., 2006)

1.4.2.3 PERK

PERK is an ER-localized type I transmembrane protein. When UPR is activated, oligomerization of PERK in the ER membranes occurs inducing its *trans*-autophosphorylation and kinase domain activation (He, 2006; Kim *et al*., 2008). PERK further phosphorylates the α subunit of eukaryotic translation initiation factor 2(eIF2α) on Ser51, resulting in the shutdown of mRNA translation and therefore reducing the load of newly synthesized proteins entering the ER lumen (Hetz *et al*.,2006). An exceptional case to this general response is that certain mRNAs gain a selective advantage for translation under conditions in which eIF2α is phosphorylated (Lu *et al*., 2004), most common is the transcription factor ATF4 which activates the transcription of prosurvival genes as well as pro apoptotic genes such as CHOP. Additionally, ATF4 is a co-factor to GADD34,

whose role is to dephosphorylate eIF2α reversing protein synthesis attenuation with a negative feedback mechanism (Novoa *et al*. 2001).

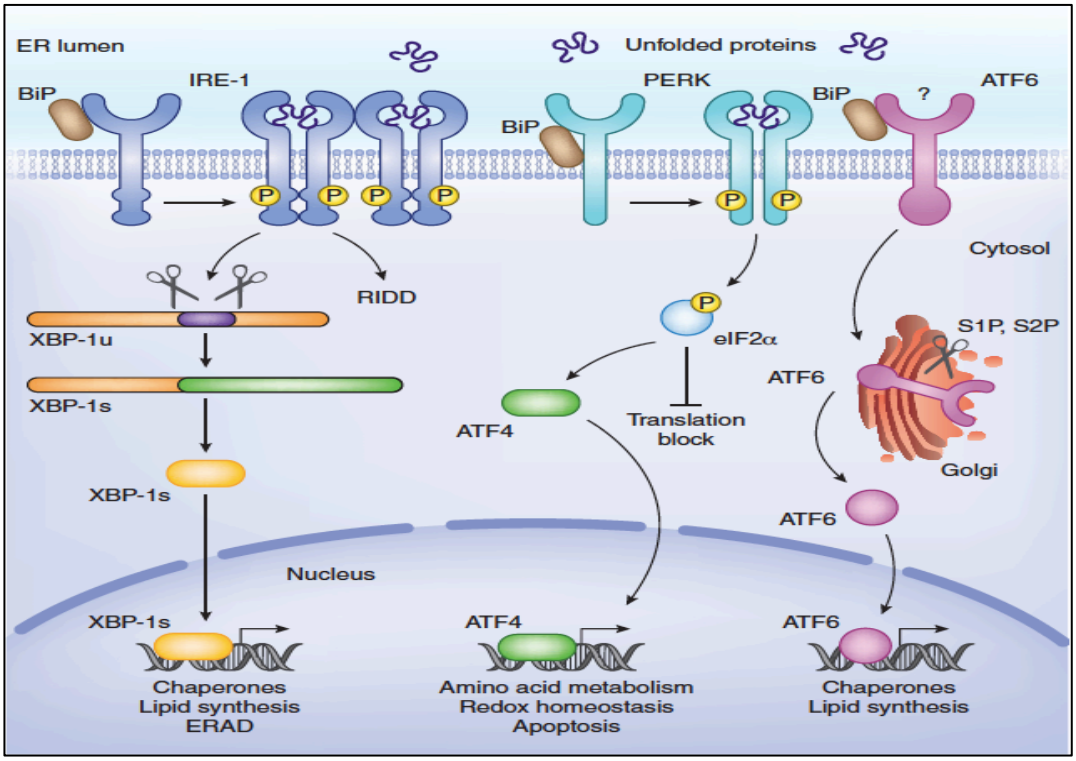

Figure 9: Unfolded Protein Response (Janssens *et al*., 2014)

1.4.3 Chemical vs Physiological Induction of UPR (Fig. 10)

There are several pharmaceutical UPR inducers with different modes of action available and routinely used in cell culture systems to induce ER stress and activate the UPR. These include Tunicamycin, Thapsigargin, Brefeldin A, dithiothreitol (DTT), and MG132. Oxidative cellular stress associated with changes in the translocon complex results to a global protein translation halt, a typical event in UPR induction through the PERK pathway. Compounds such as puromycin and aminoacid analogues lead to the aggregation of misfolded polypeptudes in the ER, eliciting stress and ultimately induce UPR (Hightower, 1980., Hammadi *et al*., 2013, Druelle *et al*., 2016, Schwenzer *et al*., 2019).

There are also some physiological UPR induction methods that have been reported to induce mild ER stress such as the deprivation of glucose to cells. The concentrations used and duration of induction are predetermined based on cell systems used and generally, the kind of output expected from an experiment (Oslowski and Urano, 2011; Bergman *et al*., 2018). ER stress and UPR induction

by either chemical or physiological inducers differs from cell to cell and activate the UPR in a specific manner. However, while these agents act in different ways, they all converge in their ability to induce an accumulation of unfolded glycoproteins in the ER, activating ER stress and ultimately UPR.

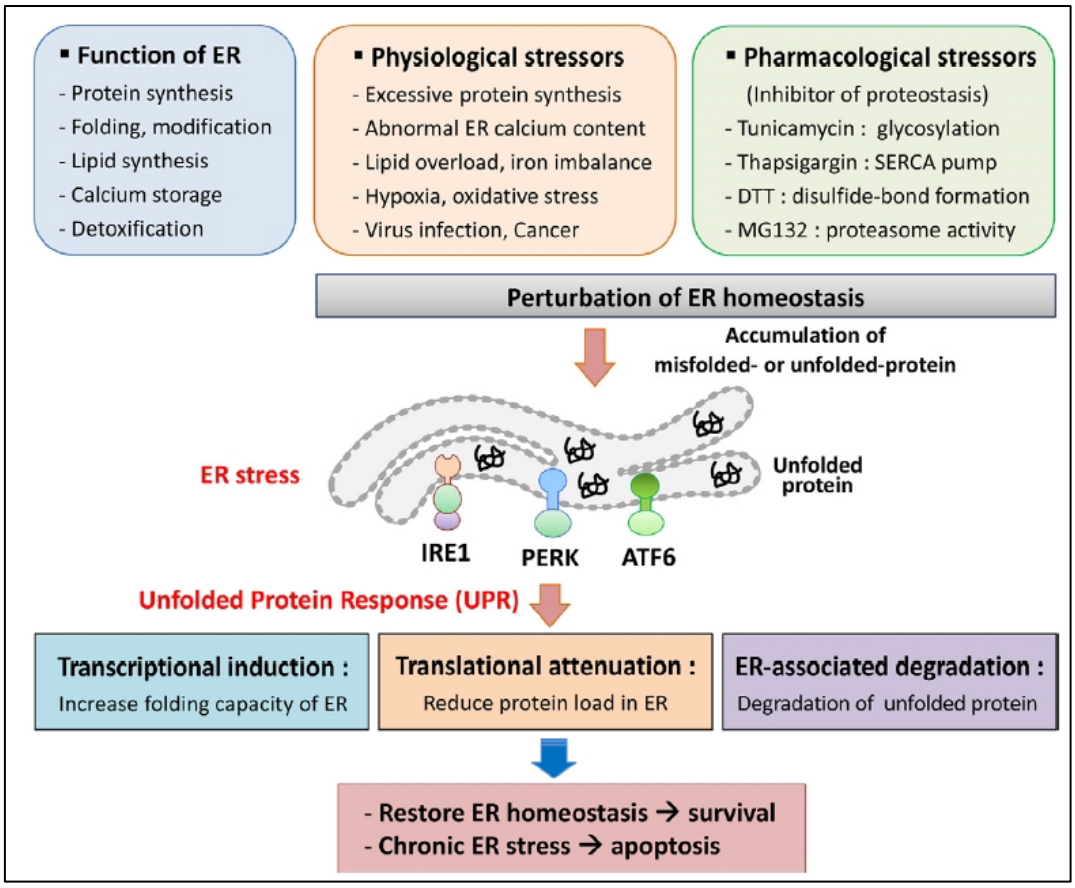

Figure 10: ER stress and Unfolded Protein Response induction (So, 2018)

Other methods of physiological induction of ER stress and UPR involve different strategies that amount to the accumulation of misfolded or unfolded proteins in the ER and by doing so achieving a more organelle-specific induction (protein overload which in theory is confined to the lumen of the ER) as opposed to general perturbation of cellular homeostasis. The strategies investigated in this study are reported herein.

siRNA interference of BiP

Apart from being a major chaperone in the ER, BiP binds the three UPR transducers in non-stressed cells and dissociates from them under conditions of ER stress and in doing so, activates the UPR. In line with this and evidence from

previous reports in HEK293 and HeLa cells (Suzuki *et al*., 2007), the depletion of BiP by siRNA transient knockdown has been shown to induce ER stress and activating UPR.

Overexpression of BiP ATPase mutants

BiP (also known as HSPA5, GRP78) is a chaperone protein in the ER with numerous functions including folding of nascent proteins, targeting misfolded proteins for degradation (ERAD) and regulating the UPR. BiP has two major domains; the N-terminal domain contains an ATP catalytic site and the C-terminal domain contains the substrate-binding site. The two domains communicate by binding and releasing ATP and unfolded peptides respectively to regulate activity and most of the activities of BiP are dependent on its ATPase activity for proper function (Mayer *et al*., 2005)

BiP ATPase mutants have amino acid substitutions within the nuclear binding domain, which renders the protein unable to carry out its activities. Some of these mutants include G227D, a non-ATP binding mutant and T37G, an ATP-conformational change induction mutant (Hendershot *et al*., 1996). The overexpression of the ATPase mutants will impair the folding capacity of the ER, thereby inducing ER stress and UPR.

Overexpression of ectopic proteins such as α1-antitrypsin mutants

The alpha 1 anti-trypsin (α1AT) is a member of the serpin family of protease inhibitors that inhibit proteases and protect tissues from damage (Fregonese *et al*., 2008).

α1AT mutants may induce either an overload of proteins in the ER (polymer aggregation) or accumulation of misfolded proteins. A common and widely studied mutant of α1AT is the null Hong Kong (NHK) mutant, a truncated variant that does not fold properly. While the wild type (α1AT) is completely secreted, only a fraction of the NHK mutant can be secreted thus inducing ER stress and activate the UPR (Ordóñez, *et al*.,2013; Ferris *et al*., 2013).

1.4.3.1 Cancer as a physiological ER stress inducer

As shown in figure 10, physiological stressors include cancers and viral infections. In general, the elicitation of UPR induction relies on the sustenance of the inducing stimuli in exerting ER stress. Cancer-induced ER stress is implicated in the initiation of transformation, unrestricted cell division, invasion and spread of tumorigenic cells. In most cancers, ER stress is accompanied by hypoxia and nutrient deprivation especially in the early stages of tumorigenesis (Chipurupalli *et al*., 2019; Madden *et al*., 2019). Transformed cells take advantage of the pro-survival mechanisms of UPR to sustain growth and proliferation of tumorigenic cells and meeting the vast protein folding demands accompanied by the progression of cancer. However, unlike in viral infections (next section, 1.4.3.2) where ER stress can be a direct result of accumulation of viral proteins as well as those of the host, the process of tumorigenesis ultimately results to a protein load, almost always solely belonging to the host cells. And depending on the circumstances and cell's condition, UPR activation may also help the resistance to treatment and production of clones less sensitive to chemotherapy. In most cases, UPR activation is a vital step for oncogenic transformation, as UPR signaling molecules interact with well-established oncogene and tumor suppressor gene networks to modulate their function during cancer development (Walczak *et al*., 2019).

1.4.3.2 Virus-induced ER stress and UPR

As previously discussed, virus replication and/or assembly of newly synthesized viral progeny for most flaviviruses occurs in the ER. This implies a large accumulation of viral proteins within the ER resulting into a protein overload in the ER lumen during infection, the essence of ER stress and subsequently UPR activation. Several studies have suggested a connection between UPR activation and either the process of viral replication (herpes simplex virus (HSV) 1, JEV, and HCV (Su *et al*., 2002; Cheng *et al*., 2005; Tardif *et al*., 2005) or the production of a specific viral protein in the ER (Zhang and Wang, 2012). For example, the ectopic

expression of the E2 protein, but not E1, core and NS3 proteins of Hepatitis C virus (HCV), has been shown to activate the expression of BiP (Liberman *et al*., 1999). HCV replicons expressing only non-structural proteins are also capable of stimulating BiP expression (Tardif *et al*., 2002).

Like innate signaling, viruses have evolved to use the UPR signaling to their advantage throughout the life cycle as reviewed by Ambrose and Mackenzie, 2013b and Green *et al*., 2013, suggesting in some instances a pro-viral function. This selective manipulation of the UPR is also different when the infection is acute or chronic.

Any viral infection whether acute or chronic is an arms race between the host cell and the virus with the host attempting to eradicate the virus and the virus trying to take advantage of the various responses including the UPR, manipulating them to its advantage.

While pro-survival is a common goal in any virus infection, as far as the UPR is concerned, the major difference is that chronic infections are skewed in that the virus targets some parts of the stress response with an aim of promoting persistence and/or latency. Indeed, such is the case in Hepatitis C which activates all three arms of the UPR but after this initial upregulation and peaking, there follows only milder stress that is long-lived. This is made possible by increased eIF2α phosphorylation alleviating the protein translation halt thus supporting the HCV chronic infection and later with diminished CHOP levels avoiding immediate cell death (Mercuiol *et al*., 2011; reviewed by Chan *et al*., 2014). HCMV is the largest human herpesvirus encoding at least 200 proteins. Its replication is relatively slow and due to its size, it is understandably stressful for the cell and particularly the ER to endure the slow replication. For this reason, HCMV has evolved to mitigate this by an upregulation of BiP throughout its cycle. BiP helps to control the prevailing UPR due to infection by protein folding, and has been shown to play some roles in virus assembly and egress (Buchkovich *et al*., 2010). In other cases, viruses may decide to only utilize certain arms of UPR and inhibit others such as HSV that strongly activates GADD34 to relieve the protein

translation inhibition while WNV activates only ATF6 and XBP1 but not PERK so as to bypass the translation halt. Different viruses and how they may manipulate the UPR to their advantage have been reviewed by Dash *et al*., 2016.

1.4.4 The UPR and antiviral immunity

The role of UPR in the remedial of ER stress has increasingly been associated with modulation of immunity and inflammation activities revealing more about functions other than ER stress management. The UPR has also now been recognized for its role in immune cell differentiation and function, and in regulating immune and inflammatory responses, including those associated with infections, tumors and autoimmune responses (reviewed by Grootjans *et al*., 2016).

When cells undergoing an acute UPR upon treatment with Tharpsigargin were treated/transfected with TLR and MDA5 agonists, there was an augmentation in TLR-induced cytokines and IFNβ production, a log-fold or more over the PRR agonist alone. In dendritic cells, this synergistic effect was shown to be dependent on the transcription of XBP1 (Smith *et al*., 2008; Hu *et al*., 2011)

This synergistic effect was not only observed upon pre-treatment with pharmacologic agents, cells expressing the misfolding α1AT mutant responded to LPS with greater cytokine production (Caroll *et al*., 2010). This synergistic effect has been observed in multiple culture cell types, human and mouse macrophages as well as dendritic cells as shown.

There is also evidence that UPR sensing of Influenza hemaglutinin (HA) triggers a direct anti-IAV response by targeting HA degradation via the ER associated degradation pathway (ERAD). The host cells detect HA as a misfolded or “nonself” protein and ER mannosidases target HA to ERAD for degradation and limit IAV replication (Frabutt *et al*., 2018).

There is increasing data showing that the UPR may be a danger signal that synergizes with PRR-sensing to elicit an antiviral state or may do so via activation of intrinsic pathways such as ERAD to limit infection (as reviewed by Janssens *et al*., 2014; So, 2018).

1.4.5 ER stress, UPR and interplay with autophagy

While the last resort for cells undergoing prolonged ER stress is cell death, autophagy can help cells to cope with mild ER stress by its contribution to elimination of misfolded and unfolded proteins suggesting a certain amount of cross-talk between them. Additionally, certain stimuli such as nutrient starvation that have been documented to induce mild ER stress can also induce autophagy. The interplay between the two has mostly been described in some specific disease conditions such as kidney and neurodegenerative diseases. Some autophagy genes have been shown to be activated after activation of ATF4, a PERK-mediated factor during the unfolded protein response. Both IRE1 and ATF6 have also at one time or another been implicated in the modulation of the cellular autophagy process (Cai *et al*., 2016; Cybulsky, 2017; Hosoi *et al*., 2017).

More generally though, in conditions where this interplay exists, UPR elicited by ER stress stimulates autophagy and the three UPR sensors may distinctively modulate certain points of the autophagy process. PERK- dependent eIF2α phosphorylation has been shown to contribute in the activation of autophagy in response to the accumulation of unfolded proteins. Activation of IRE1 has also been shown to regulate autophagy when cells were treated with ER stress inducers TM or TG or proteasome inhibitors led to an IRE1-dependent activation of autophagy which relies on the interaction of IRE1 with TRAF2 and JNK activation. These and other distinct ways on how individual arms of UPR converge into the autophagy pathway are comprehensively reviewed by Verfaillie *et al*., 2009; Senft & Ronai, 2015; Kabir *et al*., 2018.

1.5 Aim of thesis

My thesis stemmed from previous observations pertaining to the role of UPR in the elicitation of a robust antiviral state during flavivirus infections.

- As a prerequisite, my first task was to analyze the effects of UPR inducers TM and TG on cell growth and viability in our current experimental settings
- Additional to this, my central objective was rooted into the search for alternative UPR inducers, an attempt to induce UPR in a more specific manner targeting the endoplasmic reticulum, which is the site of replication for many flaviviruses but the center for protein folding and therefore central in ER stress and UPR signaling.
- Upon success, to evaluate this alternative of UPR induction in the context of antiviral signaling during TBEV infection as I also analyzed the same with the inducer Tunicamycin.

2.MATERIALS AND METHODS

2.1 Materials

2.1.1 Cells

Human cells

- U2OS: Human osteosarcoma cell line (ECACC No. 92022711)
- Vero: African green monkey kidney (ECACC No. 84113001)
- HEK 293T: Human embryonic kidney cell line with the SV40 T-antigen

Bacteria cells

- **MAX Efficiency DH10B Competent Cells** (Invitrogen – cat. no. 18297-010). Genotype: F- mcrA Δ (mrr-hsdRMS-mcrBC) ϕ80lacZ Δ M15 Δ lacX74 recA1 endA1 araD139 Δ (ara, leu)7697 galU galK λ - rpsL nupG
- **MAX Efficiency DH5α Competent Cells** (Invitrogen – cat. no. 18258012 Genotype**:** F^- Φ80*lac*ZΔM15 Δ(*lac*ZYA-*arg*F) U169 *rec*A1 *end*A1 *hsd*R17 (rk^-, mk^+) *pho*A *sup*E44 λ^- *thi*$^-$1 *gyr*A96 *rel*A1

2.1.2 Media

Human cells

- Cells were grown in Dulbecco's modified Eagle's medium (DMEM) Gibco – cat. no. 31885-023 (Life Technologies) supplemented with 10% fetal bovine serum (FBS; REF 10270-106, EU approved, Brazil, Life Technologies), 0.1 U/ml penicillin, and 0.1µg/ml streptomycin at 37°C in 5% CO_2.
- Reduced serum medium (Opti-MEM) was used during transfection. The media and serum were purchased from Gibco – cat. no. 31985-070.
- Cell freezing medium was made by 90% FBS and 10% DMSO (Sigma-Aldrich cat.no. 472301-500ML) for long-term storage.

Bacteria cells

- Luria-Bertani (LB) Medium: 10g bacto-trypton, 5g bacto-yeast extract, 10g NaCl per 1 liter medium. Ampicillin or Kanamycin was added at a concentration of 100µg/ml and 50µg/ml respectively.
  For hardening 1.5% agar-agar was added to the liquid medium.
- SOC Medium: Super Optimal Broth (SOB) medium (20g bactotrypton, 5g bacto-yeast extract, 0.5g NaCl per 1L medium) was enriched with 20mM glucose.

2.1.3 Antibodies

2.1.3.1 Primary Antibodies

Antibody	Species	Dilution	Source/Reference
4G2	Mouse	1:20000 WB	Kindly provided by Dr. Vivian Huerta Center for Genetic Engineering and Biotechnology (CIGB), Cuba
FLAG®M2	Mouse	• 1: 1000 WB • 1: 5000 FC	Sigma-Aldrich - cat. no. F1804
SV5	Mouse	• 1: 10000 WB • 1: 5000 FC	Kindly provided by Oscar Burrone; Laboratory of Molecular Immunology (ICGEB)
BiP	Mouse	1: 1000 WB	• BD Biosciences - cat. no. 610979 • Kindly provided by Oscar Burrone; Laboratory of Molecular Immunology (ICGEB)

Table 1: Primary antibodies used in this study (WB= Western Blot, FC=Flow Cytometry)

2.1.3.2 Secondary antibodies

Antibody	Species	Dilution	Source/Reference
Anti-mouse AlexaFluor 488	Donkey	1:500 FC	Molecular probes (Invitrogen cat.no. A32723)
Anti-mouse/HRP	Rabbit	1:10000 WB	DakoCytomation (cat. no. P0447)
Anti-rabbit/HRP	Goat	1:10000 WB	DakoCytomation (cat. no. P0449)
Human β-Actin Peroxidase	Mouse	1: 50000 WB	Sigma-Aldrich (cat.no. A3854)

Table 2: Secondary antibodies used in this study (WB= Western Blot, FC=Flow Cytometry)

2.1.4 siRNAs

Pools of small interfering RNAs (siRNAs) against BiP (ON-TARGET plus SMARTpool, 5nmol siRNA cat.no. L-008198-00-0005) and control pool ON-TARGETplus Non-targeting Pool, 5nmol siRNA cat.no. D001810-10-05) were purchased from Dharmacon and used according to manufacturer's instructions.

2.1.5 Vectors

Plasmid analysis was performed on SerialCloner version 2-6-1

Plasmid	**Characteristics**	**Reference/Source**
pcDNA3 BIP (grp78) human	• Encodes Wild type BiP/grp78 • AMP^R	• Kindly provided by Dr.Oscar Burrone; Laboratory of Molecular Immunology (ICGEB) • Sasset *et al*., 2015
pcDNA3 BIP (grp78) human G227D	• Encodes a non-ATP binding BiP mutant • AMP^R	

pcDNA3 BIP (grp78) human T47G	• Encodes an ATP-conformational change induction BiP mutant • AMP^R	•
pcDNA3-AAT-SV5-BAP	• Encodes an SV5-tagged wild type α1AT • AMP^R	
pcDNA3-AAT-D318-SV5-BAP	• Encodes an SV5-tagged null Hong Kong mutant of α1AT • AMP^R	
pEGFP-C1	• Encodes the GFP mutant 1 variant • $KANA^R$	• BD Biosciences Clontech cat. no. 6084-1 • Cormack *et al*., 1996
pcDNA 3.1(+)	• Empty vector • AMP^R	Invitrogen-cat.no. V79020
pl.18 TBE Hy C 3xFlag	• Encodes Flag-tagged TBE Capsid protein • AMP^R	• Kindly provided by Dr. Anna K. Överby; MIMS, Umeå Universitet, Sweden • Överby *et al*., 2010 • Tarpey and Greenwood, 2001.
pl.18 TBE Hy prM 3xFlag	• Encodes Flag-tagged TBE pre-Membrane protein • AMP^R	
pl.18 TBE Hy E 3xFlag	• Encodes Flag-tagged TBE E protein • AMP^R	
pl.18 TBE Hy NS1 3xFlag	• Encodes Flag-tagged TBE non-structural protein 1 • AMP^R	

pl.18 TBE Hy NS2A 3xFlag	• Encodes Flag-tagged TBE non-structural protein 2A • AMP^R	
pl.18 TBE Hy NS2B 3xFlag	• Encodes Flag-tagged TBE non-structural protein 2B • AMP^R	
pl.18 TBE Hy NS3 3xFlag	• Encodes Flag-tagged TBE non-structural protein 3 • AMP^R	
pl.18 TBE Hy NS4A 3xFlag	• Encodes Flag-tagged TBE non-structural protein 4A • AMP^R	
pl.18 TBE Hy NS4B 3xFlag	• Encodes Flag-tagged TBE non-structural protein 4B • AMP^R	
pl.18 TBE Hy NS5 3xFlag	• Encodes Flag-tagged TBE non-structural protein 5 • AMP^R	
pGL3 IFN-β Luc	• Encodes the Firefly Luciferase gene under control of the IFN-β promoter • AMP^R	• Lin *et al*., 2000
pEF-BOS-FLAG-RIG-IN	• Encodes Flag-tagged RIGI (active domain only, not full-length) • AMP^R	• Kindly provided by Dr. Takashi Fujita (Kyoto University) • Yoneyama *et al*., 2004

Table 3: Plasmids used in this study

2.1.6 Primers

Primers were designed using the NCBI Primer Designing Tool (**http://www.ncbi.nlm.nih.gov/tools/primer-blast/**), following optimal parameters and selecting only the primers spanning exon–exon junctions to minimize genomic DNA amplification. All primers were synthesized by and purchase from Sigma-Aldrich or Intergrated DNA Technologies (IDT).

Oligonucleotide name	**Sequence: 5’ to 3’**
β-Actin Fw	CAT GTG CAA GGC CGG CTT CG
β-Actin Rv	GAA GGT GTG GTG CCA GAT TT
BiP Fw	CCC GAG AAC ACG GTC TTT GA
BiP Rv	TCA ACC ACC TTG AAC GGC AA
CHOP Fw	TAA AGA TGA GCG GGT GGC AG
CHOP Rv	CTG CCA TCT CTG CAG TTG GA
DNAJC3 Fw	CGT TTG CGT TCA CAA GCA CT
DNAJC3 Rv	CCC GAA CTT CAC TGA GGG AC
EDEM1 Fw	AGG ACC AAG GGG GAA AGT CT
EDEM1 Rv	GTA CAC GAT TGC AGT TGG AGC
GADD34 Fw	CCC AGA AAC CCC TAC TCA TGA T
GADD34 Rv	CTC GGA GAA GCG CAC CTT T
GAPDH Fw	CAT GAG AAG TAT GAC AAC AGC
GAPDH Rv	AGT CCT TCC ACG ATA CCA AAG
IFI44 Fw	AGA CGA ATG CTA TGG GCT GC
IFI44 Rv	CCT CCC TTA GAT TCC CTA TTT GCT C
IFI44L Fw	TCA AAG CCG GGT CAT GAA TG
IFI44L Rv	CCT TCA TGG GGT CCA GTT CC
IFIH1 Fw	GAT TCA GGC ACC ATG GGA AGT
IFIH1 Rv	AGG CCT GAG CTG GAG TTC TG
IFIT1 Fw	GAA ATA TGA ATG AAG CCC TGG A
IFIT1 Rv	GAC CTT GTC TCA CAG AGT TCT CAA
IFNβ Fw	AGG ACA GGA TGA ACT TTG AC
IFNβ Rv	TGA TAG ACA TTA GCC AGG AG
OASL Fw	TAC CAG CAG TAT GTG AAA GCC A
OASL Rv	GGT GAA GCC TTC GTC CAA CA
TBEV 5’ NCR Fw	GCG TTT GCT TCG GA
TBEV 5’ NCR Rv	CTC TTT CGA CAC TCG TCG AGG

Viperin Fw	CCC CAA CCA GCG TCA ACT AT
Viperin Rv	TTG ATC TTC TCC ATA CCA GCT TCC
XBP1s Fw	CTG AGT CCG CAG CAG GTG
XBP1s Rv	GGC TGG TAA GGA ACT GGG TC
XBP1u Fw	AGC CAA GGG GAA TGA AGT GAG G

Table 4: Sequences of primers used in this study

2.1.7 Solutions and Buffers

- **1X PBS (1 litre)**

  In 800 ml of distilled water, the following were added; 8 g of NaCl, 0.2 g of KCl, 1.44 g of Na_2HPO_4, 0.24 g of KH_2PO_4. pH adjusted to 7.4 and distilled water was added to bring solution to volume of 1 liter.

- **2X HBS buffer**

  42mM HEPES (Sigma-Aldrich cat. no. H4034-100G), 274mM NaCl, 1.5mM $Na_2HPO_4.12H_2O$, 15mM D-glucose and pH adjusted to 7.

- **5X TBE (1 litre)**

  54g Tris base (Invitrogen cat.no. 15504-020), 27.5g Boric acid (Sigma-Aldrich cat.no. 31146), 20ml 0.5M EDTA (Sigma-Aldrich cat.no. E5134-1KG) and distilled water to final volume of 1 litre.

- **3.7% Paraformaldehyde (PFA)**

  5ml of 37% PFA: 1.85g of PFA powder, reagent grade crystalline (Sigma-Aldrich cat. no. P6148-500G) dissolved in 5ml of distilled water, 10µl 10M KOH. 37% PFA was diluted in 2x PHEM buffer (18.14g PIPES (ChemCruz cat.no. sc-216099); 6.5g HEPES; 3.8g EGTA; 0.99g $MgSO_4$; pH adjusted to 7 with 10M KOH) to produce 3.7% PFA.

- **6% carboxymethyl cellulose (CMC)**

  500 ml; 30g CMC powder (Sigma-Aldrich cat. no. C5013-500G) dissolved in 500ml PBS

- **1% Crystal violet solution**

  1L; 10g Crystal violet powder (Sigma- Aldrich cat.no. C6158-50G), 200ml PBS and 800ml Methanol (Sigma-Aldrich cat.no. 32213-2.5L-M)

- **SDS electrophoresis buffer (10X)**

  30.2g Tris, 188g Glycine (Sigma-Aldrich 33226-1KG), 50ml 10% SDS (Sigma-Aldrich L5750-500G), add water to 1 litre

- **10X Transfer Buffer (1 litre)**

  30.3g Tris, 144g Glycine, add water to 1 liter

    - **1X Transfer buffer (1 litre)**: 100ml 10X Transfer Buffer, 200ml Methanol and 700ml water.

- **10X TBS (1 litre)**

  60g Tris, 2g KCl, 80g NaCl, pH adjusted to 8.5 with 37% HCl, add water to 1L

    - 1X TBS-T (1 litre): 100ml 10X TBS, 900 ml water, 1ml Tween-20 (Sigma-Aldrich P2287)

- **100mM PMSF**

  17.4 mg of PMSF (Sigma-Aldrich cat.no. P7626) in 1ml of isopropanol (Riedel-de Haën cat.no. 603-117-00-0)

- **EDTA and EGTA solutions**

  EDTA (Sigma-Aldrich cat.no. E5134-1KG) and EGTA (Sigma-Aldrich cat.no. E3889-100G) dissolved in H_20.

- **Nonidet-P40 (NP-40)**

  20mM Tris HCl pH 8, 137 mM NaCl, 10% glycerol (Sigma-Aldrich cat.no. 49770-1L), 1% nonidet P-40 (Calbiochem cat.no. 492015) and 2 mM EDTA

2.1.8 Size Markers and Dyes

- PageRuler Plus Prestained Protein Ladder, Thermo Scientific cat.no. 26619
- 100bp DNA Ladder (5u/µl), Promega cat.no. G2101
- 1kb DNA ladder (100µg/ml), Promega cat.no. G571A
    - DNA markers supplied with Blue/Orange 6X Loading dye, Promega cat.no. G190A

2.2 Methods

2.2.1 Cell culture

Cells were grown at 37°C, 5% CO_2 in DMEM complete medium. Cell passaging was done by treatment with 0.05% Trypsin – 0.02 % EDTA and seeded at appropriate dilutions.

Cell culture was done in aseptic conditions, cells were routinely screened for Mycoplasma contamination and new cell stocks were revived at regular intervals.

2.2.2 Whole genomeTranscription analysis

U2OS cells were seeded into 10cm plates, the next day, they were infected with TBEV at a MOI = 1, after one hour of infection with serum free medium, this medium was replaced with complete growth medium alone for the cells with just infection or complete medium plus TM in sterile treatment and infection and treatment with TM. RNA samples were then collected at 0, 10 and 24 hours post infection in EuroGOLD TriFast lysis buffer (EuroClone EMR 507100) and total RNA was extracted. Quality of extracted RNA was checked by spectrophotometric analysis (260/280>1.8) and Agilent bioanalyzer (RNA integrity number, RIN≥8). Our collaborator Danilo Licastro, CBM-Trieste performed further analyses and I report herein the protocol that was followed.

Briefly, cDNA libraries of polyA-containing mRNA molecules were prepared using Illumina TruSeq standard protocol. Libraries were pooled and sequenced on two different Illumina Platforms. The first run was performed on Hiseq2000 4-plex run single reads, 50 bp reads while the second run was performed on HiscanSQ 8-plex run pair-end reads, 2x100bp reads. All data were subjected to quality control using FastQC software.

Briefly, bioconductor packages DESeq2 version 1.4.5. and EdgeR version 3.6.2 in the framework of R software version 3.1.0 were used to perform differential gene expression analysis of RNA-seq data. Both packages are based on the negative binomial distribution (NB) to model the gene reads counts and shrinkage estimator to estimate the per-gene NB dispersion parameters.

Specifically, rounded gene counts were used as input and the per-gene NB dispersion parameter was estimated using the function DESeq for DESeq2 while, for edgeR the function calcNormFactors with the default parameters was used. To detect outlier data after normalization, R packages

Array Quality Metrix were used and before testing differential gene expression all genes with normalized counts below 14 were eliminated to improve testing power while maintaining type I error rates. Estimated p-values for each gene were adjusted using the Benjamini-Hochberg method. Genes with adjusted $P<0.05$ and absolute Logarithmic base 2-fold change > 1 were selected.

2.2.3 Ingenuity Pathway Analysis

Significantly changed genes (up-regulated, down-regulated, or both) were analyzed by Danilo Licastro using online bioinformatics tool Ingenuity Pathway Analysis (Qiagen). Direct relationships were included with experimentally observed or highly predicted confidence from human species. Canonical pathways, diseases and disorders, and molecular and cellular functions were analyzed.

2.2.4 Plasmid transformation

DH10β or DH5α competent cells were used for transformation of all plasmids in this study. Cells were incubated with the plasmids on ice for 30 min. They were then heat-shocked at 42°C for 40 seconds, left on ice for 2 minutes before addition of SOC medium. Cells were then incubated at 37°C for 1.5 hours before they were plated onto LB agar with the required antibiotic. They were grown overnight at 37°C.On the next day, selected colonies were picked and inoculated into 5 ml of LB medium containing the required antibiotic.

2.2.5 Plasmid DNA extraction

After approximately 12-15 hours, plasmid DNA was extracted using NucleoSpin Plasmid (Macherey-Nagel cat.no.1801/003) for minipreps and/or NucleoBond Xtra Midi (Macherey-Nagel cat. no. 1803/009) for midipreps. Extracted DNA was authenticated by restriction endonuclease digestion and sequencing. Restriction

endonucleases and their specific buffers were purchased from New England Biolabs (NEB).

2.2.6 Plasmid transfection

- **Lipofectamine LTX transfection**

Plasmids were transfected into U2OS cells using Lipofectamine™ LTX Reagent with PLUS™ Reagent (Invitrogen cat.no. 15338-100) according to a standard, optimized protocol. Transfection was done using reduced serum medium (Opti-MEM) and further grown in DMEM supplemented with 10% FBS.

- **Calcium Phosphate transfection**

Transfections for luciferase reporter assay were performed in HEK293T cells using a standard, optimized protocol. Transfection was done in DMEM supplemented with 10% FBS and further incubated at 37°C, 5% CO_2 until sample collection.

2.2.7 siRNA transfection of BiP

U2OS cells were reverse transfected that is cells were seeded onto the transfection mix. siRNAs used were at a concentration of 20nM and transfection was performed using Lipofectamine RNAiMAX transfection Reagent (Invitrogen cat.no. 13778-075) according to the manufacturer's instructions. Cells were then incubated at 37°C, 5% CO_2 in DMEM complete medium for 48 hours before infection with TBEV.

2.2.8 Flow Cytometry

Efficiency of transfection was checked for all experiments involving plasmid transfection. Cell monolayers were treated with 0.05 % Trypsin – 0.02 % EDTA to prepare single cells suspensions. Cells were then washed twice with PBS. For EGFP control, cells resuspended with 500µl PBS and immediately analyzed by flow cytometry.

Anti-SV5 and FLAG assays involved the fixation of cells with 3.7% paraformaldehyde (PFA) for 15 minutes at room temperature, followed by

centrifugation at 1000 rpm for 5 minutes followed by two washes, the first with a buffer made up of a 0.1% Tween 20 in PBS solution and the second with 1X PBS, at 1000 rpm for 5 minutes per wash.

Permeabilization was done by 0.05% Saponin-0.1% BSA solution incubated for 15 minutes at room temperature followed by two washes as described above for fixation.

Primary and secondary antibodies (anti-SV5/anti-FLAG or Alexa Fluor 488) were diluted in 0.1% Tween 20 in PBS solution. Anti-SV5 was used at 1:5000, anti-FLAG at 1:50 and Alexa Fluor 488 at 1:500 dilutions. Cells were incubated with primary antibodies for 30 minutes at room temperature followed by two washes. The same conditions were used for secondary incubation but without exposure to light followed by two washes as described previously.

Cells were finally resuspended in 500µl PBS and analyzed on a FACS Calibur machine (Becton Dickinson) and the Cell Quest Pro software.

Appropriate controls were employed every time including untreated cells and those only treated with the secondary antibodies as well as empty vector controls for normalization.

2.2.9 Infection and Tunicamycin treatment of Cells

- **Virus stocks**

  Neudoerfl strain of TBEV was used for all experiments reported herein.

  Viral stocks were prepared by infection of Vero cells at multiplicity of infection of 0.1. After observation of cytopathic effects (CPE), the supernatant was collected, clarified by centrifugation, supplemented with 20 % FBS, and stored in aliquots at -80°C. Viral titres were determined by using a plaque-forming assay.

When performing infection experiments, U2OS cells were seeded in a 12 well plate at an appropriate confluence. 24 hours later, cells were infected at multiplicity of infection (MOI=1) by adding 400µl of virus stock properly diluted in serum-free medium.

After 1 hour incubation at 37°C with 5%, CO2, the inoculum was replaced with DMEM supplemented with 4 % decomplemented FBS except for the condition of Tunicamycin treatment where at medium change, the medium contained 1µg/ml of Tunicamycin (Sigma-Aldrich cat. no. T7765-1MG) or 0.5mM of Tharpsigargin (Sigma-Aldrich cat. no. T9033-1MG). T0 (0 h.p.i) is the time after this first hour of incubation with the virus and subsequent time points are counted from this initial point. Control cells, mock infected and cells untreated with inducer(s) were also used.

2.2.10 Cell Lysis

Depending on the type of analysis to be performed, cells were lysed in one of the following lysis buffers:

- Laemmli Buffer (50 mM Tris-Cl pH 6.8, 2% SDS, 10% glycerol, 100 mM DTT, 0.1% bromophenol blue-Bio-Rad cat.no. 161-0404)
- RIPA buffer (50 mM Tris-Cl pH 7.5, 150 mM NaCl, 1% NP-40, 0.1% SDS, 1mM EDTA, 1mM EGTA, 1mM PMSF, 0.5% Sodium deoxycholate (Sigma-Aldrich cat.no. D6750-100G) and Proteinase Inhibitors (Roche - 11836170001) and Phosphatase Inhibitors: Sodium Fluoride (Riedel-deHaën 30105) and Sodium Orthovanadate (Sigma-Aldrich S6508-10G 028K0117)
- 5X Reporter Lysis Buffer (RLB) Promega cat.no. E397A, diluted to 1X for harvest of luciferase samples

2.2.11 Bradford Assay

Quantification of cell lysates was performed by Bradford assay. Briefly, 250µl of 1X Bio-Rad Protein Assay Dye reagent (Bio-Rad Laboratories GmbH cat.no.500-0006) was pipetted into clear 96-well plate according to the number of samples in duplicates. Known concentrations of BSA diluted from a 10mg/ml 100X stock (Promega cat.no. R396D 24122438) ranging from 0.5 to 4µg/µl were then added into respective wells, likely 2µl of cell lysates were added into respective wells. 1X Bio-Rad Protein Assay Dye reagent was used as blank. All samples were

carefully mixed by pipetting up and down and immediately read at wavelength 595 nm on a Wallac Envision 2104 Multilabel Plate Reader (Perkin Elmer). The known concentrations were used to plot a standard curve that was subsequently used to calculate the concentrations of unknown samples.

2.2.12 SDS PAGE

Whole cell lysates were resolved by SDS-PAGE at appropriate acrylamide percentages. The lysates were boiled at 95°C for 10 minutes, centrifuged for 1 minute at RT at 1000 rpm, and subsequently loaded into the acrylamide gel. Gels were run in SDS electrophoresis buffer, initially at 80V into the stacking gel and later at 140V into the running gel.

2.2.13 Western blot

Nitrocellulose membrane (GE Healthcare – cat.no. 10600015) was used at transfer at 350mA for 1.5 hours. Blocking was done for 1 hour in 5% milk/BSA depending on protein to be checked followed by incubation with appropriate primary antibodies diluted in 5% milk/BSA for 1 hour at room temperature or 4°C overnight (O/N) depending on antibody. Secondary antibodies conjugated with HRP (DakoCytomation – cat.no. P0447/8) were diluted in 5% milk/BSA depending on protein to be checked and blots were incubated for 1 hour at room temperature. Washes were done with TBS 0.5% Tween-20 solution. Blots were developed using Immobilon®Crescendo Western HRP Substrate (Millipore – cat. no. WBLUR0500) according to manufacturer's instructions.

2.2.14 Luciferase Assay

The luciferase assay to assess the IFNβ promoter activity resulting from co-transfection of NS2B and/or RIGI-N with IFNβ was performed using 250µl of 1X RLB per well of a 12-well plate. Cells were then scraped and harvested followed by freeze and thaw cycles in dry ice and room temperature respectively to facilitate cell lysis. A centrifugation step was then carried out at 12000g for 30 seconds and supernatants were collected and stored at -20°C until analysis.

For analysis, 50µl of Luciferase substrate was pipetted into white 96-well-plates

in duplicate followed by addition of 25µl of respective samples, 1X RLB buffer was used as a blank. Samples were mixed well and measurements of IFNβ-luciferase activity in cell lysates were performed using the Wallac Envision 2104 Multilabel Plate Reader (Perkin Elmer). All measurements were normalized to individual protein concentrations that were quantified with the Bradford assay method as described previously.

2.2.15 RNA extraction, cDNA synthesis and qRT-PCR

Samples for quantitative reverse transcription PCR (qRT-PCR) were lysed and collected with EuroGOLD TriFast buffer. Total cellular RNA was extracted according to the manufacturer's protocol. RNA samples were resuspended in autoclaved water and treated with DNase I recombinant, RNase Free Kit (Roche cat. no. 04716728001) before being quantified by a Thermo Scientific™ NanoDrop 2000.

500 ng of total RNA was then reverse transcribed using dNTPs (Promega cat. no. U144B), 150ng/µl random primers (Invitrogen cat.no. P/N 58875), 5X First Strand Buffer, 0.1M DTT and M-MLV Reverse Transcriptase (Invitrogen cat.no. 28025-013) RNase Inhibitor (Promega N2518), in a reaction mix.

Quantification of mRNA was obtained by real-time PCR using the 2X qPCR SyGreen Mix Separate ROX cat.no. PB20.14-05 qPCR kit (PCR BIOSYSTEMS) on a CFX96 Bio-Rad thermocycler. The different primers used are listed in Table 4. Analysis of relative gene expression was performed using the $2^{-\Delta\Delta CT}$ method of normalization (Livak and Schmittgen, 2001) with β-Actin as the housekeeping gene of choice.

2.2.16 XBP1 splicing RT PCR

cDNA was synthesized from 500ng total RNA samples as described previously. Subsequently, RT PCR was performed using the GoTaq®G2 Flexi DNA Polymerase kit (Promega cat.no. M7805). The amplicon spanning XBP1 splicing site was amplified using the Xbp1u Fw and Xbp1s Rv primers and GAPDH as control (Table 4) under the following conditions: 95 °C for 5 minutes, 95 °C 30 seconds, 60 °C 30 seconds, 72 °C

30 seconds for 35 cycles and 72°C 2 minutes. PCR products were run on a 2% Agarose gel for 45 minutes at 80V. Gel preparation: UltraPure™ Agarose powder (Invitrogen cat.no. 16500-500) melted in 0.5X TBE buffer and mixed with Ethidium Bromide-250ng/ml. Agarose gels were visualized using the UVIdoc HD2 gel documentation system (UVITEC Cambridge)

2.2.17 Plaque assay

Viral yields quantification was done by plaque assay using Vero cells. Cells were seeded in 24-well plates in on the first day. On the next day when the monolayer was formed, cells were infected in duplicate with a 10-fold serial dilution of TBEV in a total volume of 200µl of serum-free medium. After 1 hour incubation at 37°C, 5% CO_2, the inoculum was removed and a 1ml overlay containing 6% CMC and normal medium (DMEM supplemented with 4 % decomplemented FBS) at a ratio 1:1 was added. The cells were incubated for 5 days at 37°C, 5% CO_2.

To develop, the medium/CMC solution was removed, cells were then fixed with 3.7% PFA for 20 minutes at room temperature. Cells were stained with 1% crystal violet solution and incubated for 20 minutes at room temperature. After incubation, the staining solution was removed and cells were washed with water until the plaques were visible enough for counting.

Viral yields were determined by counting the average number of plaques formed in the duplicate wells and multiplied by the dilution factor.

2.3 Figures and Statistical Analysis

At least two independent experiments in triplicate repeats were conducted unless indicated otherwise. GraphPad Prism 7 for Mac OS X was used to generate all figures and perform all statistical analyses. Mean values are shown with standard deviation and p-values, measured with an unpaired two-tailed t-test or one-way ANOVA as indicated in figure legends. Significant p-values are denoted by asterisks ($p \leq 0.05$ = *; significant, $p \leq 0.01$=**; highly significant and $p \leq 0.001$ = ***; extremely significant). Where asterisks are missing the differences are not significant.

3.RESULTS

3.1 The UPR primes an earlier and more robust antiviral signaling

Our laboratory has extensively studied the UPR and its interplay with innate immunity. When I started my doctoral degree, I was involved in a team effort to make sense of a series of observations pointing at a role of the UPR in concert with the innate signaling system in priming the host cell in its response to flavivirus infection, boosting its antiviral activity.

The key observation was that in the course of TBEV infection, the UPR pathway is active as early as 8 hours after infection, while the interferon response occurred at later time points (starting from 16 hours). When this pathway is pre-activated by Tunicamycin, a commonly used UPR inducer that inhibits protein N-linked glycosylation, there is an up regulation of IFNβ (Fig. 11B) as well as virus inhibition not just for TBEV (Fig. 11A) but also for several other members of the Flaviviridae family such as WNV, DENV and ZIKV. Similar effects were observed also with another drug Thapsigargin (TG) that inhibits ER Ca^{2+}-dependent ATPase and depletes the ER Ca^{2+} supply (Fig. 11A, C).

The results of this work have been recently published and the paper is appended to this thesis for ease of reference. Although I have been involved in replicating several experiments pertaining to this work, which helped me develop essential skills in molecular biology and virology, I am reporting in this thesis only those where I have been the principal responsible scientist, as well as follow up unpublished experiments.

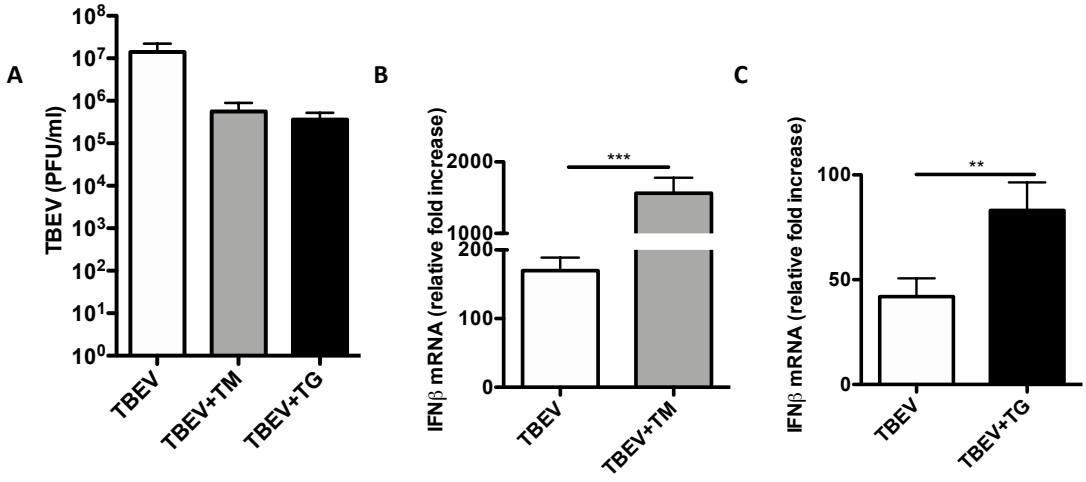

Figure 11: UPR inhibits TBEV and up regulates IFNβ: TBEV infection (white bars) and TBEV infection and treatment with either TM (grey bars) or TG (black bars) at 24 h.p.i A) TBEV yields in PFU/ml as quantified by plaque assay, B-C) IFNβ mRNA quantification by qRT-PCR on TM or TG treatments. Results presented as normalized to β-Actin and relative fold increase over T0 time point (**p≤0.01, ***p≤0.001 unpaired, student's t-test) – data obtained from Carletti and Zakaria *et al*., 2019

3.1.1 UPR inducers Tunicamycin and Tharpsigargin are not cytotoxic but cytostatic

Historically, most UPR studies employ the use of pharmaceutical inducers such as Tunicamycin (TM) and Tharpsigargin (TG); our studies on UPR are no different as can be seen from figure 10. However, majority of the said chemical inducers may act pleiotropically and this may probably have some effects to the cellular activities. This certainly depends on the concentrations and/or cell systems used.

To exclude any toxic effect of the UPR-inducing drugs and to ensure the reliability of our data obtained from routine use of the UPR inducers TM and TG, I took the initiative to test these two inducers' effects on cell growth and/or viability. The protocol implemented to perform this experiment imitated an infection experiment except the infection itself.

Briefly, as indicated in figure 12A, I seeded 50000 U2OS cells per well in a 12-well plate format; the next day, I removed the medium and added serum free medium for 1 hour like I would do in an infection experiment. After 1 hour, I added fresh complete medium to the mock control cells (U2OS) or complete

medium containing 1µg/ml TM or 0.5µM TG, concentrations that we routinely use for our experiments. After the one hour, I collected the T0 RNA samples and counted cells with Trypan blue. More samples were collected at time points 4, 8, 24 and 32 hours after treatment (subsequently referred to as T4, T8, T24, T32, T = time point). The time point beyond 24 hours was purposefully chosen to cover the infection cycle of flaviviruses that take longer than 24 hours.

When taking the cell counts, I took note of all dead and alive cells at the indicated time points to determine the percentage viability (Fig. 12C) and RNA was used in a qRT-PCR to check the expression of housekeeping genes β-Actin and GAPDH that we commonly use in our qRT-PCR analyses. This was to test whether the TM and TG had any effect on that as well.

As can be observed in figure 12B, the Mock control cells grew exponentially throughout the time course while cells treated with both TM and TG appeared to be somewhat stagnant between 0 and 8 hours but then grew consistently between 8 and 24 hours and even more between 24 and 32 even though at a slightly slower rate than the control cells. The restored growth pattern especially at 24 hours and forward is not unexpected and is quite consistent with the declining exposure of the drugs on cells as the time course progresses.

qRT-PCR of β-Actin and GAPDH revealed that the Cq values of both housekeeping genes ranged between 15 and 17 in all conditions except at 24 hours in the TG treatment where it rose to 19. When compared by a t-test, there was no significant difference between the average Cq values of both genes at all time points (Fig. 12D).

These results indicate that both TM and TG at the concentrations used in our experiments have a rather cytostatic effect on cell growth, since there was no substantial cell death as can be seen in the percentage viability plot (Fig. 12C). This suggests that at the concentrations used, TM and TG have a minimal detrimental effect if any on U2OS cells in the course of our experiments.

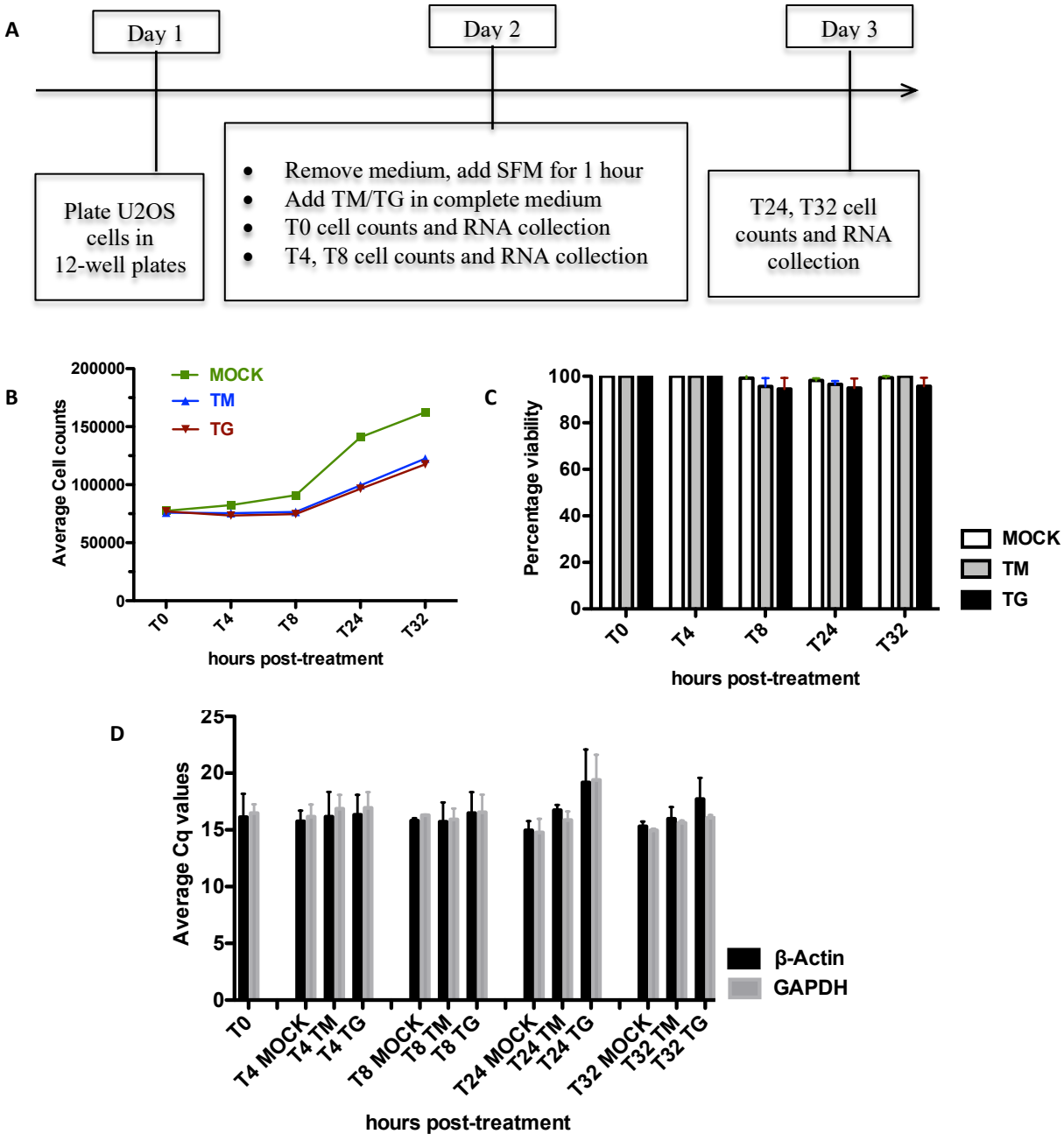

Figure 12: TM/TG cytotoxicity assay over the course of 32 hours A) schematic representation of experimental procedure B) Average cell counts of mock cells and cells under TM or TG treatment C) Percentage viability of cells counted in B, D) Average absolute Cq values of β-Actin (black bars) and GAPDH (grey bars) of mock cells and cells treated with TM or TG.

3.1.2 An antiviral signature characterizes the early UPR-driven antiviral response during TBEV infection

During TBEV infection, the kinetics of IFNβ activation are concomitant with IRF3 phosphorylation and its translocation to the nucleus in conditions of infection with a pre-activated UPR. While involving IRF3, this antiviral activity is independent of the canonical interferon signaling and IRF3 has additionally been implicated in other flaviviruses namely, DENV2, WNV and ZIKV. Specific to TBEV, the IRE1 arm of the UPR confers this antiviral activity and other arms may be valid for different viruses. These observations suggest a vital link between UPR and the cellular innate signaling and the two acting in concert to elicit a robust antiviral state against flavivirus infection. (Carletti and Zakaria *et al*., 2019).

The observation of UPR antiviral signaling being independent of the canonical IFN signaling and dependent on IRF3 instigated a whole genome transcriptome analysis (in collaboration with Dr. Danilo Licastro,CBM-Trieste,Italy) to better characterize this antiviral activity owed to UPR during TBEV infection.

The analysis was carried out on three groups of U2OS cells subjected to different treatments; first group was of cells on sterile Tunicamycin treatment (1µg/ml), second, cells only infected with TBEV and the third group, cells treated with TM and infected with TBEV, MOI = 1. All cells were subjected to their individual treatments for 8 hours, after which RNA samples were collected (Fig. 13A). RNA was extracted and checked for integrity and quality prior to analysis.

Three replicates for each condition were subjected to high-throughput RNA-Sequencing analysis and the data were analyzed using bioinformatics tools by Dr. Licastro as described in the Materials and Methods chapter.

An analysis with Ingenuity Pathway Analysis (IPA) revealed UPR as the most enriched pathway in the condition of sterile TM treatment as expected, and no pathway was particularly enriched in the condition of TBEV infection alone. However, in the condition of both TM treatment and TBEV infection, IPA revealed the following as the most up regulated pathways; “Activation of IRF by

cytosolic PRR", "Interferon signalling", "Role of PRRs in recognition of bacterial and viruses" and "Role of RIG-I like receptors in antiviral innate immunity".

Furthermore, a differential analysis was performed between the group of sterile TM treatment (UPR activation alone) and that of treatment and TBEV infection. This analysis revealed a set of 39 genes that were differentially modulated between the two conditions. Of these genes, 21 representing 53.8% of all genes were ISGs and were up regulated in the condition of both TBEV infection and TM treatment as observed in the heat map. (Fig. 13B – C).

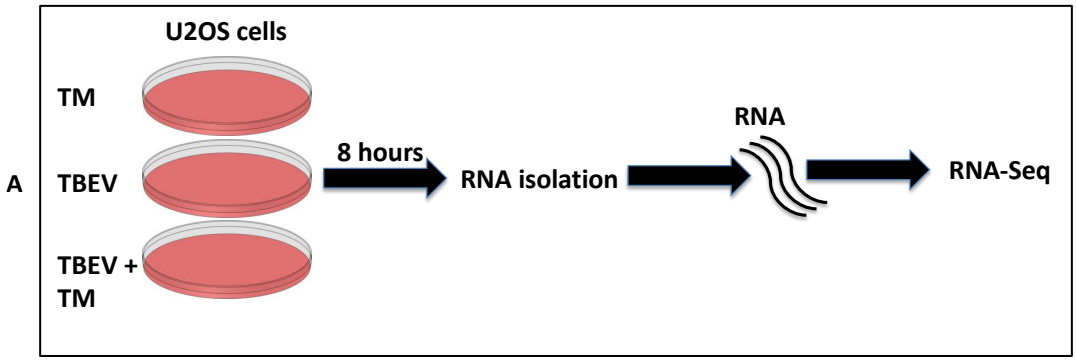

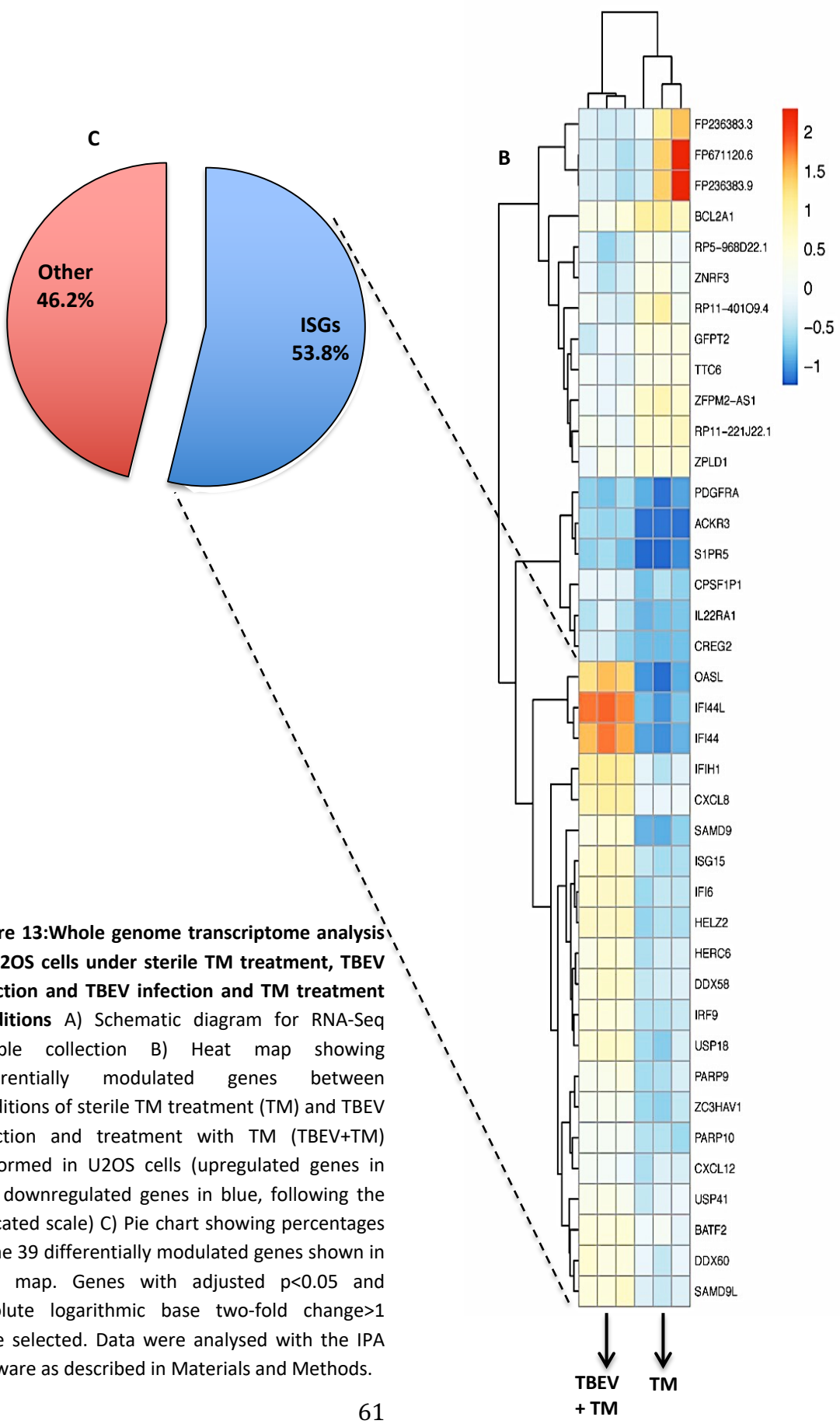

Figure 13:Whole genome transcriptome analysis of U2OS cells under sterile TM treatment, TBEV infection and TBEV infection and TM treatment conditions A) Schematic diagram for RNA-Seq sample collection B) Heat map showing differentially modulated genes between conditions of sterile TM treatment (TM) and TBEV infection and treatment with TM (TBEV+TM) performed in U2OS cells (upregulated genes in red, downregulated genes in blue, following the indicated scale) C) Pie chart showing percentages of the 39 differentially modulated genes shown in heat map. Genes with adjusted $p<0.05$ and absolute logarithmic base two-fold change>1 were selected. Data were analysed with the IPA software as described in Materials and Methods.

I followed up on the transcriptomic data (Figs. 13B, C) and validated the differential analysis findings by qRT-PCR. I followed the same experimental scheme as shown in figure 14A except that I collected samples at 10 hours and 24 hours after TBEV infection. As opposed to the 8-hour time point used in the transcriptomic analysis (Fig. 13), the 10-hour time point was used to reiterate the time points in a previous differential analysis (not reported herein) that showed UPR as a relevant up regulated response in the window of time between 10 and 24 hours. 10 hours when TBEV replication is already active but no induction of IFNβ, a delay strategy employed by TBEV and at 24 hours when both IFNβ induction and TBEV multiplication are detectable (Carletti and Zakaria *et al*., 2019). Clearly the events in the transcriptomic analysis (Fig. 13) at 8 hours are still relevant at 10 hours (Fig. 14) and this difference in time points is not at all consequential to the outcomes. From the 21 ISGs identified in the differential analysis (Fig. 13B), I chose the top 4 most up regulated genes namely: OASL, IFI44, IFI44L and IFIH1. Additionally, I tested for the induction of IFIT1 and Viperin, which are known broad antiviral ISGs that have been previously described as having antiviral activity towards several flaviviruses (Wacher *et al*., 2007; Vonderstein *et al*., 2017; Lindqvist *et al*., 2018)

The qRT-PCR data reiterated the differential analysis in that there was a significant induction of the analyzed ISGs in the condition of TBEV infection and treatment with TM (Fig. 14A-F) with OASL, IFIH1, IFIT1 and Viperin showing significant induction at both time points while IFI44 and IFI44L showing significant induction at the 10 hour and 24 hour time points, respectively. These results reinforced the results from the transcriptomic analysis on the fundamental role of ISGs in the UPR-driven antiviral state during TBEV infection.

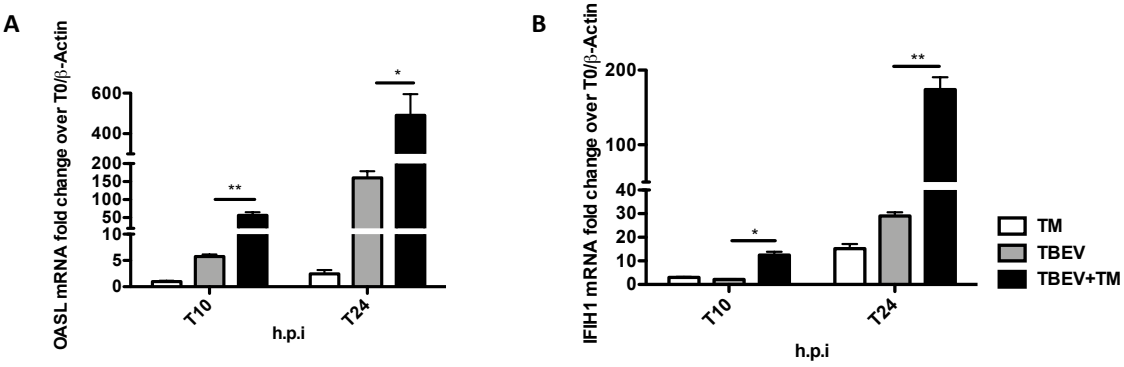

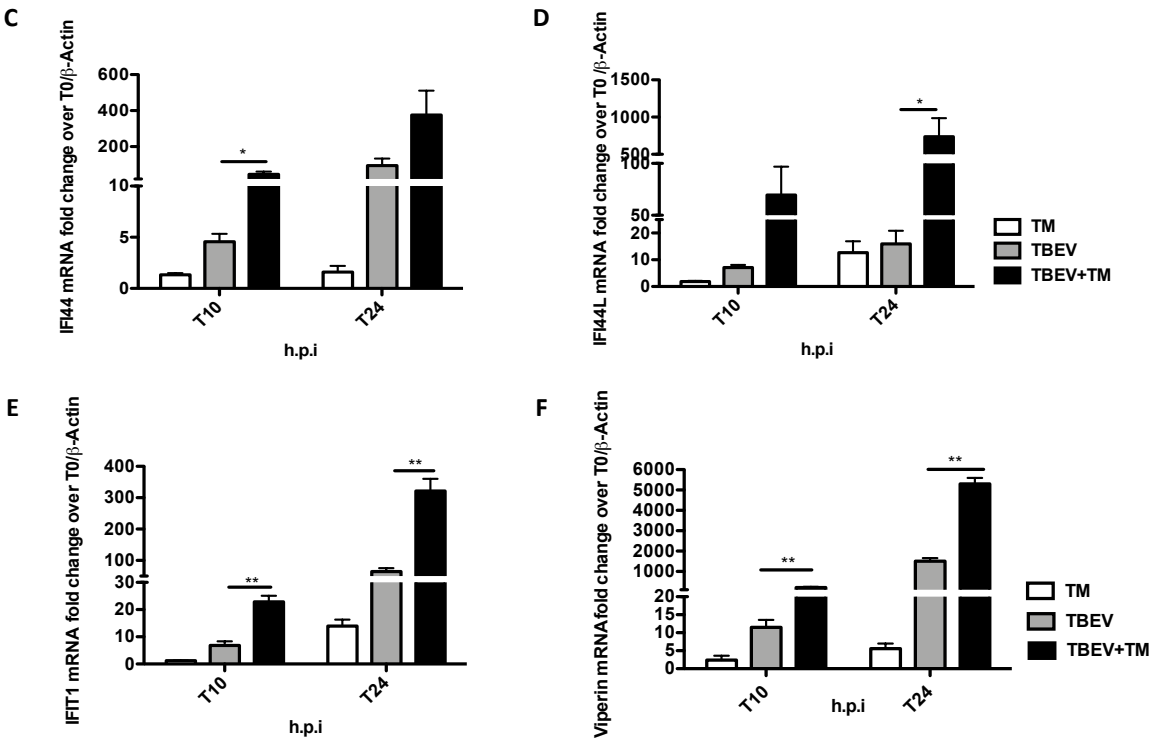

Figure 14: **Validation of selected ISGs from differential analysis (Fig.13)**; cells were subjected to conditions of sterile TM treatment (white bars), TBEV infection (grey bars) and TBEV infection and TM treatment (black bars) at 10 and 24 hours post infection. qRT-PCR quantification of A) OASL B) IFIH1 C) IFI44 D) IFI44L E) IFIT1 and F) Viperin. Results presented as normalized to β-Actin and fold change over the T0 time point (*p≤0.05, **p≤0.01, ***p≤0.001 unpaired, student's t-test).

3.2 Alternative methods of UPR induction

The results shown previously in figure 12 were certainly convincing enough of the minimal effects of TM and TG in our experimental settings. Nevertheless, I sought out to find alternatives that could possibly replace the use of pharmaceutical UPR inducers as employed from figures 11 to 14 and possibly recapitulate the observations in our previous results (Carletti and Zakaria *et al*., 2019). This was meant to reinforce our previous observations by using a different way of UPR induction but also to attempt that induction in a more organelle-specific manner that is by targeting the ER as opposed to what may be described as widespread/pleiotropic targeting by chemical inducers.

For these reasons, several approaches to induce ER stress and eventually UPR were explored and are reported herein.

3.2.1 UPR induction by depletion of the chaperone protein BiP

GRP78 alias BiP is the main ER chaperone that sequesters the three transmembrane proteins; ATF6, IRE1 and PERK that are principle effectors of UPR and dissociates from them under conditions of ER stress. Taking advantage of this fact, I attempted to deplete BiP and in essence on one hand, making it absent to handle the folding of the incoming protein load but also the elicitation of ER stress due to impairment and/or lack of the sequestration of the UPR effector proteins that is carried out by BiP.

To this end, I reverse-transfected U2OS cells with 20mM of small interfering RNA targeting BiP or the control siRNA following the manufacturer's protocol. After 48 hours of incubation at 37°C, I infected the cells with TBEV, MOI = 1, and collected supernatants, cell lysates and RNA samples at time points 0, 8 and 24 hours after infection.

The depletion of BiP by siRNA was confirmed by an anti-BiP western blot (Fig. 15A) and in this condition, while not as potent as TM, qRT-PCR analysis showed substantive induction of the spliced form of XBP1 and IFNβ mRNAs at all time points with increasing levels throughout the time course as compared to the siCTRL (Fig. 15B, C), suggestive of an active UPR and innate signaling just as has been observed in our previous results (Carletti and Zakaria *et al*., 2019).

XBP1s mRNA is considered the classical marker of an active IRE1, the most conserved arm of the UPR (Zhang *et al*., 2016) and is typically used as the readout for an active UPR.

It is important to note that this induction of XBP1s and IFNβ mRNAs at the T0 time point is purely a consequence of the depletion of BiP and not infection as this time point is only after 1 hour of infection.

However contrary to our previous observations, there was no difference in viral yields between the condition of BiP depletion and siCTRL, in fact, the yields were

similar in both conditions and both more than those observed in the condition of treatment with TM (Fig. 15D). A possible reason could be that as efficient as the knockdown was to induce XBP1s and IFNβ mRNA, this may not be efficient enough to reflect in virus inhibition.

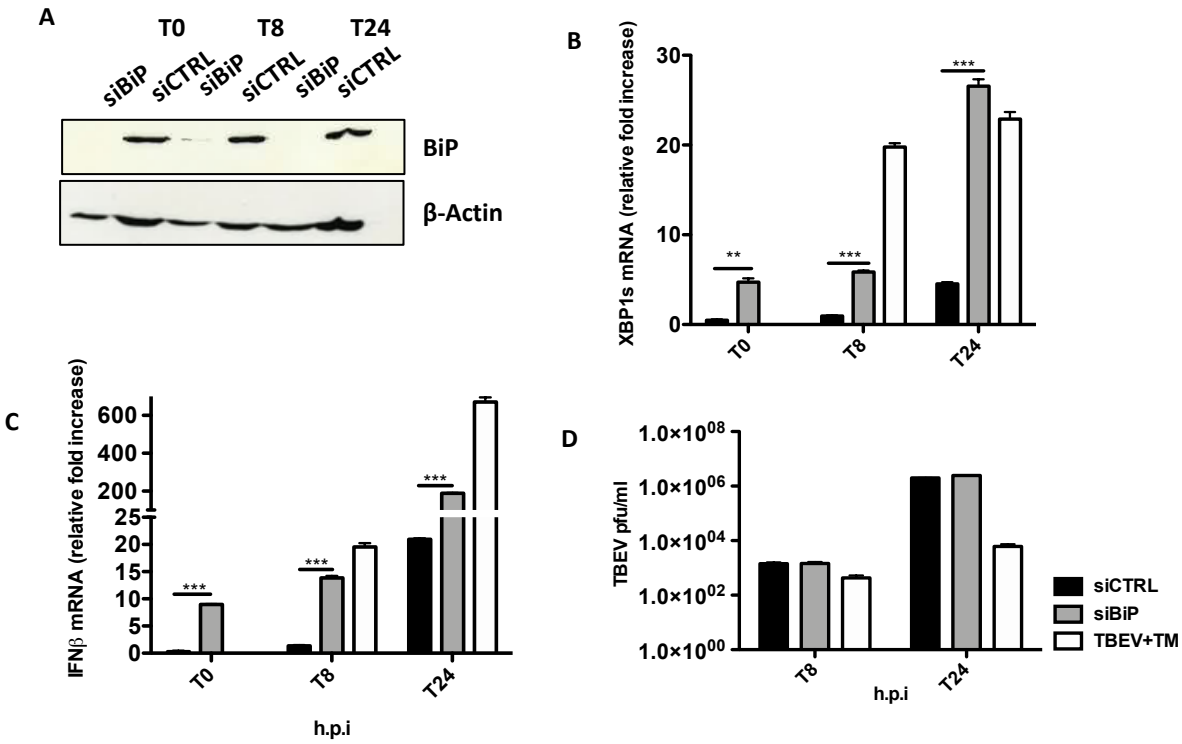

Figure 15: UPR induction by depletion of BiP followed by TBEV infection: siCTRL and TBEV infection (black bars), siBiP and TBEV infection (grey bars), TBEV infection and treatment with TM (white bars), A) Anti-BiP western blot confirming depletion of BiP by siRNA B) qRT-PCR quantification of spliced XBP1 and C) IFNβ mRNAs after BiP depletion and TBEV infection (results presented as normalized to β-Actin and fold change over siCTRL) D) Quantification of TBEV viral yields in PFU/ml as quantified by plaque assay after BiP depletion and TBEV infection (**p≤0.01, ***p≤0.001 unpaired, student's t-test)

3.2.2 Expression of BiP mutants does not induce UPR

Next I attempted inducing UPR by ectopic expression of two mutants of the chaperone protein BiP; namely G227D and T37G. These mutants are impaired in their ATPase-dependent nuclear binding domains; the ATPase activity is pivotal in the ability of BiP to fold nascent proteins that come into the ER. It was

therefore, plausible to reason that the mutants' impairment in protein folding would lead to an increase in the de novo protein load, thereby overloading the ER and in so doing, enable the induction of ER stress and then UPR.

To address this, I seeded 50000 U2OS cells per well of a 12-well plate, the next day I transfected the cells with 500ng of respective plasmids. Transfection was performed using Lipofectamine LTX following astandard, optimized protocol and after approximately 5 hours of incubation at 37°C, the transfection mix was replaced with complete medium and incubated further overnight. The positive control cells were treated with TM for the same amount of time as the transfected cells. After approximately 16 hours, I collected cell extracts and RNA samples. Cell lysates were analyzed for expression by western blot with anti-BiP antibody, while RNA was used for cDNA synthesis and analyzed by qRT-PCR for quantification of the spliced form of XBP1.

Efficiency of transfection was measured by flow cytometry and ranged between 50% and 65% for all constructs. Expression of the BiP proteins was confirmed by an anti-BiP western blot (Fig. 16A) and the difference in expression between ectopic expression and baseline levels as observed in the 3 controls (cells transfected with an empty vector, cells treated with Lipofectamine LTX alone and untreated U2OS cells) is quite obvious.

However, the mutants G227D and T37G were not able to sufficiently induce UPR as observed in the quantitative measurement of the mRNA of the spliced form of XBP1s showing minimal levels such as those seen in the BiP WT (Fig. 16B). This was also true for the induction of IFNβ mRNA (Fig. 16C). The minimal induction of IFNβ in the TM condition is consistent with what is expected in the condition of sterile treatment with TM i.e in the absence of infection (Fig. 14)

One possible reason for this result could be compensation in protein folding by the endogenous BiP in the case of BiP mutants' expression. A possibly more feasible approach could be to perform a co-transfection of the mutants and wild type BiP with a secretory protein and in this case, the protein folding ability or lack thereof in the case of the mutants would be more comparable.

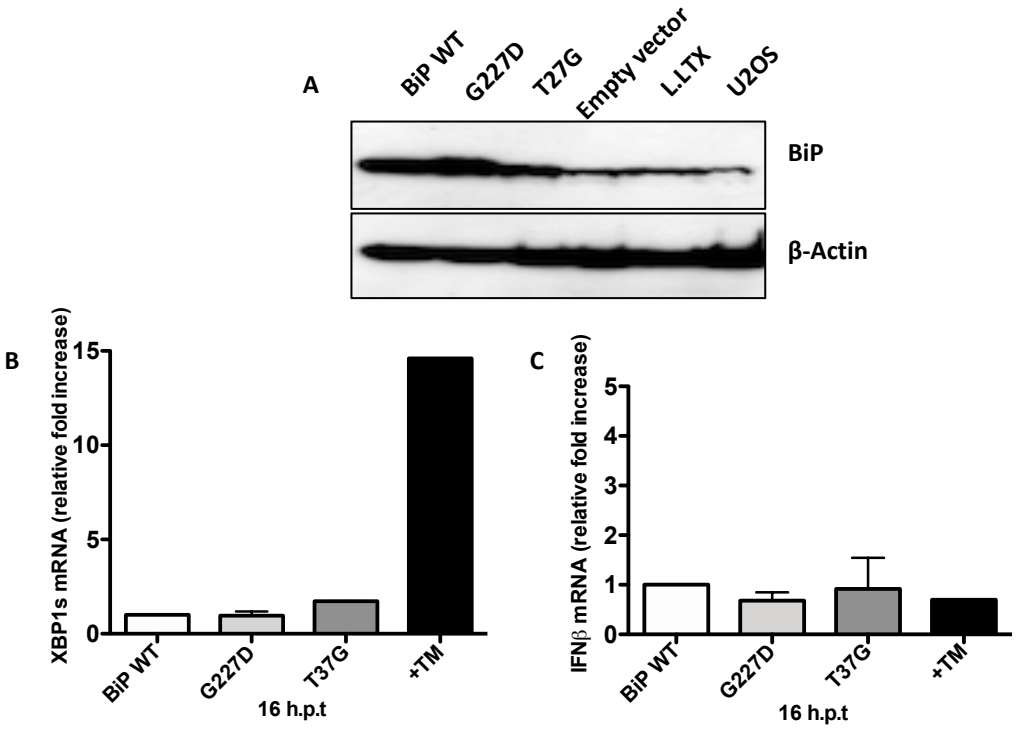

Figure 16: UPR induction by Expression of BiP mutants A) Anti-BiP western blot showing expression of BiP WT, G227D and T37G mutants B) Quantification of XBP1s mRNA after 16 hours transfection by qRT-PCR, reults presented as normalized to β-Actin and fold change over BiP WT (L.LTX=Lipofectamine LTX)

3.2.3 UPR induction by expression of Null Hong Kong

The next attempt involved yet again an ectopic expression approach only this time, it was of a verified UPR inducer; null-hong kong (NHK) a truncated mutant of the alpha 1 anti-trypsin (α1AT) that does not fold properly and therefore overloads the ER and induces the UPR (Ordóñez *et al*., 2013). While α1AT is completely secreted, NHK is considered secretion-incompetent and only a portion of it can be secreted.

To do this, I performed the experiment following the same scheme as in figure 16, this time transfecting SV5-tagged NHK or the control α1AT plasmids using Lipofectamine LTX and like before TM treatment was included as a positive control for UPR induction. Whole cell lysates were collected and tested for protein expression and secretion by anti-SV5 western blot while RNA was used for cDNA synthesis. Successively; these samples were analyzed for their ability to

induce UPR by quantification of the mRNA of XBP1s by qRT-PCR. An anti-SV5 flow cytometry analysis was also performed to check for transfection efficiency using a standardized protocol and results normalized to an empty vector. The transfection efficiencies ranged between 60% and 64% for all constructs.

Expression and secretion of both proteins was confirmed by an anti-SV5 western blot and a difference in size that reflects the difference in amino acids is clearly visible between α1AT and NHK, and only a small portion of NHK was secreted as is expected (Fig. 17A). And as previously documented in the literature, NHK seemed to significantly induce the spliced form of XBP1 (Fig. 17B) but not IFNβ mRNA (Fig. 17C).

While NHK could not induce significant IFNβ levels, its ability to significantly induce XBP1s prompted the next step which was a follow-up with TBEV infection to check whether in the condition of NHK expression and infection, there would be a UPR-driven inhibition of the virus as was observed in the case of infection and treatment with TM.

The same experimental scheme as in figures 17A-C was followed but with an additional step of infection on the following day. Whole cell lysates, supernatants and RNA were then collected at T0, T4, T12 and T24 time points and analyzed by anti-SV5 WB and qRT-PCR.

Upon infection, there was modest induction of IFNβ as a consequence of NHK transfection at T4 and T8, this induction was however not significant. Moreover, an up-regulation in the induction was observed at T24 most likely due to increasing virus multiplication and this was the case in all treatments (Fig. 17D). While this result was not supportive of our hypothetical model, I noticed a trend of modest inhibition of TBEV replication in the condition of expression of NHK from T12 (Fig. 17E), which like the induction of IFNβ mRNA in figure 17D was not significant.

Moreover, I was not able to reproduce this phenotype of the inhibition in TBEV replication in subsequent experiments even with further optimization of the experimental scheme in attempt to improve the efficiency of transfection even more than it was initially.

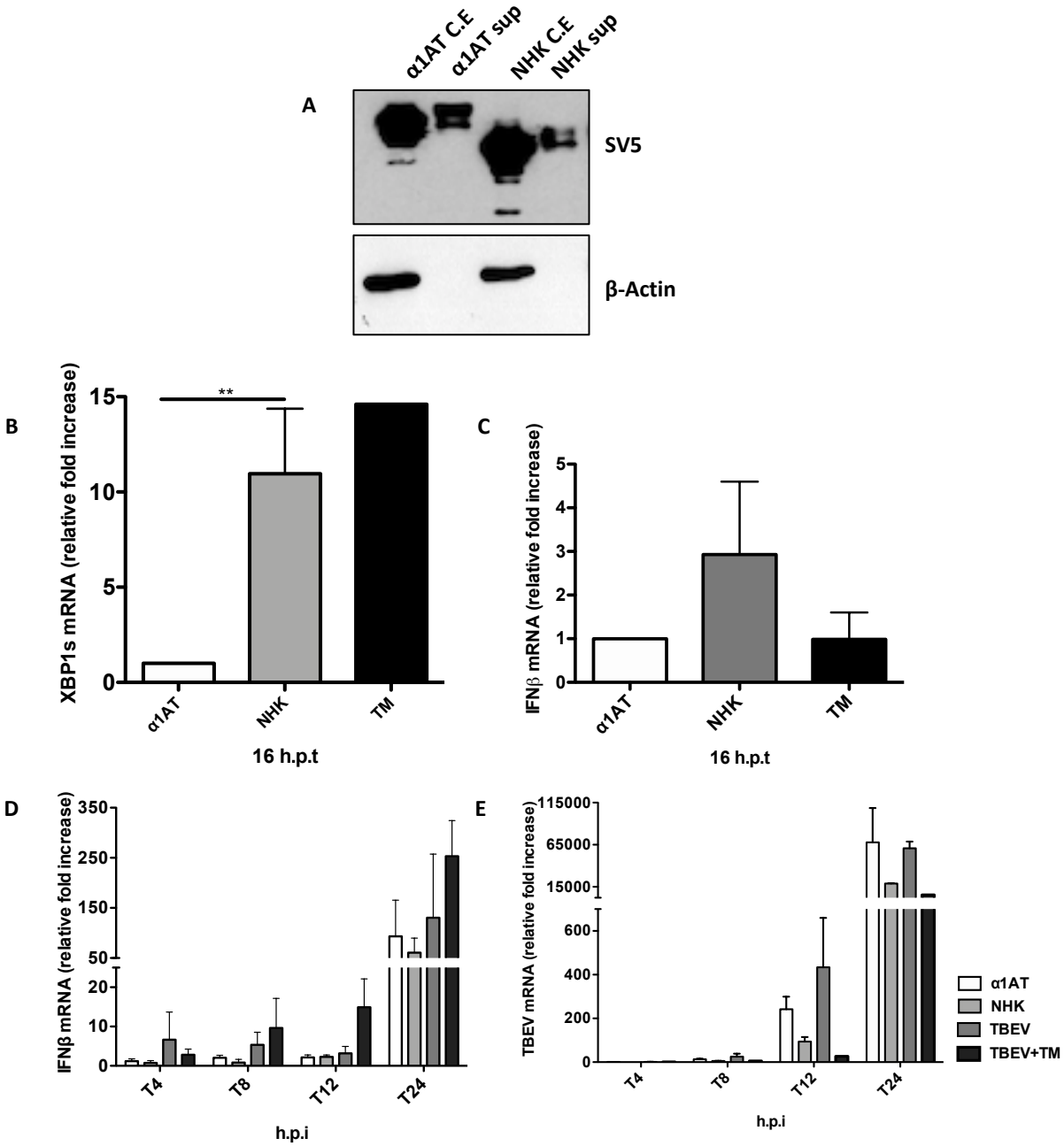

Figure 17: UPR induction by expression of Null Hong Kong A) Anti-SV5 western blot showing expression and secretion of α1AT and NHK B) qRT-PCR quantification of spliced XBP1 C) IFNβ and D) TBEV mRNAs in the conditions of infection with α1AT, NHK transfection or treatment with TM as positive control. Results presented as normalized to β-Actin and fold change over α1AT (A, B) or T0 time point (D, E). C.E=cell extract, sup= supernatant (**p≤0.01, student's t-test)

3.2.4 A screen of TBE viral proteins identifies some potent UPR inducers

Since previous attempts to induce UPR by inducing protein overload were deemed unsuccessful, I decided to shift my focus to the physiological route of UPR induction following TBE virus infection. From our previous observations and the literature, the process of infection occurs with an unscheduled overload of the viral proteins on the host cell's machinery and more specifically the ER, thus inducing stress and UPR. In TBEV infection, kinetics of UPR induction range between 8 and 12 hours after infection (Carletti and Zakaria *et al*., 2019).

By this logic, it was plausible to reason that ectopic expression of TBE viral proteins would also be able to induce the response like it happens during infection. An additional advantage to this approach was the possibility of identifying the viral component(s) that could be responsible for induction of UPR in the course of TBEV infection.

To accomplish this, I began by a screen of all TBE viral proteins to identify candidates for ER stress and UPR induction. All 3 structural and 7 non-structural proteins, a kind gift from Dr. Anna K. Överby; have been individually cloned in a high expression plasmid pl.18 and contain a FLAG tag (Table 3) at her lab in MIMS, Umeå Universitet, Sweden.

To do this, I performed the experiment following the same scheme as in the figures 15 and 16, this time transfecting each construct as well as an empty vector. Additionally, untreated cells (U2OS) and cells treated with TM were included as controls. After approximately 16 hours of transfection, whole cell lysates were collected for anti-FLAG WB and RNA samples for qRT-PCR analysis. Cells treated with TM for the same amount of time were used as a positive control. Assessment for transfection efficiency was performed by an anti-FLAG flow cytometry analysis and normalized to an empty vector. Transfection efficiencies ranged from 50% to 95% for all constructs.

All 10 viral proteins were expressed successfully as confirmed by an anti-FLAG western blot (Fig. 18A) and from the analysis of qRT-PCR data on the quantification of the spliced form of XBP1, 3 out of the 10 viral proteins E, NS1

and NS2B showed a significant induction either comparable or more than the positive control, TM (Fig. 18B). This was also true for the induction of IFNβ for the three proteins in addition to the prM protein (Fig. 18C). These results imply that the ectopic transfection of TBE viral proteins is a viable method of inducing UPR in U2OS cells and some of these proteins can activate the IRE1-XBP1 pathway of UPR and IFNβ mRNAs suggestive of an active UPR, specifically the IRE1 arm and innate signaling respectively.

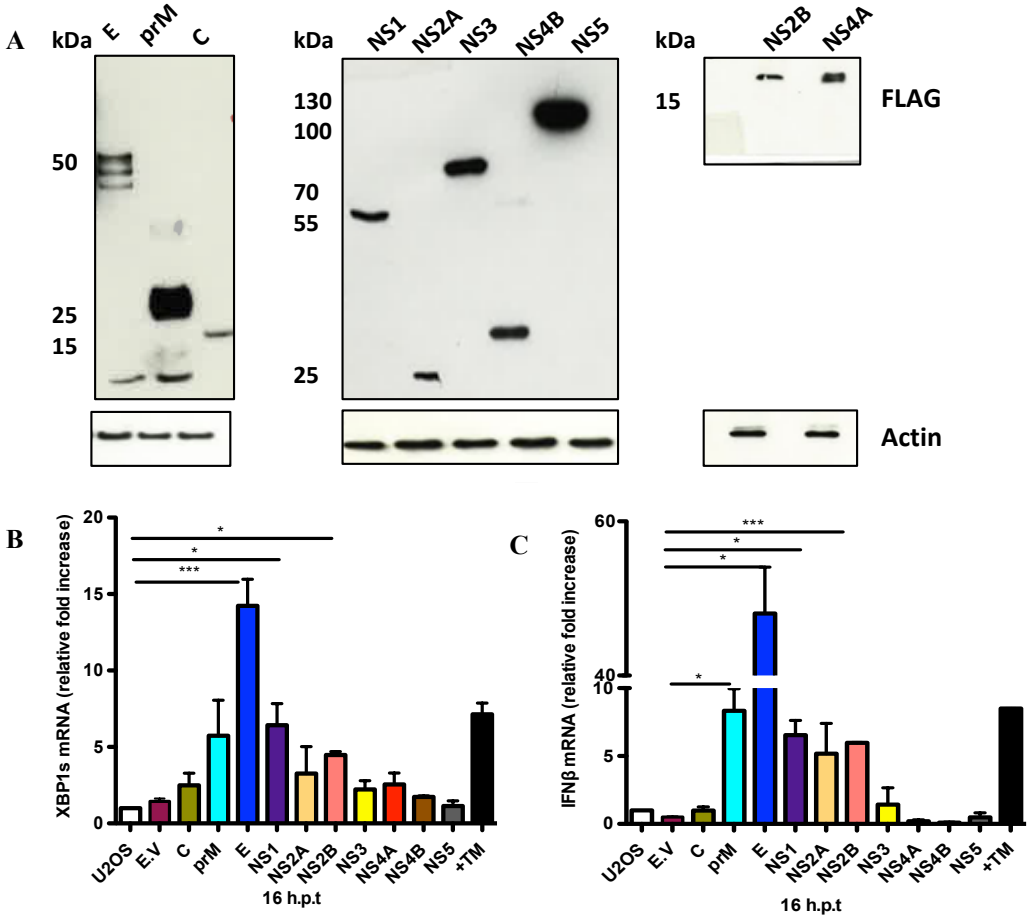

Figure 18: UPR induction by ectopic expression of TBE viral proteins: A) Anti-FLAG western blot showing expression of 10 TBE viral proteins B) spliced form of XBP1 and C) IFNβ mRNAs quantification by qRT-PCR, results presented as normalized to β-Actin and fold change over untreated U2OS cells – E.V= empty vector, (*p≤0.05, **p≤0.01, ***p≤0.001, one-way ANOVA test).

3.3 UPR induction and Innate signaling by candidate TBE proteins E, NS1 and NS2B

From the above findings, the identified TBEV viral proteins E, NS1 and NS2B were analyzed further in the context of UPR induction and innate signaling and then subjected to TBEV infection. The prM protein was not included in further investigation because while it could significantly induce IFNβ, the same wasn't true for XBP1s admittedly this could just be a consequence of varying efficiencies between experiments. Nonetheless, the fact that prM is a glycoprotein same as E and NS1 proteins as opposed to NS2B, the effects of UPR induction as a consequence of expression of a glycoprotein at least for the purposes of this study were more than adequately represented by the two. However, this is not to say prM should be completely omitted for investigation in other aspects pertaining to similar interests as those of this project. Although showing an upward trend in the induction of both XBP1s and IFNβ, NS2A was also disregarded from further analyses, as these inductions were not statistically significant (Fig. 18B, C)

As stated previously, E protein and NS1 are glycoproteins and ideally, during their formation require the endoplasmic reticulum where they undergo folding and further modifications in the Golgi before being secreted. This in essence also means their overexpression is therefore quite targeted and indeed more successful in overloading the ER, thereby inducing stress and ultimately resulting into the induction of the unfolded protein response.

Conversely, NS2B, being a transmembrane protein whose most widely studied function has been as the co-factor to NS3 and therefore contributing to protease activity of the NS2B3, poses some intrigue in its ability to induce UPR. This is partly due to its lack of properties for direct UPR induction as compared to the glycoproteins thus favoring an alternative mechanism of UPR induction.

3.3.1 Expression of TBEV E, NS1 and NS2B proteins induces UPR

The three candidate proteins (Fig. 18) identified from the screen of TBE viral proteins were expressed again in subsequent experiments (Fig. 19A) and tested initially for their ability to induce several UPR markers in addition to XBP1s.

As observed previously in the quantification of XBP1s by qRT-PCR (Fig. 18B), all three TBE viral proteins showed substantial splicing of XBP1 as compared to the empty vector by XBP1s mRNA quantification by qRT-PCR and by conventional RT-PCR for XBP1 splicing (Fig. 19B). XBP1s RT-PCR is a qualitative method of analyzing XBP1 splicing, the PCR is performed with primers that amplify both spliced and unspliced forms of XBP1. The two forms can then be observed as two bands or a single band on an agarose gel indicating splicing and therefore an active UPR and lack of it, respectively. The existence of the two bands in an event of splicing is due to a 26bp difference between the spliced and unspliced forms of XBP1. This method provides a visual advantage that adequately reiterates and/or complements the qRT-PCR quantification (schematic diagram of amplification by both methods: Fig. 19B, upper panel).

I additionally tested for EDEM1, a downstream marker of IRE1 activation and an ER-resident protein responsible for the disposal of misfolded proteins through the ER-associated degradation pathway (ERAD). EDEM1 was significantly induced by NS1 and NS2B as compared to the control (Fig. 19C), suggesting activation of the ERAD pathway at least by expression of these two TBE proteins.

It is a known fact that an increasing protein load to the ER leads to an up regulation of chaperone and co-chaperone proteins so as to increase the ER's protein folding capacity and bring back the ER homeostasis. For this reason, I tested for BiP, the major ER chaperone protein and a marker downstream of the UPR arm ATF6. Indeed, BiP was significantly up regulated by the expression of all three viral proteins (Fig. 19D) and so was the co-chaperone DNAJC3, a downstream effector of XBP1s (Fig. 19E). The PERK arm of UPR is responsible for protein translation halting and in cases of extreme ER stress, the pro-apoptotic protein CHOP alias DDIT3 is induced downstream of this pathway. As compared

to the control, the levels of CHOP/DDIT3, a pro-apoptotic protein and GADD34, a target protein for CHOP and a phosphatase that functions as a negative regulator of PERK through the dephosphorylation of eIF2α for protein translation halt recovery were significantly upregulated when all three proteins were expressed (Fig. 19F, G)

These results indicate an activation of not just IRE1-XBP1 pathway of UPR but also other UPR genes that implicate the other two arms of UPR by this approach albeit at varying levels of induction by individual TBE proteins.

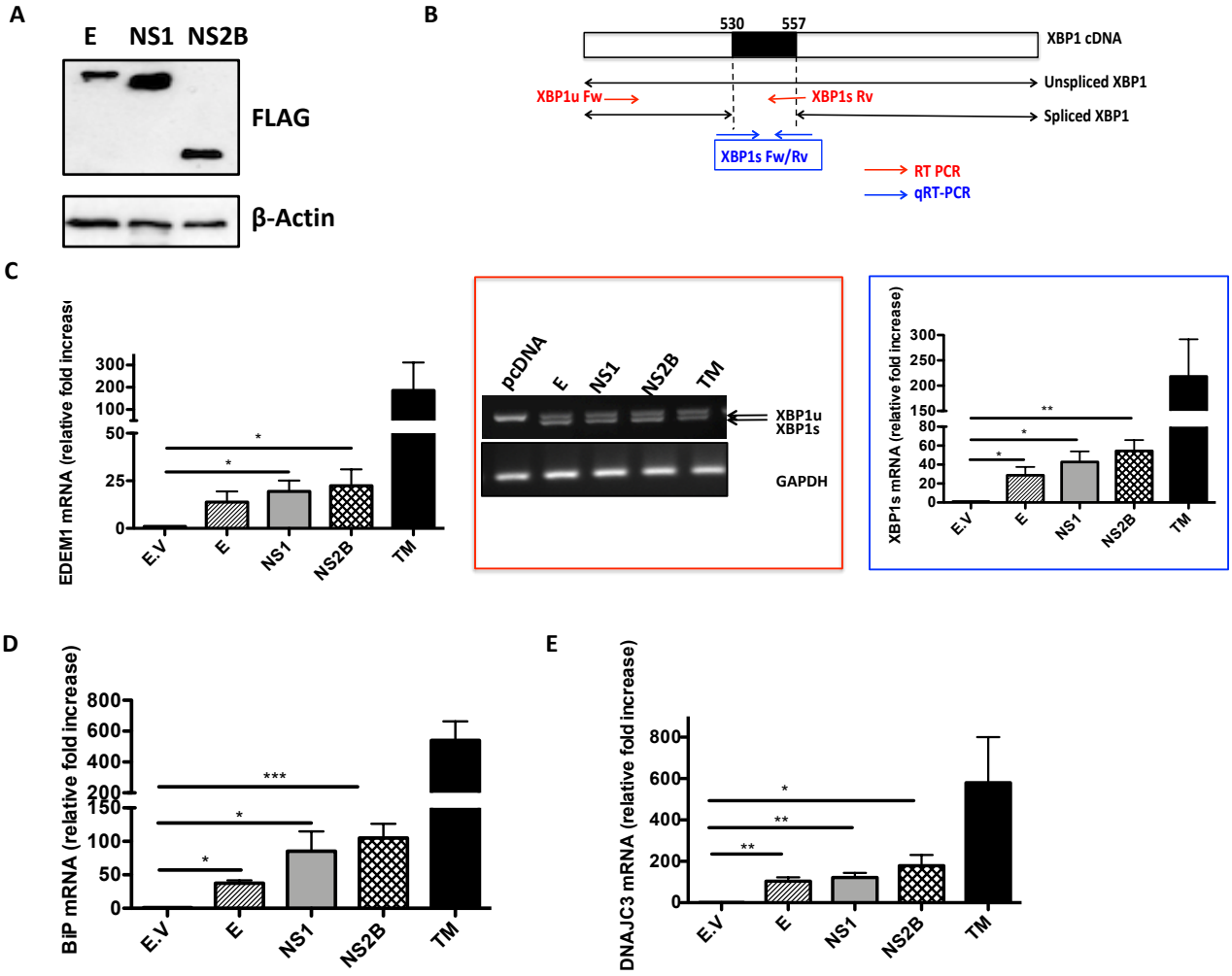

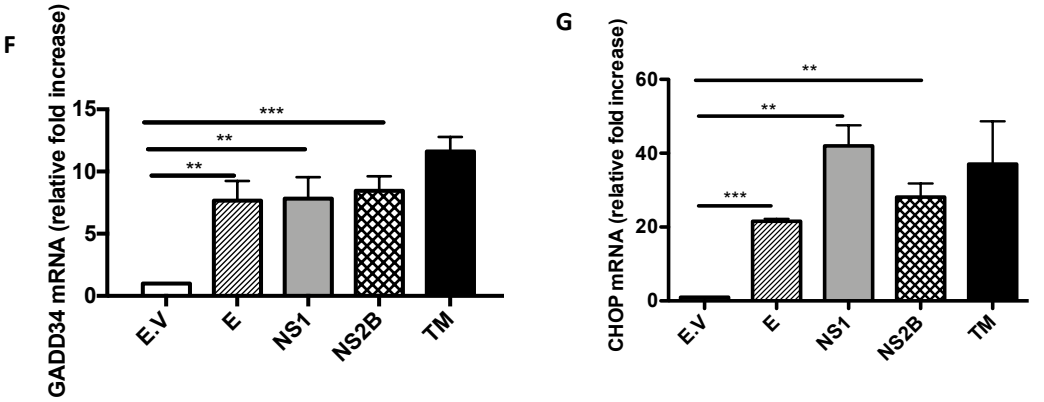

Figure 19: Expression of TBEV proteins E, NS1 and NS2B induces UPR A) Anti-FLAG western blot showing expression of E, NS1, NS2B B) XBP1 splicing; Upper panel; schematic presentation of RT-PCR and qRT-PCR (lower left, blue box) primer amplification of XBP1, Lower panel; Gel electrophoresis showing XBP1 splicing after RT-PCR (red box) and XBP1s mRNA quantification by qRT-PCR (blue box) C) EDEM1 D) BiP E) DNAJC3 F) CHOP/DDIT3 and G) GADD34 mRNAs quantification by qRT-PCR. Results presented as normalized to β-Actin and fold change over E.V = empty vector (*p≤0.05, **p≤0.01, ***p≤0.001 unpaired, student's t-test).

3.3.2 ISG induction in response to expression of TBE viral proteins

The UPR-driven antiviral signaling and maintenance of a robust antiviral state against TBEV is mediated by a subset of ISGs through IRF3 (Carletti and Zakaria *et al*., 2019). All the candidate proteins showed substantive potential in the induction of UPR (Fig. 19). Additionally, having observed that even 10 hours of sterile TM treatment can induce some amounts of antiviral ISGs (Fig. 14A-F) and the overall transfection time was approximately 16 hours, it was plausible to also check for the ability of the expression of the candidate proteins in inducing some antiviral ISGs. I selected from the strongest induced ISGs that were a result of the differential analysis in figure 13B, that is OASL, IFIH1/MDA5, IFI44, IFI44L (Fig.14A-D) as well as IFIT1 and Viperin (Fig. 14E, F) broad antiviral ISGs against flaviviruses.

Indeed, all three TBE proteins significantly induced Viperin, IFIT1 and IFI44 as compared to the empty vector control (Fig. 20A-C) while only NS2B was able to significantly induce IFI44L (Fig. 20D). However, the ISGs OASL and IFIH1 were not induced to any significant amounts by any of the viral proteins (Fig. 20E, F)

These results suggest a selective induction of ISGs by TBE E, NS1 and NS2B proteins with NS2B being the strongest of the three proteins in the induction of Viperin, IFIT1, IFI44 and IFI44L ISGs.

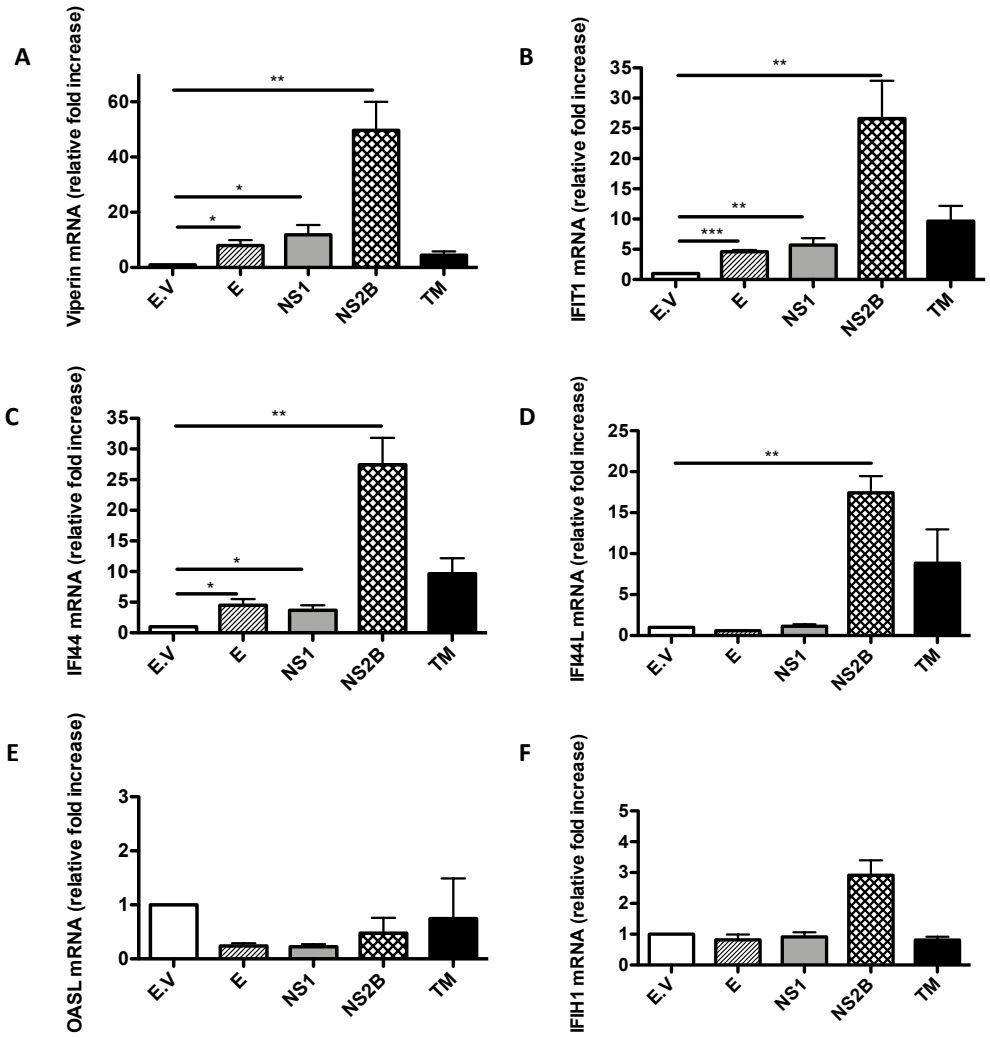

Figure 20: Expression of E, NS1 and NS2B leads to an induction of antiviral ISGs: qRT-PCR quantification of A) Viperin B) IFIT1 C) IFI44 D) IFI44L E) OASL and F) IFIH1 mRNAs. Results presented as normalized to β-Actin and fold change over E.V=empty vector (*p≤0.05, **p≤0.01, ***p≤0.001 unpaired, student's t-test)

3.4 Expression of E, NS1 and NS2B in the course of TBEV infection

The UPR-driven antiviral state translates into an up regulation of antiviral ISGs and inhibition of TBEV and other flaviviruses of clinical importance (Fig. 14, Carletti and Zakaria *et al*., 2019). In line with this, I performed a TBEV infection in a time course experiment in this system of UPR induction by ectopic expression of E, NS1 and NS2B TBE proteins.

3.4.1 Expression of E, NS1 and NS2B protein inhibits TBEV replication

The experimental scheme in this case followed the same procedure as the performed in figures 19 and 20 with an additional step of infection. After an overnight transfection, I infected the cells with TBEV, MOI = 1 and replaced the infection medium with complete medium after 1 hour of incubation. I then collected supernatants, RNA and cell extracts at time points 0, 4, 8 and 24 hours after infection (approximately 16, 20, 24 and 40 hours respectively after transfection).

500ng of RNA was used for cDNA synthesis followed by qRT-PCR quantification of TBEV mRNA and an anti-4G2 western blot for TBEV E protein expression was carried out. Supernatants were used to quantify viral yields by plaque assay as described in the Materials and Methods chapter.

After 8 hours of infection, there was a significant reduction of TBEV viral yields in the conditions of expression of E, NS1 and NS2B proteins as compared to the empty vector as well as untransfected cells. This was also true after 24 hours of infection, notably with increased virus production across all conditions as would be expected at this time point (Fig. 21A).

This phenotype is additionally corroborated with the decreased amounts of TBEV at the protein level as can be observed by an anti-4G2 western blot where in the conditions of ectopic expression of E, NS1 and NS2B at 24 h.p.i, TBEV E protein due to infection is less than that of empty vector and/or TBEV infection alone, whose amounts are quite comparable (Fig. 21B).

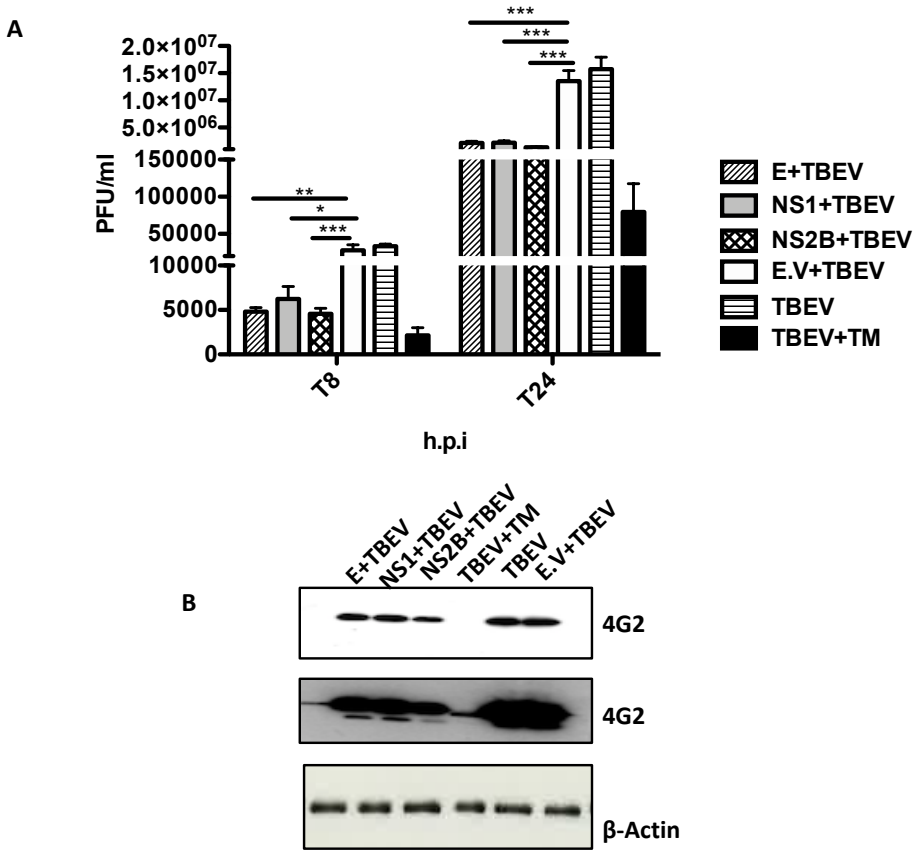

Figure 21: Expression of E, NS1 and NS2B inhibits TBEV A) TBEV yields quantification by plaque assay in PFU/ml C) Anti-4G2 western blot showing TBEV E protein expression at 24 h.p.i, middle panel inserted to show expression under TBEV+TM condition (*p≤0.05, **p≤0.01, ***p≤0.001 unpaired, student's t-test)

3.4.2 Expression of E, NS1 and NS2B proteins induces some antiviral ISGs during TBEV infection

The next set of experiments was prompted from the observations that TBE viral proteins E, NS1 and NS2B can induce both UPR and some antiviral ISGs (Fig.19, 20), but more importantly was the observation that there was TBEV inhibition in conditions of expression of the three proteins. I wanted to check whether this inhibition was due to a UPR-driven antiviral state that is facilitated by ISGs.

From the RNA samples in the experiment shown in figure 21, I tested for the same ISGs that were previously tested (Fig. 14, 20).

Generally, the expression was not as strong as was observed by transfection alone (Fig. 20) and this was to be expected due to an increased length of time since transfection because until the 24th hour post infection, it is approximately 40 hours of transfection and being a transient transfection, the number of transfectants are most likely dwindling at this point. Additionally, TBEV might have strategies to inhibit the expression of these antiviral genes, a state that is magnified and augmented with the increasing TBEV multiplication at this time point. It is therefore quite possible that at this time, the virus is overpowering the cell machinery in the experimental setting employed.

Despite this fact, there was notable induction of IFIT1, Viperin and IFI44L mRNAs by only NS2B as compared to the empty vector and/or untransfected cells at 4 and 8 hours after infection (Fig. 22A, B, C). Additionally, while transfection alone could not induce OASL (Fig. 20E), at 4 hours of infection, it showed an up-regulation trend by all three proteins but only significantly by NS2B (Fig. 22D). However, at 4 and 8 hours post infection, all proteins could sufficiently induce significant amounts of IFI44 (Fig. 22E) and IFIH1 was not induced by any of the proteins (Fig. 22F) like it was the case with transfection only (Fig. 20F)

Despite a general less expression as compared to transfection alone (Fig. 20), it seems that the ISGs induced by transfection of the proteins is maintained until few hours into infection (Fig. 22) and the effect is enough to inhibit TBEV even until 24 hours post-infection (Fig. 21).

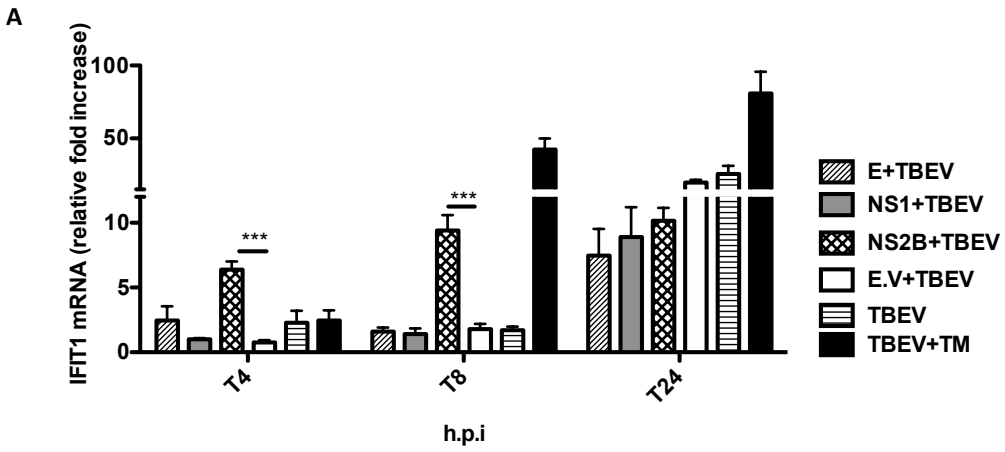

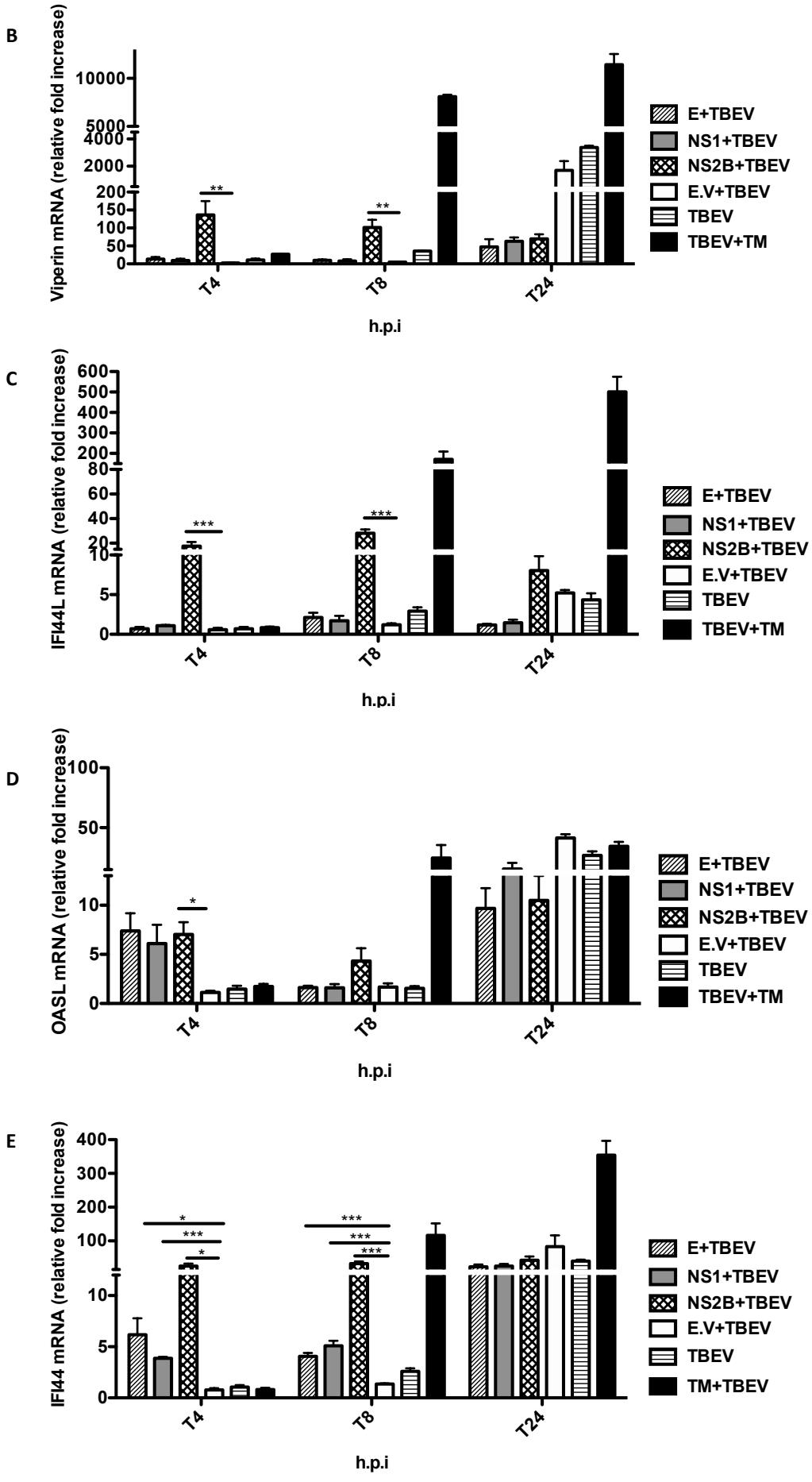
B
Viperin mRNA (relative fold increase)
10000
5000
4000
2000
200
150
100
50
0
**
**
T4
T8
T24
h.p.i
E+TBEV
NS1+TBEV
NS2B+TBEV
E.V+TBEV
TBEV
TBEV+TM
C
IFI44L mRNA (relative fold increase)
600
500
400
300
200
80
60
40
20
10
5
0
***
***
T4
T8
T24
h.p.i
E+TBEV
NS1+TBEV
NS2B+TBEV
E.V+TBEV
TBEV
TBEV+TM
D
OASL mRNA (relative fold increase)
100
50
10
5
0
*
T4
T8
T24
h.p.i
E+TBEV
NS1+TBEV
NS2B+TBEV
E.V+TBEV
TBEV
TBEV+TM
E
IFI44 mRNA (relative fold increase)
400
300
200
100
10
5
0
*
***
*
***
***
***
T4
T8
T24
h.p.i
E+TBEV
NS1+TBEV
NS2B+TBEV
E.V+TBEV
TBEV
TM+TBEV

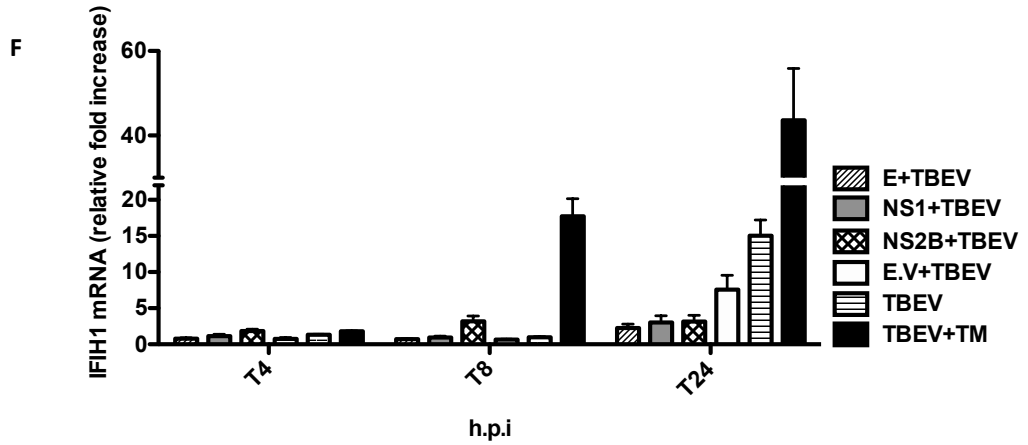

Figure 22: Expression of E, NS1 and NS2B proteins induces some antiviral ISGs during TBEV infection A) qRT-PCR quantification of IFIT1 B) Viperin C) IFI44L D) OASL E) IFI44 and F) IFIH1 mRNAs at 4, 8 and 24 time points after TBEV infection. Results presented as normalized to β-Actin and fold change over T0 time point. E.V=empty vector (*p≤0.05, **p≤0.01, ***p≤0.001 unpaired, student's t-test)

3.5 NS2B together with RIG-I augment IFNβ promoter activity

A successful innate response relies on the recognition of viral molecular signatures (PAMPs) by specialized cellular receptors (PRRs) that are unique to the said signature. After this recognition event ensues a signaling cascade that encompasses RLR conformational changes and a recruitment of an adaptor protein that is dictated by the initial signal. Adaptor proteins converge at IRFs such as NF-κB and in the case of TBEV, IRF3, the activation of which depends on its phosphorylation by kinases that are deployed in the cascade. The culmination of this complex series of events is the translocation of phosphorylated IRF3 that activates IFNβ molecules and consequently ISGs that are the actual antiviral effectors. However, some ISGs can be induced as a direct consequence of activated IRFs (Fig. 8).

RIG-I recognizes the dsRNA intermediates during TBEV infection. Induction of IFNβ and/or ISGs that characterize the UPR-driven antiviral state (Fig. 11,14) depends on IRF3 activation, which in retrospect depends on the initial PRR-PAMP recognition event and in this case, the RIG-I receptor. For this reason, it was plausible to check whether NS2B being the strongest ISG inducer (Fig. 20, 22), participates in the signaling and/or the mechanism of action of the IFNβ

promoter and the resulting effect on the promoter when expressed together with RIGI.

I took advantage of the well-studied IFNβ Luciferase reporter system and the high efficiencies of transfection that can be achieved in HEK293T cells since the readout is solely contingent on what is transfected into the cells and not any cellular responses. Briefly, HEK293T cells were transfected with plasmids encoding NS2B, RIG-I, or both together with a reporter plasmid carrying the firefly luciferase (Fluc) gene under the control of the IFNβ promoter. The same was done with an empty vector in place of NS2B. After an overnight transfection, cell lysates were collected at approximately 16 hours of total transfection time. In every experiment and/or analysis, all samples were analyzed in duplicates and the relative luciferase activity was normalized to total protein concentration in each condition. Total protein concentration was quantified by Bradford assay as described in the Materials and Methods chapter.

As can be observed in figure 23A, all transfected components were successfully expressed as confirmed by an anti-FLAG western blot. The IFNβ promoter activity was significantly up regulated when NS2B was transfected and even more so when only RIG-I was transfected. However, when both NS2B and RIG-I were co-transfected, there was a drastic increase in the IFNβ promoter activity, significantly more than either NS2B or RIG-I transfections alone (Fig. 23B). These results are indicative of an inherent ability of NS2B to potentiate RIG-I activity on the IFNβ promoter and innate signaling. Additionally, it accentuates the UPR-driven activity of NS2B and its role in innate signaling.

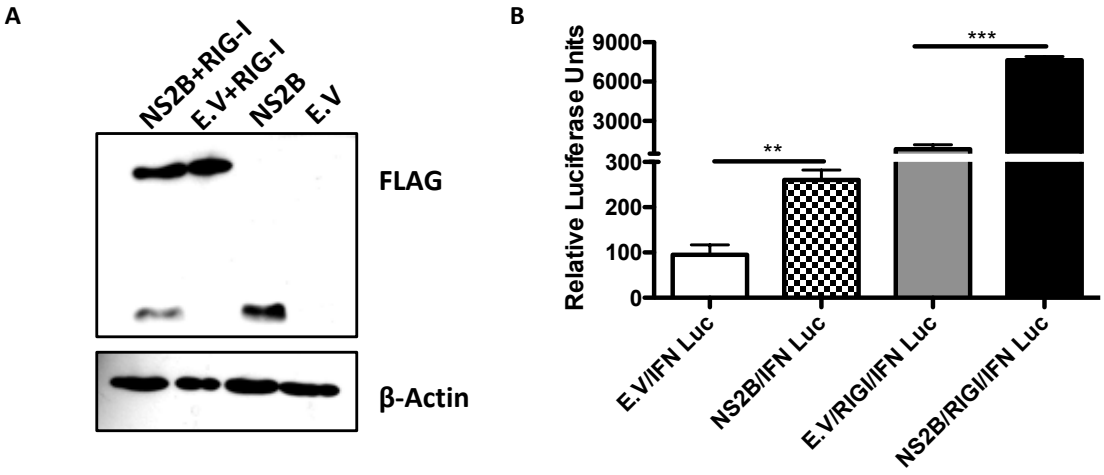

Figure 23: Expression of NS2B with RIG-I augments IFNβ promoter activity A) Anti-FLAG western blot showing expression of RIG-I and NS2B and B) Luciferase assay showing the IFNβ promoter activity after expression of NS2B and RIG-I expression, an empty vector (E.V) was used as a control. (**p≤0.01, ***p≤0.001 unpaired, student's t-test)

4.DISCUSSION

Flavivirus infections have devastated mankind at least since the 18th century with the record of the first dengue-like epidemic in Asia, Africa and North America between 1776 and 1780 (Gubler, 1998; 2002). Subsequently, the importance of Flaviviridae has increased well into the 21st century with over 40 discovered pathogens within the family causing a myriad of infections affecting global populations both in morbidity and mortality rates.

The struggle in the control of flaviviral infections is largely owed to the rapid evolving nature of viruses in general and even more so, RNA viruses. Viruses continuously evolve to evade host cell responses. The interplay between viruses and the innate immunity is therefore becoming excessively important, the understanding of which is fundamental in the search for sustainable control of viruses in terms of both vaccines and therapies.

4.1 UPR as an innate immunity signaler

UPR has been extensively studied as a homeostasis process to remediate consequences of ER stress. However, there is a vast wealth of knowledge implicating ER stress and several UPR genes in chronic non-communicable diseases ranging from diabetes to cancer as well as a multitude of autoimmune disorders (Morito and Nagata, 2012; Barrera *et al*., 2018; Madden *et al*., 2019, Walczak *et al*., 2019). Generally, the UPR is quite dynamic with different but systematically integrated actors orchestrating an attempt to recover ER homeostasis. Different ER stress stimuli at varying lengths of exposure activate different UPR sensor(s), in different kinetics and activation patterns. Ultimately, there's different signaling to the downstream effector UPR genes and put together all these factors define the fate of the cell (Hetz *et al*., 2015, 2018). This systematically designed system also somewhat applies to viruses in their ability to activate different arms and /or take advantage of one or more arms because the stimuli and other surrounding factors somewhat dictate the ultimate outcome.

In the recent past, the role of ER stress and UPR in infections and of particular interest viral infections is being actively explored. Viruses being dependent on

the host cell machinery disturb the functioning of the cell and particularly the ER. While serving as a remedial process, it is quite possible to imagine how the UPR can also be a danger signal in response to this disruption of cellular processes by viral infections. Indeed, it has been proposed that the UPR can act to potentiate immune system responses and specifically antiviral signaling (Smith, 2018)

This is the case in flaviviral infections and extensive studies in our laboratory have proven the central role of UPR in innate immune signaling. Infections with multiple flaviviruses, have shown an induction of UPR much earlier before innate signaling. Without any intervention, innate signaling only kicks in at around 16 hours after infection. However, when pre-activated, the UPR potentiates an earlier and more robust antiviral state that significantly inhibits clinically important flaviviruses (Carletti and Zakaria *et al*., 2019)

This is the basis of the study reported herein and sets the precedent on which this work builds on. My doctoral work has focused on UPR-induced antiviral signaling taking into consideration all our vital findings especially the strong induction of ISGs that plays a significant role of the antiviral signaling (Fig. 14) and indeed the involvement of RLR-sensing in this antiviral signaling that is owed to the UPR.

4.2 Pharmaceutical induction of UPR on cellular viability and growth.

Our findings presenting evidence to these facts have been obtained from experiments performed with chemical inducers of UPR. These are chemicals designed to disrupt the functioning of the endoplasmic reticulum and in doing so interrupting normal activity of the ER, inducing stress and ultimately the UPR. Chemical UPR inducers get this done seamlessly but in some cases their effects may be widespread and pleiotropic. For this reason, there is always some concern on what the drugs do to the general functioning of the cell but also to the antiviral activity that is inherent to some of these drugs such as Tunicamycin, which is a naturally occurring antibiotic active against several viruses, bacteria and fungi (Foufelle and Fromenty, 2016).

With that in mind my first task was to rule out any excessive cytotoxic effects of Tunicamycin and Tharpsigargin on cell growth. Ideally, any experimental outcome of a UPR study depends on but not limited to drug concentration, cellular system used, and more importantly the research questions to be answered. For the sake of our studies, the concentrations we use have to be strong enough to induce a notable UPR response without overshadowing the resulting antiviral response in that it has to be possible to distinctly separate the antiviral response that is a result of UPR from any activity that is intrinsic to the drug such as TM. Additionally, ours being infection experiments, the concentrations used should be ones that do not overpower the system; cells need to remain viable enough to support both cellular function and virus infection for the length of the time course.

I was able to show that the concentrations we use for both drugs indeed slow down the cell growth but without significantly impacting viability. Average cell viability ranged between 95% to 100% (Fig. 12C) and growth picked up over time in the course of 32 hours as was shown by cell counts (Fig. 12B). The same was true for the amplification of β-Actin and GAPDH genes (Fig. 12D). While the expression of these genes could be regulated differently in the presence of UPR inducers, the values were not variable compared to my untreated controls all through the time course except for GAPDH at 24 hours after treatment. This was eventually more like the other conditions at 32 hours and this difference was not significant. While this may have just been an odd spike that was probably inconsequential to qRT-PCR data normalization, subsequent data was normalized to β-Actin that was more consistent throughout the time course with the exception of XBP1s RT-PCR that used GAPDH as control (Fig. 19B).

4.3 The pursuit for alternative UPR induction methods

Next came the search for and testing of several alternatives for their ability to induce ER stress and UPR with an aim to eventually minimize or eliminate the use of pharmaceutical inducers that we, like the rest of the UPR field have been accustomed to. Eventually, to check whether this would recapitulate the

induction of antiviral signaling that was a product of UPR induction in the course of flavivirus infections (Carletti and Zakaria *et al*., 2019).

Simply put, ER stress and UPR induction happens when there is chaperone malfunction, impaired post-translational modification, difficult-to-fold client proteins (Marciniak *et al*., 2015) among other factors. In the classical model of ER stress and UPR activation, one or more of these factors ultimately leads to a rather direct increase in the intrinsic protein load. The same is true when the ER is provided with an ectopic load of unfolded and/or misfolded proteins. However, it has been suggested severally that activation of the IRE1 arm of the UPR may happen independently of this classical induction as would happen in B-cell development where the response is not due to secretory protein overload but rather a developmental switch as an anticipatory move to be ready for protein folding of the large incoming load (as reviewed by Walter and Ron, 2011). Sundaram *et al*., 2018 also observed a direct interaction of IRE1α with misfolded secretory proteins and activate preformed IRE1α complexes under conditions of ER stress, stressing on what would be a minor role of BiP in such cases.

The approaches and experiments reported herein have mostly relied on providing the ER with an overload of proteins aiming to imitate the classical model, but not omitting the possibility of an alternative model of UPR induction. What is more relevant however is whether this induction would translate into innate signaling and virus inhibition.

The depletion of BiP by siRNA (Fig. 15) while not as potent as TM was enough to induce significant XBP1s (Fig. 15B) seemingly in line with its function of the sequestration of UPR sensors. The same was true for the induction of IFNβ (Fig. 15C) as was our hypothetical model. However, on the contrary, the viral yields were the same for both the knockdown and control conditions (Fig. 15D). While not following the model to the letter, the increase in virus titres is not completely surprising; knock down of BiP has previously been shown to increase the replication of Hepatitis A virus (HAV), this effect was augmented when BiP was knocked out by CRISPR/Cas 9 in Huh7 cells (Jiang *et al*., 2017). The same has

been proposed for Hepatitis B virus whose titres increased when BiP was depleted in HepG2 cells (Ma *et al*., 2009; Zheng *et al*., 2017). While these studies were not interested in UPR, their findings may partially provide some insight into the observed increase in virus titres (Fig. 15D). Knocking down BiP is probably only enough to induce ER stress and then UPR but this induction is not enough to render the system competent to inhibit TBEV.

On the other hand, the use of BiP mutants could not induce XBP1s (Fig. 16B) or IFNβ (Fig. 16C). One explanation at least for the earlier would be the compensation by an up regulation of intrinsic BiP, other chaperones and co-chaperones in the case of expression of the mutants. This was an observation in a study by Luo *et al*., 2006 that showed an up regulation of PDI and GRP94 in $Grp78^{+/-}$ mutant mice when compared to their wild-type counterparts in a set-up where BiP activity was considered to be at about 50%. On the other hand, the role of endogenous BiP cannot be underscored either; transient transfection employed in this case was probably not enough to overcome the role of intrinsic BiP in protein folding. Experimentally though, the ER stress or UPR as measured in this experiment relied on XBP1s as the readout, taking into consideration the struggle with superior transfection efficiencies and what may be the role of endogenous BiP, another perhaps indirect UPR readout would probably be more appropriate. An experimental set-up that would allow a co-transfection of BiP and/or its mutants with a secretory protein would enable an assessment of the protein folding ability of the WT versus the mutants by quantifying not only the classical markers but also establish the collective amount of unfolded proteins bound to BiP which would probably be less in the WT than in the case of mutants. Such alternatives to study UPR have been reviewed by Lajoie *et al*., 2014.

Despite the possibilities and ideas outlined to improve the experimental set-up, I did not pursue this route of targeting BiP any further partly because of the challenge that I continuously experienced in transfection of U2OS cells as explained earlier which would make a co-transfection that much more limiting.

At the same time, I was looking into other approaches that at the time seemed more feasible.

The approach of expressing NHK to induce ER stress and UPR is largely supported by data based on study of diseases involving the serpin family of protease inhibitors and/or interest in ER stress in diseases specifically implicating the ERAD pathway. The overexpression of NHK, a cellular truncated mutant of α1AT has been shown to activate the XBP1-IRE1 pathway and is an appropriate substrate of ERAD, a pathway that serves to dispose off misfolded proteins (Hosokawa *et al*., 2001; Ordoñez *et al*., 2013; Jang *et al*., 2015). EDEM proteins play a major role in the first steps of substrate recognition of NHK and other misfolded proteins and this is crucial for efficient degradation in the ERAD pathway (Jang *et al*., 2015).

While also not as potent as TM, NHK expression was able to induce considerable XBP1s mRNA as compared to its wild type control (Fig. 17B) and this difference was complemented by the observation of more secreted α1AT than NHK suggesting its accumulation (Fig. 17A). However, there wasn't significant induction of IFNβ, which has previously characterized the UPR-driven immune response. This however was not reason enough to suspend further experiments considering that XBP1s was significantly induced which fulfilled the minimal requirement but also from previous experiments, TM and TG themselves can induce only minimal IFNβ in the absence of infection (Figs.14, 15C, 16C, 17C).

Upon infection, the lesser TBEV mRNA on expression of NHK as compared to α1AT was not significant and somewhat mirrored the induced IFNβ. In essence it is easy to think that the reduced TBEV mRNA trend observed is what caused the low IFNβ induction observed on expression of NHK (Fig. 17C, D) as opposed to an up regulation of IFNβ as a consequence of UPR that inhibits TBEV as observed in the TM positive control (Fig. 17E) and in previous experiments (Fig. 11B, C). As per our working hypothesis, UPR potentiates innate signalling that results to virus inhibition. This implies that success of the antiviral signalling and virus inhibition depends on and requires an active UPR. It has been previously established that dimers of NHK are much more aggregative than do monomers,

this is because ERAD has to disassemble dimers into monomers which are the actual substrates of EDEM proteins (Hosokawa *et al*., 2006) suggesting a longer retention of NHK dimers in the ER than its monomers. If the UPR observed in this experimental set-up on exogenous expression of NHK is due to monomer aggregates, it is plausible to speculate that the resulting response may be short-lived and probably not enough to translate into proper IFNβ induction and TBEV inhibition.

4.4 TBE viral proteins: viable UPR inducers

It is common knowledge that multiple viral infections result into the activation of ER stress (He, 2006; Asha and Sharma-Walia, 2018). RNA viruses are no exception; in fact, most of the recorded ER remodeling as a result of virus infections is due to positive-stranded RNA viruses because their replication and assembly relies almost exclusively on the ER. Replication factories for viruses are a product of ER membrane invaginations that eventually provide physical support during replication and viruses additionally use them as protective shields from innate sensors, a strategy adopted by multiple flaviviruses (Romero-Brey and Bartenschlager, 2016, Miorin *et al*., 2012, 2013). This evidence points to the obvious and vital relationship between flavivirus infection and the ER and a direct link to ER stress during viral infection. A great deal of literature exists providing insights into stress responses and UPR in the course of flavivirus infections, including but not limited to the ways different flaviviruses modulate the response, which of the three arms are activated in response to specific viruses and aspects surrounding apoptosis, autophagy and generally the relationships and/or interplays during infection which many times influence disease pathogenesis (Li *et al*., 2013; Yu *et al*., 2013;Blázquez et al., 2014; Perera *et al*., 2017; Gladwyn-Ng *et al*., 2018; Tan et al., 2018; Alfano *et al*., 2019; Zhao *et al*., 2019). And while there is no doubt on the induction of ER stress by viral infection, all this information opens up an avenue for the inquisition into what could be a specific viral protein(s) responsible for inducing the response. The

screen of TBE proteins as a way of inducing ER stress and UPR was therefore an approach presenting an opportunity for both at least in TBEV infection.

Indeed, ectopic expression of TBE viral proteins proved to be a feasible and worthwhile approach as it revealed multiple, viable candidates that could strongly induce ER stress and UPR, but also significant innate signaling (Fig. 18-20) same as was already observed in previous experiments that used pharmaceutical inducers of UPR (Fig. 14). While there isn't much available literature-wise, the search for and identification of viral proteins that induce ER stress is not a completely untapped area (Brunner *et al*., 2012; Fung *et al*., 2015; Frabutt *et al*., 2018; Siddiquey *et al*., 2018)

Glycoproteins such as E protein and NS1 being secretory proteins with a necessary requirement to go through the ER, provides them with a somewhat expected ability to induce ER stress in cases of ectopic expression, in fact, NS1 glycoproteins of JEV and DENV2 have been shown to increase XBP1 splicing (Yu *et al*., 2006). Frabutt and colleagues (2018) showed the induction of ER stress by an up regulation of BiP and XBP1s mRNAs after IAV infection. They followed up and showed the specific potency of IAV HA in inducing XBP1 splicing using a luciferase-based reporter assay to measure IRE1-mediated XBP1 activation in transient transfection of HAs of IAV H1 and H5 subtypes as well as Env glycoproteins of HIV-1 of NL43, JRFL, and SF162 strains using NHK as a positive control. This analysis further revealed the specific involvement of the ERAD pathway and highlights on the glycosylation aspect of the proteins regulating ER stress and specifically phosphorylation of IRE1α that defines the host response and pathogenesis (Hrincius *et al*.,2015; Frabutt and Zheng,2016).

The relevance of this is that different viral proteins of different viruses may indeed induce ER stress or fail to do so like was the case of some glycoproteins examined by Frabutt *et al*., 2018 and indeed in my analysis (Fig. 18). But more importantly, it stresses on how ER stress is central in defining infection outcomes and pathogeneses in viral infections which makes it that much more vital in our understanding of viral infections and even more so as we dissect some mechanistic aspects of the processes involved therein.

What seemed like an odd candidate in this screen though is the NS2B protein. NS2B is one of the 4 small, membrane-anchored proteins of flaviviruses and unlike the glycoproteins; it does not require the use of the ER like glycoproteins do in fact, its hydrophobic terminal regions function to anchor the NS2B3 protease to the ER membrane (Clum *et al*., 1997).

Admittedly, ectopic expression of NS2B may indeed cause an overload of proteins to the ER but this could be by a different mechanism as opposed to the glycoproteins, which have the biochemical attributes to suggest that they can directly overload the ER as described previously. While NS2B has not been well described in ER stress and UPR studies, NS2B3, the flavivirus protease complex responsible for several cleavages of the polyprotein has been observed to induce ER stress in DENV (Cheng *et al*., 2016) and much more than NS2B or NS3 alone (Yu *et al*., 2006). These two studies are both favoring the possibility of protease activity being involved in ER stress induction as opposed to what I have observed in my tests (Fig.18-19)

This begs the question as to whether NS2B induces the UPR in a mechanism different from the classical one and this aspect is worth looking into especially with the accumulating literature implicating some non-structural proteins in the formation of replication complexes that are the hallmark of ER membrane rearrangements that accompany infection (Leung *et al*., 2008; Rothan and Kumar, 2019) and even more specific to TBEV, a polyprotein made up of all non-structural proteins except NS5 has been proven to form replication complex-like structures independent of viral replication fortifying the knowledge that NS proteins drive the remodeling that accompanies infection at least in TBEV (Yau *et al*., 2019) NS2B proteins of DENV and JEV have been suggested to possess membrane permeability and destabilizing properties (Chang *et al*., 1999; León-Juárez *et al*., 2016). While membrane remodelling per se has not yet been proven to induce UPR, the above findings may contribute to some of the speculation that NS2B could be one of the non-structural proteins involved in ER membrane rearrangements during infection.

It is important to restate the emphasis of IRE1 pathway in all the analyses carried out in this work. The IRE1 arm is the most conserved UPR transducer in yeast, plants and metazoans (Maurel *et al*., 2014). Apart from XBP1s being the classical marker of UPR activation as stated previously, the IRE1 is the effector of choice in the UPR-driven antiviral activity in the course of TBEV infection albeit using a mechanism that does not rely on its RNase activity which leads to splicing of XBP1 and IRE1-dependent decay of RNA (Carletti and Zakaria, 2019). And while this is the current hypothesis, it is admissible to probe into the involvement of one or both of the other arms since this is a different way of UPR induction as compared to TM. Indeed, I observed an up regulation of XBP1s by two different methods as well as its downstream effector of the ERAD pathway, EDEM1 by all three proteins (Fig.18, 19B, C). The upregulation of BiP, DNAJC3, CHOP and GADD34 (Fig. 19) by all three proteins may suggest a partial involvement by more than the IRE1 arm but this observation would be more concrete if the phosphorylation of PERK and/or translocation of ATF6 would be analyzed in these conditions in future experiments pertaining to this work.

If indeed there is involvement of another arm of the UPR, this may be a consequence of individual expression of viral proteins as opposed to infection where multiple proteins may act in concert, modulating each other and somehow dampening or accentuating what could be an effect of a single protein as observed in this case and this logic goes for both induction of UPR as well as innate signaling.

4.5 UPR-driven Innate signaling by E, NS1 and NS2B

As discussed previously, the UPR is increasingly becoming important in innate signaling. An important aspect of the UPR-driven antiviral signaling during TBEV infection is the role played by ISGs. (Fig.14, Carletti and Zakaria, 2019). Some work has shown cross talks between certain arms of the UPR with the NF-κB pathway. Phosphorylation of eIF2α has been shown to activate canonical signaling of NF-κB, same as through the catalytic activity of IRE1 on treatment with TM or TG (Schmitz *et al*., 2018). Innate sensing that is UPR-driven or

modulated has been observed in multiple factors of the response suggesting an element of UPR being a danger signal in viral infection (Smith, 2014).

The induction of ISGs following expression of viral proteins (Fig. 20) is therefore not completely surprising especially after having confirmed that expression of these proteins can induce UPR (Figs. 18, 19). Same as is the case in HCMV where cytokine stimulation can be mediated by interactions between envelope entry proteins and TLR2 (Boehme *et al*., 2006), the ability of individual viral proteins to induce some innate response and even more when viral proteins are overexpressed is not completely unlikely.

The ISG induction after transfection of E protein, NS1 and NS2B while a significant observation, it was important to see whether this induction is maintained when cells were infected and more importantly if it inhibits the virus as was the case on infection and treatment with TM (Figs. 11, 14). Quite remarkably, the ISGs observed earlier (Fig. 19) are maintained for some time well into early hours of infection (Fig. 21), and visibly suppressing TBEV multiplication as analyzed by viral yield quantification and western blot (Fig. 22). Most notably is IFI44 that is induced by all 3 proteins after transfection until 8 hours after infection. The function of IFI44 is not well studied but has been shown to target HIV-1 LTR promoter activity facilitating viral latency (Power *et al*., 2015) and has additionally been speculated to be a natural homolog of Ribavirin, a potent known drug against HCV (Hallen *et al*., 2007). Ribavirin while quite potent in HCV inhibition, when tested in TBEV, it presented weak or no inhibition activity as opposed to other nucleoside analogues in the same studies (Eyer *et al*., 2015, Lenz *et al*., 2018). In addition to IFI44, induction of IFIT1 and Viperin (alias RSAD2) was observed during transfection, but this induction was only sustained by NS2B until 8 hours of infection with TBEV. IFIT1 and Viperin are well known broad antivirals against viruses beyond the Flaviviridae family (Helbig and Beard, 2014; Ng and Hiscox, 2018, Richard Lindqvist and Anna K. Överby, 2018) targeting viral protein synthesis and replication steps respectively (Fig. 7, Schoggins, 2019). IFI44L was only induced by NS2B on ectopic expression and this induction lasted until 8 hours of TBEV infection same as IFIT1 and Viperin.

Like IFI44, IFI44L is not a well-studied ISG but was identified in a FACS-based phenotypic screen of ISGs and proposed to have some antiviral activity against HCV (Schoggins *et al*., 2011; reviewed by Metz *et al*., 2013). It was also identified in a microarray analysis as one of the highly induced ISGs underlying inhibition of HIV-1replication by endogenous TRIM56 on treatment with IFNα (Kane *et al*., 2016).

Quite surprising though is OASL that is not induced with transfection but is significantly induced only at 4 hours after TBEV infection suggesting the possibility of involvement of an infection component in its induction, this induction proves to be a short-lived as it does not last longer than that. OASL belongs to the OAS family of ISGs, which in other mammals targets viral RNA for degradation by an enzyme RNAsel, which is lacking in humans. However, OASL has been suggested to promote antiviral activity by enhancing the sensitivity of RIG-I activation the sensor of dsRNA intermediates of infection (Zhu *et al*., 2014, 2015) and favoring replication for some DNA viruses (Ghosh *et al*., 2017; Bussey *et al*., 2018) suggesting a differential activity in different infections.

Whatever the mechanism of action and/or targets of these ISGs is beyond the current scope of this work but their collective effect seems to translate to TBEV inhibition and quite interestingly, while at 24 hours all the ISGs are not induced to any level of significance, the earlier effects of induction sustain TBEV inhibition until 24 hours after infection (Fig. 22). These results point to a role of ISGs in TBEV inhibition achieved by the UPR-driven activation by E, NS1 and NS2B proteins and pointing to NS2B as the protein with an ability of sustaining longer kinetics of ISG induction. Additionally, it brings forth IFI44 (Fig. 22E) as an important ISG that is induced by all the 3 proteins until 8 hours of infection and probably plays the most central role in TBEV inhibition at least in the conditions of E and NS1 expression (Fig. 21).

4.6 TBEV NS2B, more than just a protease cofactor?

A rather surprising aspect of this what work has been all the findings with NS2B (Fig.18-23). NS2B has stood out in its potency in inducing UPR and ISG induction

and presents us with an appealing and scarcely studied viral protein that future work may focus on.

Having observed some of the strongest effects on UPR induction and ISG induction in the condition of NS2B expression (Fig. 18-20), the ability of NS2B to increase the IFNβ reporter activity was just another piece to the puzzle that is NS2B (Fig. 23B). This effect was highly significant when NS2B was co-transfected with the sensor RIGI that is the PRR of choice in TBEV infections. The ability of certain viral proteins to initiate the first wave of innate signaling has been suggested in the past (Mogensen and Paludin, 2001) as it would seem is the case with NS2B. And while RIG-I is constitutively expressed, albeit at low levels, its expression is enhanced by activation of IFN-α/β signalling that is also the case when NS2B is transfected (Fig. 23A, B).

However, it would be interesting to understand the mechanism of action of NS2B and its link to the antiviral activity exhibited to a regulatory factor downstream of RLR-sensing such as IRF3.

4.7 Concluding Remarks

In my doctoral study, I embarked on a journey to analyze the effects of current UPR inducers to cell growth in the experimental settings employed for most experiments reported herein and find alternatives if any for ER stress and UPR induction.

The findings of this work have divulged a feasible approach of inducing UPR in U2OS cells using TBE viral proteins and in doing so gave us a way of narrowing down from 10 TBE viral proteins to what may be the culprits of UPR induction during infection. E protein, NS1 and NS2B proteins of TBEV may be the viral components that drive ER stress and UPR induction during TBEV infection. Moreover, they hold promise as tools to investigate the UPR in a more controlled, authentic stance and provide an alternative to the current pharmaceutical inducers.

The induction of UPR by these proteins is accompanied by innate immune signalling and TBEV inhibition, complementing quite well recent findings from our laboratory (Carletti and Zakaria *et al*., 2019) highlighting a key role played by ISGs in the UPR-induced antiviral state achieved by treatment with TM (Fig. 13), as is observed in the expression of E, NS1 and NS2B viral proteins (Figs. 19, 20)

Molecular mechanisms of action of these proteins in their induction of ER stress remains an area to be explored and while the mechanism of E protein and NS1 can be speculated, NS2B is rather more fascinating in this case. This will provide more insights on flavivirus NS2B as a stand-alone protein quite distinctly from how it has been known and studied in literature under the shadow of the NS2B3 protease complex.

NS2B brings forth even more the notion that non-structural proteins may be key players in membrane rearrangements that accompany infection. Whether membrane remodelling is enough to induce UPR independent of infection remains a question to be answered but this question offers one line of speculation as to how NS2B may induce ER stress and UPR. The established ability of NS2B to up regulate the IFNβ promoter activity (Fig. 22) adds to a role it

plays in the collective innate signalling that is observed on transfection of this protein.

Further probing into some of these aspects may be useful in establishing the mechanism(s) of UPR induction and innate signalling achieved on transfection of all proteins studied but even more so for NS2B, having confirmed that it acts in concert with RIG-I, the receptor of choice in TBEV infection.

These factors make NS2B subject to more investigation and may add more to the gap of knowledge in the study of membrane rearrangements that is a common feature among flaviviruses.

5.APPENDICES

Appendix 1:Carletti and Zakaria *et al*., 2019

Carletti, T., Zakaria, M. K., Faoro, V., Reale, L., Kazungu, Y., Licastro, D., and Marcello, A. 2019. Viral priming of cell intrinsic innate antiviral signaling by the unfolded protein response. *Nature Communications*, *10*(1), 3889. https://doi.org/10.1038/s41467-019-11663-2

nature COMMUNICATIONS

ARTICLE

https://doi.org/10.1038/s41467-019-11663-2 OPEN

Viral priming of cell intrinsic innate antiviral signaling by the unfolded protein response

Tea Carletti[1,4], Mohammad Khalid Zakaria[1,3,4], Valentina Faoro[1], Laura Reale[1], Yvette Kazungu[1], Danilo Licastro[2] & Alessandro Marcello[1]

The innate response to a pathogen is critical in determining the outcome of the infection. However, the interplay of different cellular responses that are activated following viral infection and their contribution to innate antiviral signalling has not been clearly established. This work shows that flaviviruses, including Dengue, Zika, West Nile and Tick-borne encephalitis viruses, activate the unfolded protein response before transcription of interferon regulatory factor 3 induced genes. Infection in conditions of unfolded protein response priming leads to early activation of innate antiviral responses and cell intrinsic inhibition of viral replication, which is interferon regulatory factor 3 dependent. These results demonstrate that the unfolded protein response is not only a physiological reaction of the cell to viral infection, but also synergizes with pattern recognition sensing to mount a potent antiviral response.

[1] Laboratory of Molecular Virology, International Centre for Genetic Engineering and Biotechnology (ICGEB), Trieste, Italy. [2] CBM scrl, Trieste, Italy. [3] Present address: The Pirbright Institute, Ash Road, Pirbright, Woking, Surrey GU24 0NF, United Kingdom. [4] These authors contributed equally: Tea Carletti, Mohammad Khalid Zakaria Correspondence and requests for materials should be addressed to A.M. (email: marcello@icgeb.org)

Flaviviruses are a family of relevant human pathogens delivered by mosquitoes or ticks. Dengue virus (DENV), Zika virus (ZIKV), West Nile virus (WNV), and tick-borne encephalitis virus (TBEV) are only few examples affecting tropical countries and Europe[1,2].

The genome of Flaviviruses is a single RNA filament of positive polarity encoding a polyprotein precursor, which is processed into structural and nonstructural proteins[3]. The RNA genome is replicated by the viral RNA-dependent RNA polymerase through a complementary template of negative polarity, which forms transient double-stranded RNA (dsRNA) intermediates. Infection induces important rearrangements of cytoplasmic membranes of the endoplasmic reticulum (ER) with the formation of characteristic replication vesicles containing dsRNA and replicative proteins[4–6].

Target cells respond to viral infection by activating innate defense mechanisms. Cytoplasmic pattern recognition receptors (PRRs) recognize viral RNA intermediates as pathogen-associated molecular patterns (PAMPs) to trigger the interferon (IFN)-mediated antiviral response[7]. The innate immune response is generally associated to the activity of IFN leading to the induction of interferon-stimulated genes (ISGs) endowed with antiviral activity. However, at very early time points post infection, cell intrinsic mechanisms of defense play an important role in mediating an antiviral response, while IFN remains essential to protect neighboring uninfected cells and to contain the spread of infection.

Virus infection can also lead to ER stress by unscheduled accumulation of viral proteins or modification of ER membranes. Accumulation of unfolded or misfolded proteins in the ER leads to a stress response by activating the unfolded protein response (UPR) pathway, which restores ER homeostasis[8,9]. Three transmembrane ER proteins mediate the UPR: the inositol-requiring enzyme 1 (IRE1), the protein kinase RNA-like ER kinase (PERK), and the activating transcription factor 6 (ATF6). Activated IRE1 cleaves the X-box binding protein 1 (XBP1) mRNA in the cytoplasm leading to the spliced form, which is translated into an active transcription factor (XBP1s). Activated PERK phosphorylates the eukaryotic translation initiation factor 2α (eIF2α) causing inhibition of protein synthesis, but also enhanced translation of the activating transcription factor 4 (ATF4). ATF4 in turn promotes transcription of several genes including the CCAAT/enhancer-binding protein-homologous protein (CHOP), a proapoptotic transcription factor, and feedback regulators, which counteract the phosphorylation of eIF2α. Activation of the ATF6 pathway leads to the processing of ATF6 into a cleaved product that translocate to the nucleus to activate UPR-regulated genes including Xbp1.

It has been previously shown that sterile co-stimulation of the UPR with certain PAMPs such as lipopolysaccharide or Polyinosinic:polycytidylic (poly I:C) acid greatly potentiates the expression of IFNβ[10–12]. These observations led to the intriguing hypothesis that UPR and PRR signaling synergize during infection to provide optimal antiviral immunity[13].

In this work, transcriptome analysis of TBEV infected cells shows upregulation of a number of genes involved in the UPR. Careful temporal analysis demonstrates that the IFN response is a late event preceded by the UPR. Most importantly, preactivation of the UPR during flavivirus infection causes a decrease of viral titers, an earlier induction of IRF3 phosphorylation and translocation, and of IFN and ISGs transcription. IRF3 depletion rescues flavivirus replication induced by UPR priming. Furthermore, depletion of IRE1, but not of ATF6 or PERK, enhance viral replication and rescue specifically TBEV from antiviral priming of the UPR. This IRE1 function is independent of its RNAse activity, but dependent on IRF3 and RIG-I. Hence, these data demonstrate that the UPR is a very early cellular response to TBEV infection, which triggers an IRF3/RIG-I dependent cell intrinsic antiviral response through IRE1.

Results

Transcriptome analysis of TBEV infection. In previous studies a consistent delay of the IFN beta (IFNβ) response, following flavivirus infection, was described[14,15]. Viral replication could be detected as early as 8 h post-infection (h.p.i.), while IFNβ mRNA appeared only after 16 h.p.i. Starting from this observation, in order to investigate the cellular pathways that could be activated in the infected cells before IFNβ induction, an unbiased transcriptome analysis of infected cells was conducted. Newly synthesized TBEV RNA was already high as early as 10 h.p.i., a time point, when IFNβ mRNA could not be detected. As expected, IFNβ mRNA was eventually upregulated at 24 h.p.i. These two time points were chosen to conduct the transcriptome analysis of the infected cells. Total RNA was extracted from infected cells in triplicate independent experiments and subjected to high-content sequencing. Differential analysis of the transcriptome of U2OS cells infected with TBEV at 24 versus 10 h.p.i. showed significant upregulation of 437 genes (fold change ≥2) and downregulation of 318 genes (fold change ≤2) with a false discovery rate of <0.05 (DESEQ2 statistical analysis) (Fig. 1a). Ingenuity Pathway Analysis (IPA) indicated the UPR as the most highly significant canonical pathway (−log (*p*-value) = 7.37) followed by ER stress (−log (*p*-value) = 3.93). Several genes showed upregulation, including *HSPA5* (Heat-Shock 70 kDa Protein 5, *BiP*), *Xbp1/Xbp1s*, *DDIT3* (CHOP), and the chaperones DnaJ (Hsp40) Homolog, Subfamily C, Member 3 (*DNAJC3/P58IPK*), and Subfamily B, Member 9 (*DNAJB9*). To conclude, significant early activation of UPR-related genes was observed during TBEV infection.

UPR is induced before the interferon response following infection. The kinetics of UPR induction was analyzed temporally following TBEV infection. As shown in Fig. 1, TBEV infection of U2OS cells was productive as early as 10 h.p.i. (Fig. 1b) with TBEV RNA being detectable at 8 h.p.i. (Fig. 1c). At variance, IFNβ mRNA appears only after 16 h.p.i. (Fig. 1d). UPR genes such as *Xbp1*, *DNAJC3*, and *DNAJB9* also appear at late time points, concomitantly with IFNβ mRNA (Fig. 1e and Supplementary Fig. 1A and 1B). However, the spliced form of Xbp1 mRNA, an indicator of IRE1 activation, could be detected as early as 12 h.p.i. (Fig. 1f). Similarly, the PERK-dependent activation of CHOP occurred before the IFNβ response (Fig. 1g). Indeed, PERK phosphorylation could be detected at 8 h.p.i. followed by phosphorylation of the eIF2α (Fig. 1h). The third arm of the UPR response is initiated by nuclear translocation of ATF6. To monitor the ATF6 pathway, GFP-ATF6 was transfected in U2OS cells followed by TBEV infection[16]. As shown in Supplementary Fig. 1C and quantified in Fig. 1i, translocation of GFP-ATF6 into the nucleus of infected cells occurred from 8–12 h.p.i. Consistently, UPR genes that are activated downstream of the ATF6 pathway, such as *BiP* (Fig. 1j), were also induced following TBEV infection.

Induction of UPR leads to early activation of an innate antiviral response during flavivirus infection. To summarize the above findings, all three arms of the UPR were activated at early time points following TBEV infection, prior to IFNβ induction. Therefore, the UPR could be a prerequisite for a proper antiviral response. To address this hypothesis, U2OS cells were exposed to Tunicamycin (TM), a well-known inducer of the UPR, immediately after TBEV infection. As shown in Fig. 2a, b, viral yields and

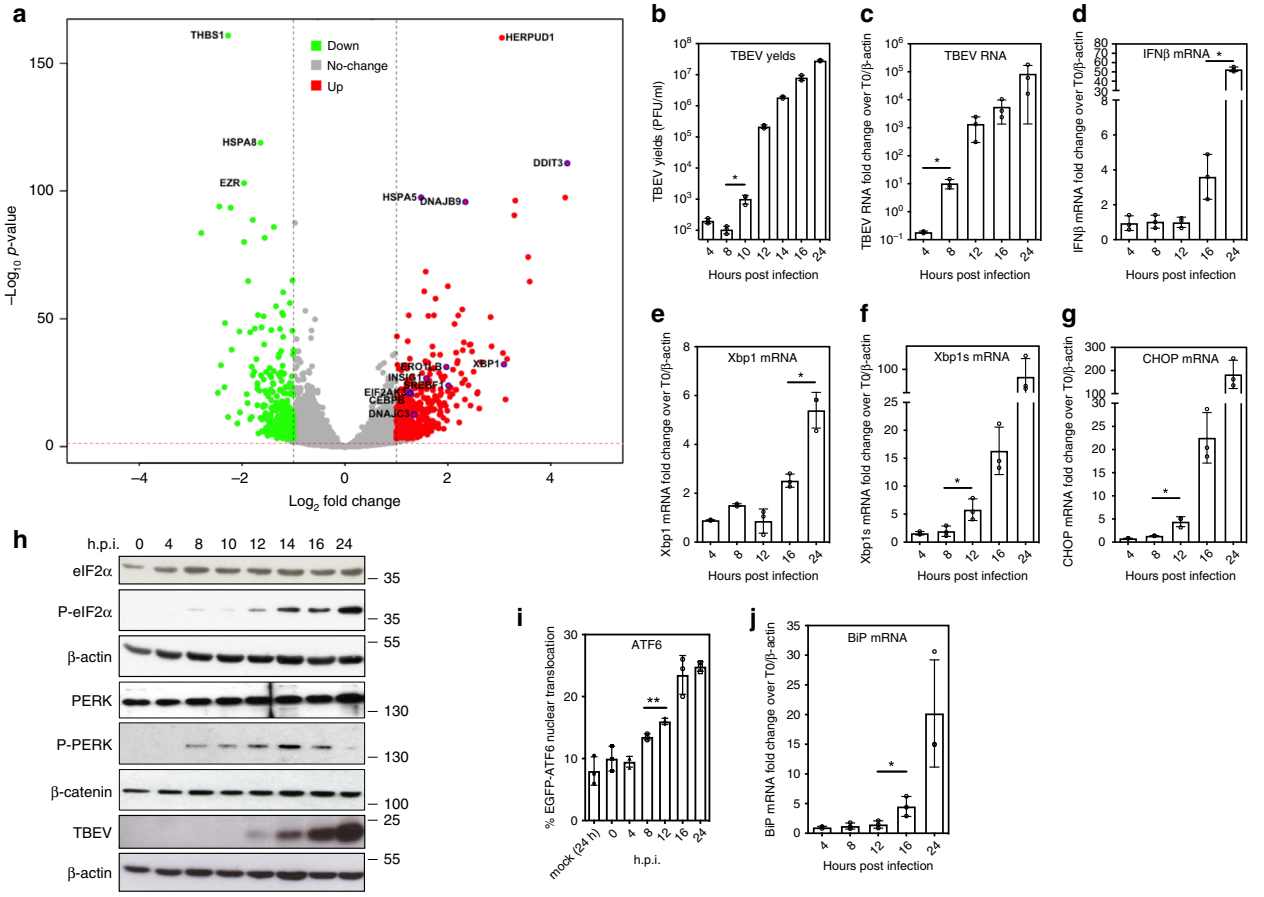

Fig. 1 Temporal analysis of the UPR response to TBEV infection. **a** Difference in total transcript expression following TBEV infection. Total RNA was extracted from TBEV infected cells at 0, 10, and 24 h.p.i. in triplicate independent experiments and processed for high-content sequencing (~24.6 million reads for each time point). The volcano plot shows the differential gene expression at 24/0 versus 10/0 h.p.i. Horizontal and vertical dashed lines indicate cutoff values (FDR value of 0.05 corresponding to 1,30 Score and absolute logarithmic fold-change >2, respectively). Genes having a significant altered expression are emphasized in red (upregulated) and green (downregulated). Upregulated hits from the UPR pathway are encircled in blue. **b** Time course of viral yields. U2OS cells were infected with TBEV at moi = 1. Supernatant from infected cells were used to infect Vero cells to measure virus yields (PFU/ml). **c**–**g**, **k** Time course of viral RNA and UPR-related mRNAs. U2OS cells were infected as in **b**. Total RNA extracted at the indicated time points and used as template for qPCR using primers specific for TBEV (5′-NCR) (**c**). TBEV RNA amplification products were normalized to β-actin RNA and plotted as fold change from time 0. Data and statistics are plotted as in Fig. 1b. The same protocol was used to quantify mRNA of IFNβ (**d**), Xbp1 (**e**), Xbp1s (**f**), CHOP (**g**), and BiP (**j**). **h** Time course of PERK activation. U2OS cells were infected with TBEV at moi = 1. At the indicated time points, the total protein content was extracted and subjected to immunoblotting with the indicated antibodies. **j** Time course of ATF6 translocation. Cells treated as in (**b**) were quantified for ATF6 nuclear translocation. GFP positive cells were manually counted for ATF6 nuclear translocation at each time point. The graph shows the results from two independent experiments, 200 cells for each time point. Typically three biologically independent experiments ($n = 3$) in triplicate repeats were conducted for each condition examined. Average values are shown with standard deviation and p-values, measured with a paired two-tailed t-test. Significant p-values are indicated by asterisks (**$p < 0.01$; *$p < 0.05$). Source data are provided as a Source Data file

viral RNA were markedly reduced following TM treatment. Since TM inhibits N-linked glycosylation and could potentially affect viral infectivity, viral RNA levels were also investigated. To note, at 8 h.p.i., while viral yields were not yet increasing (Fig. 2a), there was a significant inhibition of viral replication in the presence of TM (Fig. 2b), demonstrating that this early antiviral effect is independent of any unspecific activity on the glycosylation of viral proteins. As a control of TM activity, Xbp1s mRNA was also induced at early time points in the presence of TM (Fig. 2c). Interestingly, induction of IFNβ mRNA occurred much earlier following preactivation of the UPR. As shown in Fig. 2d, treatment of U2OS cells with TM alone (gray bars) stimulated a weak tenfold increase of IFNβ mRNA only after 24 h of treatment. However, upon both TBEV infection and TM treatment, IFNβ was clearly induced as early as 8 h.p.i. (white bars).

To rule out any unspecific effect of TM, the same approach was repeated using Thapsigargin (TG), which activates UPR by blocking the ER calcium ATPase. As shown in Supplementary Fig. 1D and E, both TM and TG inhibit TBEV, but, while TM showed a partial effect on E protein glycosylation as expected, TG did not affect the viral protein. TG was first verified for being able to induce Xbp1s in U2OS at the concentration used (Supplementary Fig. 1F). Next, cells were infected with TBEV followed by treatment with TG. As shown in Fig. 2e, f, TG behaves similarly to TM in inducing an early IFNβ response and inhibiting virus yields. As observed with TM, IFNβ mRNA was induced at low levels by TG alone after 24 h of treatment, but synergized with TBEV infection to potentiate the innate response.

A similar analysis was conducted on other members of the flavivirus family such as DENV2 (Fig. 2g, h), WNV (Fig. 2i, j),

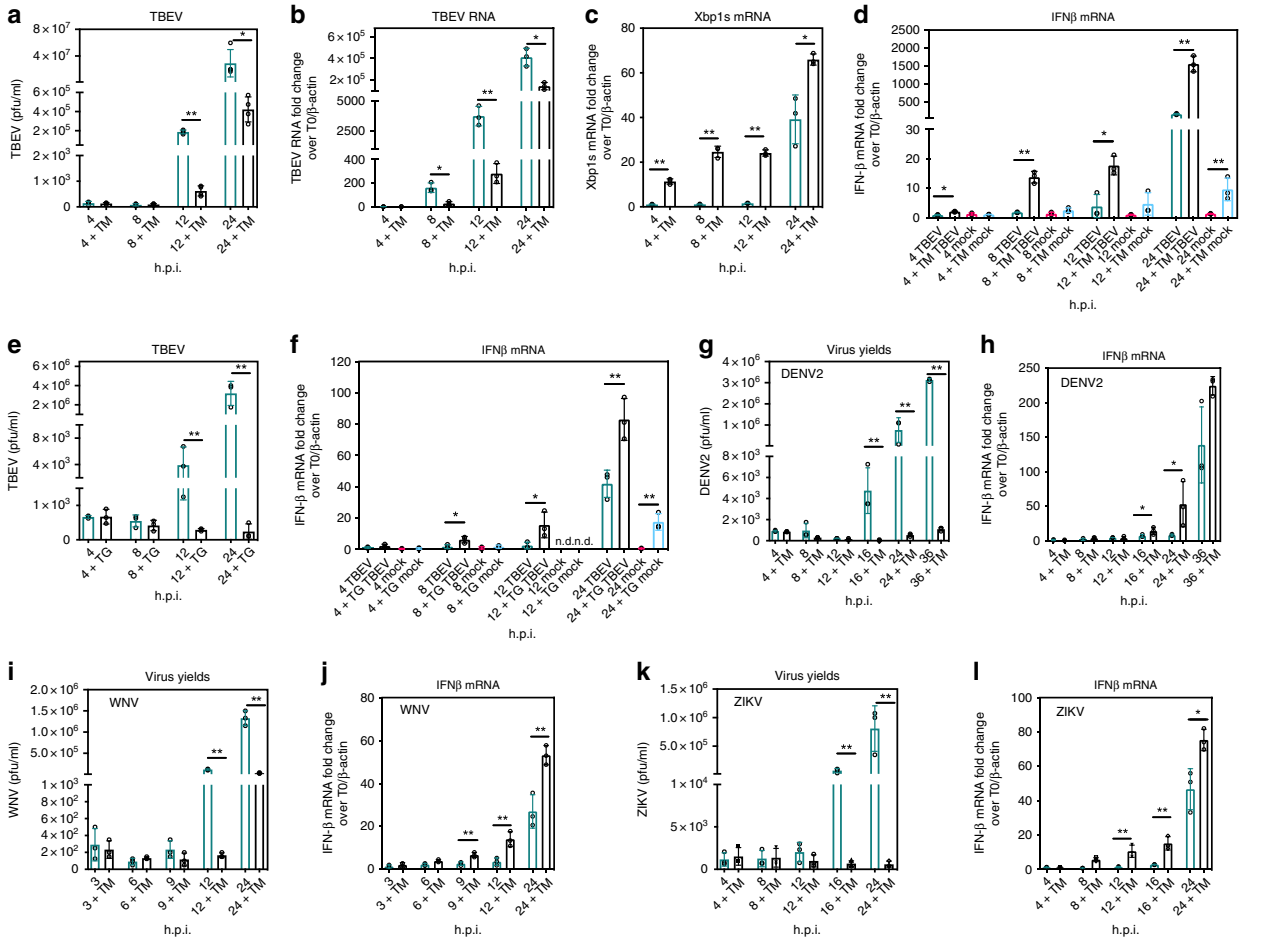

Fig. 2 Modulation of the interferon response to flavivirus infection by the UPR. **a** Tunicamycin treatment inhibited TBEV yields. U2OS cells were either infected with TBEV at moi = 1 (blue bars) or treated with 1 μg/ml Tunicamycin (TM) immediately after infection (black bars). At the indicated time points, supernatants from infected cells were used to infect Vero cells to measure virus yields (PFU/ml). **b**–**d** Tunicamycin treatment inhibited TBEV RNA, increased Xbp1s and led to early IFNβ induction. U2OS cells were infected as in **a**. Total RNA was extracted at the indicated time points and used as template for qPCR using primers specific for TBEV 5′-NCR (**b**), Xbp1s (**c**) or IFNβ (**d**). β-actin was used for normalization and data plotted as fold change from time 0. Values of IFNβ mRNA from mock-infected cells treated with Tunicamycin alone were also indicated (**d**, azure bars). **e**, **f** Thapsigargin treatment inhibited TBEV yields and led to early IFNβ induction. U2OS cells were infected with TBEV at moi = 1 (blue bars) or treated with 0.5 μM Thapsigargin (TG) immediately after infection (black bars) and treated as above (**b**, **d**). **g**–**l** Tunicamycin treatment inhibited DENV2, WNV, and ZIKV yields and led to early IFNβ induction. U2OS cells were either infected (blue bars) or treated with Tunicamycin (TM) immediately after infection (black bars). At the indicated time points, supernatants from infected cells were either used to infect Vero cells to measure virus yields (DENV2 **g,** WNV **i**, ZIKV **k**) or total RNA was extracted and used as template for real-time qPCR to quantify IFNβ mRNA (DENV2, **h**; WNV, **j**; ZIKV, **l**). Statistics as already described in the legend of Fig. 1. Source data are provided as a Source Data file

and ZIKV (Fig. 2k, l). Likewise, induction of the UPR by TM resulted in a decrease of virus yields and an early IFNβ response demonstrating that early activation of the UPR leading to a sustained IFNβ response is a general mechanism within flaviviruses.

The UPR-induced antiviral response is independent of canonical interferon signaling. Since early IFN activation was consistently observed following flavivirus infection in the presence of UPR inducers, it was plausible to hypothesize that the decrease of virus titers could depend on interferon-dependent antiviral signaling. In order to address this, primary embryonic murine fibroblasts, derived from IFN receptor knockout mice (MEF *ifnar-/-*), were infected in the same experimental conditions. Noteworthy, as shown in Fig. 3, wild-type MEF reproduced the same phenotype observed as in U2OS cells, reinforcing the previous observations also in a nontransformed primary murine cell model. MEF *ifnar-/-* showed an antiviral response and an early induction of IFNβ in the presence of TM, which was kinetically similar to that observed in wild-type MEFs (Fig. 3a, b). This observation points to an IFN-signaling independent antiviral activity.

A subset of ISGs, with antiviral activity, that are known to be induced directly by the transcription factor IRF3, have been previously described[17,18]. IRF3 phosphorylation, measured following infection, occurred at earlier time points and to a greater magnitude in TM-treated cells as compared with control (Fig. 3c). Consistently, nuclear translocation of IRF3 was significantly increased at 8 h.p.i. compared with infection alone in the same experimental conditions (Fig. 3d, e). Transcriptional induction of IRF3-dependent ISGs, such as IFIT1 or Viperin, showed early activation kinetics in the presence of TM, comparable with what was observed for IFNβ, (Fig. 3f, g).

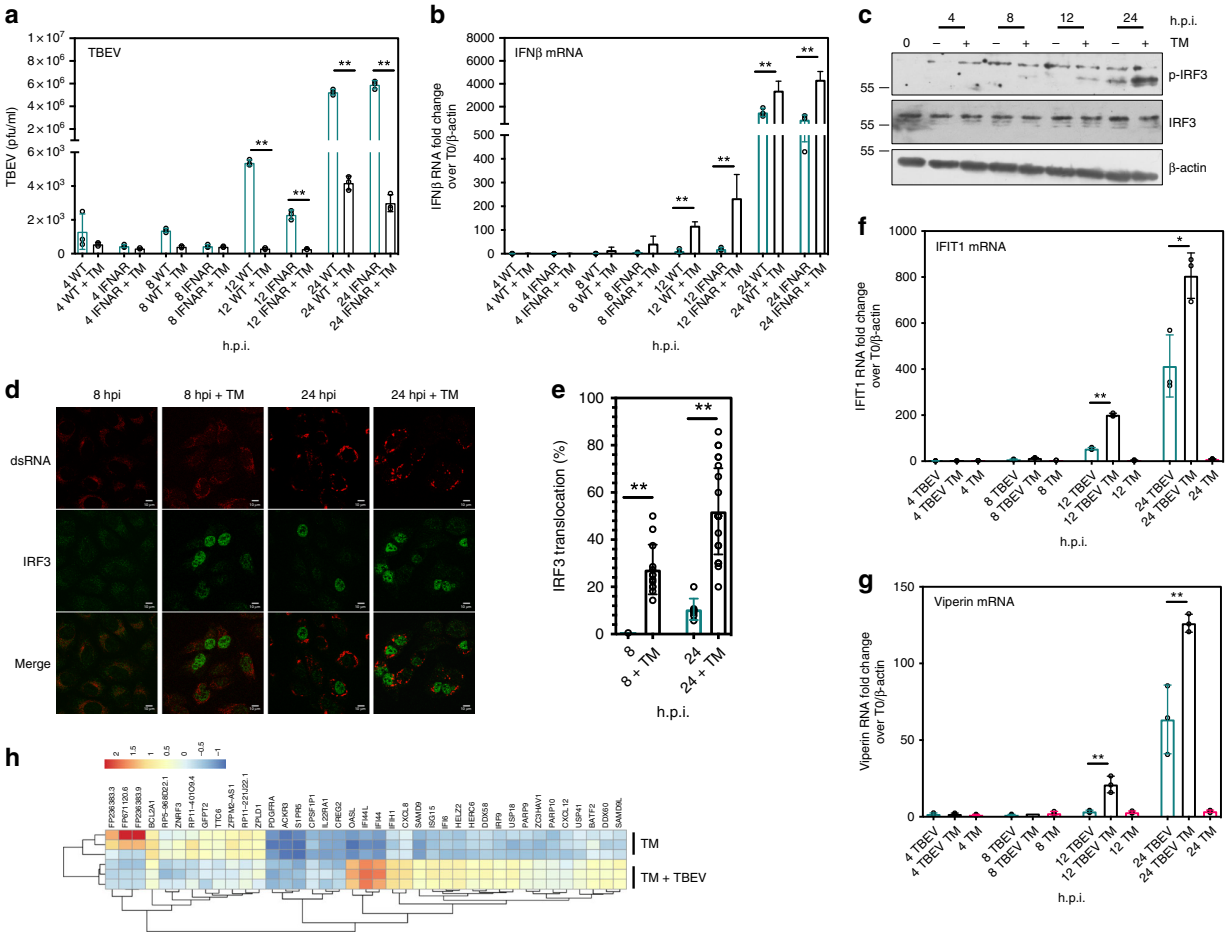

Fig. 3 UPR-induced antiviral signaling following infection is independent of interferon signaling. **a** Tunicamycin treatment inhibited TBEV yields independently of IFNAR. Primary embryonic MEF *Ifnar*$^{-/-}$ cells were either infected with TBEV (blue bars) or treated with TM immediately after infection (black bars). At the indicated time points virus yields were measured (PFU/ml). **b** Tunicamycin treatment of TBEV infected cells led to early IFNβ induction. Total RNA from MEF *Ifnar*$^{-/-}$ infected as above in **a** was extracted at the indicated time points and used as template for real-time qPCR using primers specific for IFNβ. **c** Tunicamycin treatment led to early IRF3 phosphorylation. U2OS cells were infected with TBEV and treated with TM immediately after infection. At the indicated time points the total protein content was extracted and subjected to immunoblotting with the indicated antibodies. **d** Tunicamycin treatment led to early IRF3 nuclear translocation. U2OS cells were infected with TBEV and treated with TM immediately after infection. At the indicated time points, cells were fixed and stained for IRF3 (AlexaFluor 488, green) and dsRNA (AlexaFluor 594, red). Scale bar = 10 μm. **e** Quantification of IRF3 translocation following TBEV infection and Tunicamycin treatment. Cells treated as in **d** were manually quantified for IRF3 nuclear translocation at each time point. The graph shows the results from two independent experiments, ~ 200 cells for each time point. **f**, **g** Tunicamycin treatment of TBEV infected cells led to early ISG induction. Total RNA from U2OS cells infected with TBEV moi = 1 was extracted at the indicated time points and used as template for real-time qPCR using primers specific for IFIT1 or Viperin. Values of ISG mRNA from mock-infected cells treated with Tunicamycin were also indicated (magenta bars). **h** Tunicamycin treatment of TBEV infected cells led an early ISG signature. Transcriptome analysis of cells infected with TBEV compared with infected and treated with TM was performed at 8 h.p.i. in U2OS cells. The cluster of 39 genes differentially regulated in the two conditions is shown in the heatmap (upregulated, red, downregulated, blue, following the indicated gradient). Statistics as already described in the legend to Fig. 1. Source data are provided as a Source Data file

In order to better characterize this phenomenon a transcriptome analysis was conducted on: (i) cells infected with TBEV at 8 h.p.i.; (ii) cells treated with TM for 8 h and (iii) cells both infected and treated with TM at the same time point. IPA indicated the UPR as the most highly enriched canonical pathway (p-value = 7.97^{-12}) induced by sterile TM treatment, while for TBEV infected cells alone at 8 h.p.i. no enriched pathways were indicated, which is in line with the observation that UPR is activated from 10 h.p.i. (Fig. 1). IPA indicated 'activation of IRF by cytosolic PRR" as the most highly enriched canonical pathway (p-value = 3.04^{-05}) for the dataset of cells infected with TBEV and treated with TM. Other top-ranked pathways were 'interferon signaling", 'role of PRRs in recognition of bacteriae and viruses", and 'role of RIG-I like receptors in antiviral innate immunity" strongly supporting the hypothesis. Differential analysis of the two groups, i.e., treated with TM alone and infected +TM, indicated that the 39 genes that were differentially modulated in the two conditions partition in two functional clusters that defined each condition as clearly visible in the heatmap (Fig. 3h). The cluster of genes differentially regulated during infection in conditions of UPR induction showed a high prevalence of ISGs. In particular ISG15, IFI6, IFI44L, IFI44, IFIH1, DDX60, SAMD9, SAMD9L, ZC3HAV1, PARP10, DDX58, and OASL have been already described as antiviral effectors[19–23]. A subset of these ISGs that include OASL, IFIH1, IFI44, and IFI44L have been validated by RT-qPCR

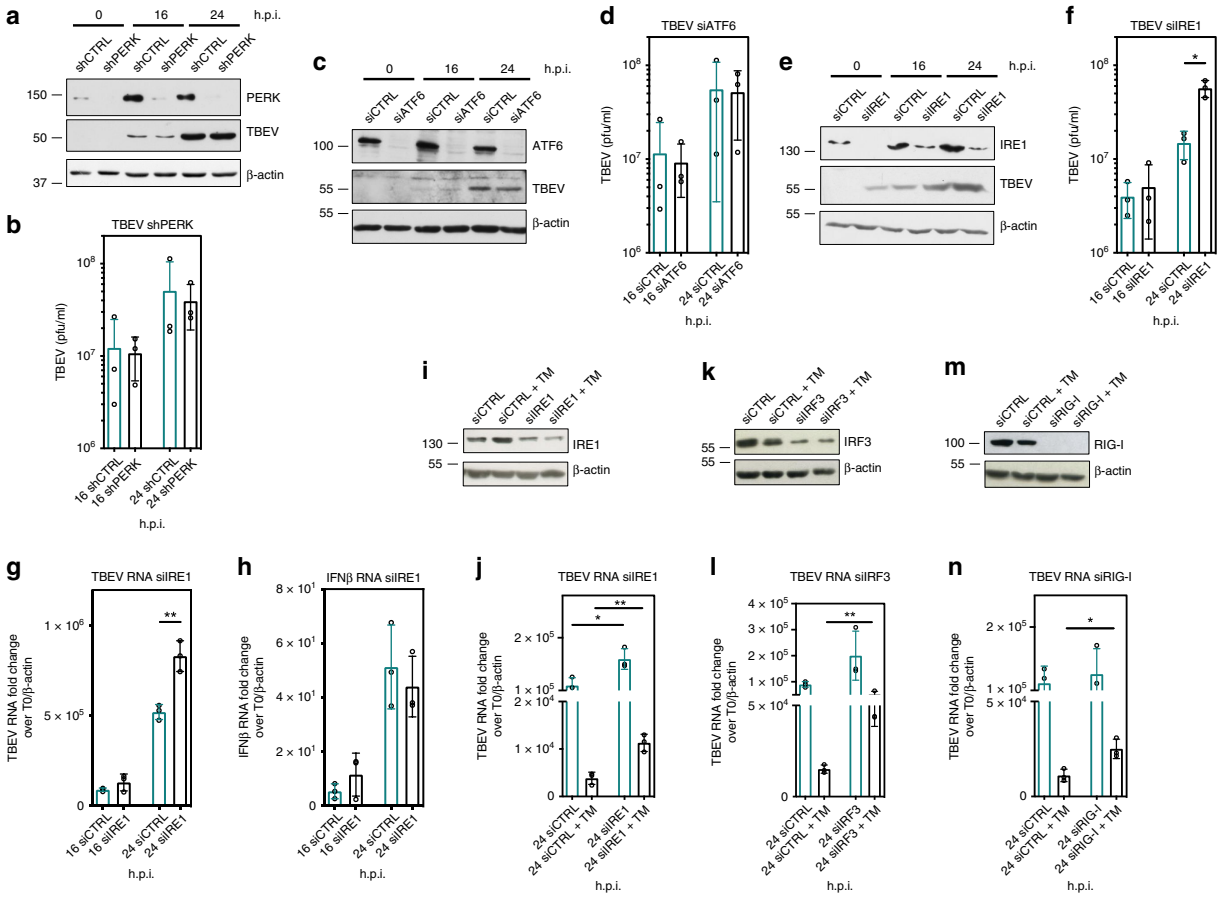

Fig. 4 UPR-induced antiviral signaling following TBEV infection requires the IRE1 pathway. **a**, **b** PERK depletion did not affect TBEV yields. U2OS cells stably transduced with shPERK under puromycin selection were infected with TBEV and harvested for immunoblotting at 16 and 24 h p.i., Actin is the protein loading control (**a**). At the indicated time points, supernatants from infected cells were used to infect Vero cells to measure virus yields (**b**). **c**, **d** ATF6 depletion did not affect TBEV yields. U2OS cells were transfected with siATF6/siCTRL and after 48 h infected with TBEV. Cells were harvested for immunoblotting at 16 and 24 h.p.i. Actin is the protein loading control (**c**). At the indicated time points, supernatants from infected cells were used to infect Vero cells to measure virus yields (**d**). **e**, **f** IRE1 depletion increased TBEV yields. U2OS cells were treated as above (**c**, **d**) with siIRE1. **g**, **h** IRE1 depletion increased TBEV replication but did not affect IFNβ mRNA. U2OS cells were depleted for IRE1 as above (**e**). Total RNA was extracted at the indicated time points and used as template for real-time qPCR using primers specific for TBEV (**g**) or IFNβ (**h**). TBEV RNA amplicons were normalized to β-actin RNA and plotted as fold change from time 0. **i**, **j** IRE1 depletion partially rescued TBEV replication in TM-treated cells. U2OS cells were either infected with TBEV (blue bars) or treated with TM immediately after infection (black bars) in conditions of IRE1 depletion. Immunoblot for IRE1 and TBEV RNA quantification was performed at 24 h.p.i. **k**, **l** IRF3 depletion partially rescued TBEV replication in TM-treated cells. U2OS cells were treated as above (**i**, **j**) in conditions of IRF3 depletion. Immunoblot for IRF3 and TBEV RNA quantification was performed at 24 h.p.i. **m**, **n** RIG-I depletion partially rescued TBEV replication in TM-treated cells. U2OS cells were treated as above (**i**, **j**) in conditions of RIG-I depletion. Immunoblot for RIG-I and TBEV RNA quantification was performed at 24 h.p.i. Statistics as already described in the legend to Fig. 1. Source data are provided as a Source Data file

(Supplementary Fig. 2). Therefore, an ISG antiviral signature characterized the early response triggered by the UPR during TBEV infection.

The UPR-dependent anti-TBEV response is IRE1 and IRF3/RIG-I dependent. The UPR activates three signaling pathways mediated by the ER transmembrane proteins ATF6, IRE1, and PERK. Each of them was targeted by RNAi to investigate their involvement in antiviral signaling following TBEV infection. U2OS cells were treated with siRNA (IRE1 and ATF6) or with shRNA (PERK) to deplete cells of the respective proteins. As shown in Fig. 4a–d, depletion of PERK or ATF6 did not result in significant changes of viral yields. Depletion of PERK was also obtained by siRNA transfection with similar results (Supplementary Fig. 3A and 3B). Conversely, depletion of IRE1 resulted in a higher TBEV titer (Fig. 4e, f) and enhanced TBEV RNA levels (Fig. 4g), but not IFNβ mRNA (Fig. 4h). Therefore, the IRE1 pathway appears principally responsible for UPR-mediated antiviral signaling for TBEV. Indeed, IRE1 depletion partially rescued replication of TBEV following TM treatment (Fig. 4i, j). From previous studies it was discovered that the IFN response against TBEV infection depends on the activity of the PRR RIG-I leading to IRF3 induction[15]. In order to understand if the antiviral activity triggered through IRE1 was dependent on IRF3, U2OS cells were treated with a siRNA against IRF3 and then infected and subjected to TM treatment. As shown in Fig. 4k, l, IRF3 depletion almost completely rescued viral replication in conditions of UPR priming. Hence, the UPR primes infected cells for IRF3-mediated antiviral activity. Depletion of RIG-I also partially rescued TBEV replication indicating that PRR sensing contributes to this pathway together with IRE1 (Fig. 4m, n). One possible mechanism could be related to the RNAse activity of

IRE1, which leads to Xbp1 splicing and IRE1-dependent decay of RNA (RIDD) activity. Xbp1 transcription factor has been shown to directly activate IFN, while the RIDD activity has been proposed to generate substrates for RIG-I signaling[24,25]. However, pretreatment of TBEV infected cells with 4μ8C, a specific inhibitor of IRE1 RNAse activity capable of inhibiting Xbp1 splicing (Supplementary Fig. 3C), didn't show any modulation of virus infectivity (Supplementary Fig. 3D). These data indicate that IRE1-mediated pathways other than Xbp1 splicing and RIDD activity need to be considered to explain the UPR-dependent antiviral signaling induced by TBEV infection.

Other flaviviruses, such as WNV, DENV2, and ZIKV, which have been shown previously to be inhibited by early induction of the UPR with TM (Fig. 2g–l), also respond in terms of rescued viral replication in conditions of IRF3 depletion (Supplementary Fig. 4A–4F). These experiments reinforce the notion that there is a causal link between virus-induced ER stress and innate immune sensing and that this feature is shared among different flaviviruses. However, WNV replication inhibited by TM could not be rescued in IRE1 depleted cells (Supplementary Fig. 4G and 4H). This observation indicates that while TBEV appears to depend principally on the IRE1 pathway, other flaviviruses may require the contribution of ATF6 or PERK.

Discussion

In this work, virus-induced UPR is shown to play a pivotal role in the cell intrinsic innate antiviral response to flaviviruses. UPR and innate sensing have been shown previously to synergize following sterile stimulation[10–13]. However, evidence of this mechanism in infected cells is lacking. The experimental evidence presented here in the context of flavivirus infection points to a direct role of the UPR to trigger a suboptimal activation of the IRF3 pathway, which synergizes with PRR signaling to mount a potent antiviral defense.

This work stems from previous observations that identified a delayed IFN response following flavivirus infection[14,15]. Transcriptome analysis of TBEV infected cells identified the UPR and ER stress pathways as early responses of the cell to infection prior to the IFN response. Similar findings were recently observed for cells of neuronal origin infected with TBEV[26]. Hence, a temporal analysis of UPR activation was performed to better understand the order of cellular events that follow infection.

ATF6 nuclear translocation, following TBEV infection, increased from 8 h.p.i. (Fig. 1i) confirming earlier observations taken at 24 h.p.i.[27]. ATF6-dependent genes, such as *Xbp1* and *BiP*, also increased following infection (Fig. 1e, j). However, ATF6 depletion did not affect viral yields indicating that the ATF6 pathway is dispensable during infection (Fig. 4c, d). These observations are consistent with DENV2 infection, which has been shown to induce ATF6 nuclear translocation but was not affected in ATF6 MEF knockouts[28,29]. Conversely, WNV_{KUN} infection, which also induces activation of the ATF6 branch of the UPR at 12–18 h.p.i., showed decreased titers in $ATF6^{-/-}$ MEFs[30,31]. ATF6 could have a cytoprotective role during milder infections such as WNV_{KUN}, while remains nonessential for more pathogenic viruses such as DENV or TBEV. Indeed, a more lethal strain of WNV has been shown to degrade ATF6 in a proteasome-dependent manner[32].

PERK phosphorylation, following TBEV infection, was visible from 8 h.p.i. and eIF2α phosphorylation increased from 12 h.p.i. (Fig. 1h). PERK depletion did not affect viral yields (Fig. 4a, b). Conversely, WNV_{KUN} infection did not induce strong phosphorylation of eIF2α, but infection of PERK KO cells led to an increase of viral replication[30]. Similarly, PERK was shown to negatively regulate DENV2 infection and induced phosphorylation of eIF2α at 9 h.p.i., but at later time the phosphorylation of this factor was negatively regulated[28]. Another report suggested a proviral role of PERK in DENV2 infection with decreased virus titers in $PERK^{-/-}$ MEFs[33]. These data suggest that TBEV, WNV, and DENV2 are regulating the PERK pathway during infection, but its role is still a matter of debate and may depend upon the cell type used or to the virus with differential kinetic properties.

Xbp1 splicing during TBEV infection was activated as early as 12 h.p.i. (Fig. 1f). Earlier studies already demonstrated Xbp1 splicing following TBEV infection, but only at later time points[27]. Other Flaviviruses, such as WNV_{KUN}, DENV2, and JEV, also activate Xbp1 splicing early during infection[28–30]. The transcription activity of Xbp1s is preserved in TBEV infected cells, as demonstrated by the activation of its target genes *DNAJB9* and *DNAJC3* (Supplementary Fig. 1A and 1B). This is in agreement with what has been observed for JEV and DENV2[29]. Notably, IRE1 depletion resulted in an increase of TBEV titers suggesting a role in antiviral signaling (Fig. 4e, f). These data are in contrast to DENV infection that has been shown to yield significant lower infectious virus in $IRE1^{-/-}$ MEFs[28]. However, besides being different viruses that adapted differently to the host, genetic knockout may activate compensatory pathways that influence the outcome of the assay. Interestingly, several reports indicate that targeting the Xbp1 pathway downstream of IRE1 had no effect on the infection by DENV, JEV, and WNV_{KUN}[28,30,32]. Also for TBEV, the use of 4μ8C, a specific inhibitor of the RNAse activity of IRE1 required for Xbp1 splicing, did not impact infectivity suggesting alternative explanations (Supplementary Fig. 3C and 3D).

Next, the causal link between the UPR and innate responses was explored. UPR induction in the context of TBEV infection led to phosphorylation of IRF3 and its nuclear translocation at early time points (Fig. 3c–e). Transcriptome analysis following viral infection and UPR induction caused an early signature of innate response with the activation of several ISGs with antiviral activity (see heatmap in Fig. 3h and Supplementary Fig. 2). These observations point to a direct role of the UPR, in particular through the IRE1 arm for TBEV, to trigger a suboptimal activation of the IFNβ pathway, which then synergizes with PRR signaling to mount antiviral defenses. Indeed, depletion of IRE1 or IRF3/RIG-I in the context of UPR induction preserved from the antiviral effect (Fig. 4). IRF3 depletion induced a rescue of viral replication also for WNV, DENV2, and ZIKV, indicating a general mechanism of UPR priming of antiviral innate immunity. However, IRE1 dependence could be demonstrate for TBEV, but not for WNV (Supplementary Fig. 4G and 4H). This observation is in line with the differences in UPR response among flaviviruses as mentioned above and will require further analysis.

PRR signaling is believed to depend on the unmasking of specific viral PAMPs during infection, particularly RNA replication intermediates for flaviviruses[15]. Disruption of these compartments that allow PRR access to agonist RNA is therefore required for full activation of the IFN response. It is possible to conceive that the UPR also triggers the modification of membranes or membrane-associated protein complexes that eventually unmask the viral RNAs allowing PRR function. Recent loss-of-function screens identified novel ER-associated factors required for flavivirus replication, which could provide hints on the cellular factors involved in this process[34,35].

To conclude, several lines of evidence point to a direct relationship between the UPR and PRR-mediated activation of cell intrinsic innate antiviral signaling. Independent pathways cooperate to respond to viral infection and to overcome viral subversion strategies in the incessant battle between flaviviruses and the host cell.

Materials and methods

Cells and viruses. TBEV represents a good model of the Flavivirus genus because it is easily manipulated leading to robust infection in vitro. Furthermore, U2OS cells were shown previously to maintain an intact PRR-IFNβ signaling pathway with respect to TBEV infection[15].

Vero clone E6 (ATCC C1008) and human osteosarcoma U2OS cells (ATCC HTB-96) were grown under standard conditions in Dulbecco's modified Eagle medium (DMEM) supplemented with 10% fetal bovine serum. Primary murine embryonic fibroblasts (MEF *Ifnar*-/-) from mice lacking the α-chain of the IFN-α/β receptor on a B6 background were kindly provided by U. Kalinke (TWINCORE Germany). Pregnant female mice at 13–14 days of gestation were sacrificed and uterus were removed with the help of forceps and washed with sterile PBS to remove blood. Embryos were carefully separated from the uterus of pregnant mice at 13–14 days of gestation and their head and liver was removed. Each embryo was minced, treated with trypsin EDTA and plated in growth medium. Low-passage MEFs were used for the experiments. Wild-type MEF were similarly obtained from isogenic B6 animals. Animal care and treatments were conducted in conformity with institutional guidelines in compliance with national and international laws and policies.

Working stocks of TBEV (strain Neudoerfl), West Nile virus (strain NY99), Dengue virus type 2 (strain New Guinea), and Zika virus (strain Uganda #976) were routinely propagated and titrated on Vero E6 cells.

UPR inducers Tunicamycin or Thapsigargin (Sigma-Aldrich) were added to cells 1 h after infection (0 h.p.i.). IRE1 Inhibitor 4μ8C (Tocris) was added to U2OS at 0 h.p.i. at a concentration of 30 μM.

LV Production and shRNA delivery. Lentiviral silencing vectors were derived from pLKO.1 TRC (Addgene). The control short hairpin RNA (shCTRL) was the pLKO.1 scramble from Addgene. For PERK targeting, a specific sequence was designed and cloned into pLKO.1 TRC (shPERK) using the oligonucleotides 5′-CCGGGGAACGACCTGAAGCTATAAACTGCAGTTTATAGCTTCAGGTCGTTCCTTTTTG-3′ and 5′-AATTCAAAAAGGAACGACCTGAAGCTATAAACTGCAGTTTATAGCTTCAGGTCGTTCC-3′.

Packaging in HEK 293T cells was performed according to standard procedures using the packaging plasmid psPAX2 and pMD2.G (Addgene). Cell supernatants were filtered and kept at −80 °C until use. U2OS cells were transduced in presence of polybrene (hexadimethrine bromide, Sigma-Aldrich) following manufacturer's protocol. Transduced cells were selected using 2 μg/ml puromycin.

RNA interference. Pools of small interfering RNAs (siRNAs) were obtained from Dharmacon. ON-TARGET plus Nontargeting Pool was used as a control in all experiments. ON-TARGET plus SMARTpool siRNA was used for the depletion of ATF6 IRE1, PERK, IRF3, and RIG-I. U2OS cells were transfected with siRNAs at a concentration of 100 nM, using Lipofectamine RNAiMAX transfection Reagent (Invitrogen) according to the manufacturer's instructions.

Western-blotting and immunofluorescence. For immunoblotting, whole-cell lysates were resolved by SDS-PAGE and blotted onto nitrocellulose membranes. The membranes were blocked in 4% nonfat milk in Tris-buffered saline (TBS) plus 0.1% Tween 20 (TBST), followed by incubation with the primary antibody diluted in the same solution at 4 °C overnight. After washing three times with TBST, secondary horseradish peroxidase (HRP)-conjugated antibodies were incubated for 1 h at room temperature. The blots were developed using a chemioluminescent HRP substrate (Millipore). For immunofluorescence (IF), cells were washed with PBS, fixed with 4% paraformaldehyde for 15 min, incubated for 5 min with 100 mM glycine, and permeabilized with 0.1% Triton X-100 for 5 min. Subsequently, the cells were incubated at 37 °C for 30 min with PBS, 1% bovine serum albumin, and 0.1% Tween 20 before incubation with antibodies. The coverslips were rinsed three times with PBS, 0.1% Tween 20 (washing solution) and incubated for 1 h with secondary antibodies. The coverslips were finally washed three times with washing solution and mounted on slides using Vectashield mounting medium (Vector Laboratories). Fluorescence images of fixed cells were captured on a Zeiss LSM510 Meta confocal microscope with a 63 × numerical-aperture 1.4 Plan-Apochromat oil objective. Further details can be found in previous publications[36,37]. The following antibodies were used in this study: a rabbit polyclonal against the TBEV E protein produced in our laboratory following immunization with the inactivated virions (1:100 IF, 1:1000 WB); a rabbit polyclonal against TBEV prM kindly provided by Franz Heinz, Vienna (1:100 WB); a rabbit polyclonal against human eIF2α from SCBT (1:100 WB, cat.no. sc-11386); a rabbit polyclonal against phosphorylated (Ser51) human eIF2α from Cell Signaling (1:500 WB, cat.no. 9721); a rabbit polyclonal against human PERK from SCBT (1:500 WB, cat.no. sc-13073); a rabbit monoclonal against human PERK from Cell Signaling (1:1000 WB, cat.no. 3192); a rabbit polyclonal against phosphorylated (T981) human PERK from SCBT (1:200 WB, cat.no. sc-32577); a mouse monoclonal against human PKR from SCBT (1:200 WB, cat.no. sc-6282); a mouse monoclonal against human β-catenin from BD Transduction Lab (1:2000 WB, cat.no. 610153); a mouse monoclonal against human β-actin conjugated with peroxidase from Sigma-Aldrich (1:50000 WB, A3854); a rabbit monoclonal against IRF3 from Cell Signaling (1:1000 WB, cat.no. 4302); a mouse monoclonal against dsRNA from English & Scientific Consulting (1:100 IF, cat.no. J2-1101) a rabbit monoclonal against phospho-IRF3 from Cell Signaling (1:500 WB, cat.no. 4947); a mouse monoclonal against ATF6 from Abcam (1:500 WB, cat.no. ab122897); a rabbit monoclonal against IRE1 from Cell Signaling (1:1000 WB, cat.no. 3294); a mouse monoclonal against RIG-I from Adipogen (WB 1:500, cat. No. AG-20B-0009). Secondary antibodies conjugated with AlexaFluor 488/594 were from Life Technologies (1:500 IF, cat.no. anti-mouse 594 A21207 and anti-rabbit 488 A-21206) and peroxidase conjugates from Dako (1:5000 WB, cat.no. anti-rabbit P0448 and anti-mouse P0447).

Real-time quantitative reverse transcription PCR. For real-time quantitative reverse transcription PCR (qPCR) total cellular RNA was extracted with the UPzol according to the manufacturer's protocol (Biotechrabbit) and treated with DNase I (Invitrogen). 500 ng were then reverse-transcribed with random primers and M-MLV Reverse Transcriptase (Invitrogen). Quantification of mRNA was obtained by real-time PCR using the Kapa Sybr fast qPCR kit on a CFX96 Bio-Rad thermocycler. Primers for amplification are listed in Supplementary Table 1.

Transcriptome analysis by RNAseq. For the first transcriptome analysis (Fig. 1) Human U2OS cells were infected with TBEV at a moi of 1 PFU/cell. Cells were lysed using UPzol (Biotechrabbit) and total RNA was extracted at time 0, 10, and 24 h post-infection (h.p.i.). For the second transcriptome analysis (Fig. 3) U2OS cells were infected with TBEV at a moi of 1 PFU/cell and after 1 h media were replaced with normal growth medium or DMEM plus TM. Cells were lysed with UPzol and total RNA was extracted from each condition at 0 and 8 h.p.i.

Quality of extracted RNA was checked by gel electrophoresis (ribosomal 18S and 28S), spectrophotometric analysis (260/280 > 1.8), and Agilent bioanalyzer (RNA integrity number, RIN ≥ 8). All cDNA libraries of polyA-containing mRNA molecules were prepared using Illumina TruSeq standard protocol. Libraries were pooled and sequenced on two different Illumina Platforms. The first run was performed on Hiseq2000 4-plex run single reads, 50 bp reads, while the second run was performed on HiscanSQ 8-plex run pair-end reads, 2 × 100 bp reads. All data were subjected to quality control using FastQC software. Single reads were mapped against the human genome RNA reference from NCBI using CLCbio software, while pair-end reads were mapped against Homo sapiens GRCh38.77 reference from UCSC using STAR software[38]. Bioconductor pakages DESeq2 version 1.18.1[39] and IHW[40] version 1.6.0 in the framework of R software version 3.4.3 was used to perform differential gene expression analysis of cells infected with TBEV at 24versus 10 h.p.i and cells infected with TBEV and treated with TM at 8 h.p.i versus uninfected cells treated with TM at the same time point. The package is based on the negative binomial distribution (NB) to model the gene reads counts and shrinkage estimator to estimate the per-gene NB dispersion parameters. Specifically, rounded gene counts were used as input and the per-gene NB dispersion parameter was estimated using the function DESeq for DESEQ2. The RNA-seq workflow recommendations[41] were used to detect outlier data after normalization and to improve testing power, while maintaining type I error rates Independent Hypothesis Weighting was used as multiple testing procedure.

Estimated *p*-values for each gene were adjusted using the Benjamini–Hochberg method[42]. Genes with adjusted $P < 0.05$ and absolute logarithmic base twofold change >1 were selected. Data were finally analysed with the IPA software.

Statistics. Typically three independent experiments in triplicate repeats were conducted for each condition examined. Average values are shown with standard deviation and *p*-values, measured with a paired two-tailed *t*-test. Only significant *p*-values are indicated by the asterisks above the graphs ($^{**}p < 0.01$ highly significant; $^{*}p < 0.05$ significant). Where asterisks are missing the differences are calculated as nonsignificant (n.s).

Reporting summary. Further information on research design is available in the Nature Research Reporting Summary linked to this article.

Data availability

Data underlying Figs. 1 B–J, 2 A–L, 3 A–C and E–H, 4 A–N, Supplementary Figs. 1A, B and D–F, 2 A–F, 3 A–H, and 4 A–H are provided as Source Data files. All other data are available from the corresponding author upon reasonable requests. RNAseq data have been deposited with links to BioProject accession number PRJNA474353 in the NCBI BioProject database [https://www.ncbi.nlm.nih.gov/bioproject/]. Sequence Read Archive (SRA) submission: SUB4111543—1st of June 2018, SRA accession: SRP149625.

Received: 15 August 2018 Accepted: 19 July 2019
Published online: 29 August 2019

References

1. Weaver, S. C. et al. Zika virus: history, emergence, biology, and prospects for control. *Antivir. Res.* **130**, 69–80 (2016).

2. Carletti, T., Zakaria, M. K. & Marcello, A. The host cell response to tick-borne encephalitis virus. *Biochem. Biophys. Res. Commun.* **492**, 533–540 (2017).
3. Lindenbach, B. D.,Thiel, H. J., Rice C. M. *Fields Virology* (eds Knipe, D. M., Howley, P. M., Griffin, D. E., Lamb, R. A., Martin, M. A.) 1101–1152 (Lippincott, Williams & Wilkins, Philadelphia, 2007).
4. Welsch, S. et al. Composition and three-dimensional architecture of the dengue virus replication and assembly sites. *Cell Host Microbe* **5**, 365–375 (2009).
5. Gillespie, L. K., Hoenen A., Morgan G., Mackenzie J. M. The Endoplasmic reticulum provides the membrane platform for biogenesis of the flavivirus replication complex. *J. Virol.* **84**, 10438–47 (2010).
6. Miorin, L. et al. Three-dimensional architecture of tick-borne encephalitis virus replication sites and trafficking of the replicated RNA. *J. Virol.* **87**, 6469–6481 (2013).
7. Akira, S., Uematsu, S. & Takeuchi, O. Pathogen recognition and innate immunity. *Cell* **124**, 783–801 (2006).
8. Ron, D. & Walter, P. Signal integration in the endoplasmic reticulum unfolded protein response. *Nat. Rev. Mol. Cell Biol.* **8**, 519–529 (2007).
9. Schroder, M. & Kaufman, R. J. The mammalian unfolded protein response. *Annu. Rev. Biochem.* **74**, 739–789 (2005).
10. Smith, J. A. et al. Endoplasmic reticulum stress and the unfolded protein response are linked to synergistic IFN-beta induction via X-box binding protein 1. *Eur. J. Immunol.* **38**, 1194–1203 (2008).
11. Hu, F. et al. ER stress and its regulator X-box-binding protein-1 enhance polyIC-induced innate immune response in dendritic cells. *Eur. J. Immunol.* **41**, 1086–1097 (2011).
12. Zeng, L. et al. XBP-1 couples endoplasmic reticulum stress to augmented IFN-beta induction via a cis-acting enhancer in macrophages. *J. Immunol.* **185**, 2324–2330 (2010).
13. Smith, J. A. A new paradigm: innate immune sensing of viruses via the unfolded protein response. *Front. Microbiol.* **5**, 222 (2014).
14. Overby, A. K., Popov, V. L., Niedrig, M. & Weber, F. Tick-borne encephalitis virus delays interferon induction and hides its double-stranded RNA in intracellular membrane vesicles. *J. Virol.* **84**, 8470–8483 (2010).
15. Miorin, L., Albornoz, A., Baba, M. M., D'Agaro, P. & Marcello, A. Formation of membrane-defined compartments by tick-borne encephalitis virus contributes to the early delay in interferon signaling. *Virus Res.* **163**, 660–666 (2012).
16. Chen, X., Shen, J. & Prywes, R. The luminal domain of ATF6 senses endoplasmic reticulum (ER) stress and causes translocation of ATF6 from the ER to the Golgi. *J. Biol. Chem.* **277**, 13045–13052 (2002).
17. Grandvaux, N. et al. Transcriptional profiling of interferon regulatory factor 3 target genes: direct involvement in the regulation of interferon-stimulated genes. *J. Virol.* **76**, 5532–5539 (2002).
18. Daffis, S., Samuel, M. A., Keller, B. C., Gale, M. Jr. & Diamond, M. S. Cell-specific IRF-3 responses protect against West Nile virus infection by interferon-dependent and -independent mechanisms. *PLoS Pathog.* **3**, e106 (2007).
19. Schoggins, J. W. & Rice, C. M. Interferon-stimulated genes and their antiviral effector functions. *Curr. Opin. Virol.* **1**, 519–525 (2011).
20. Meng, X. et al. A paralogous pair of mammalian host restriction factors form a critical host barrier against poxvirus infection. *PLoS Pathog.* **14**, e1006884 (2018).
21. Fusco, D. N. et al. HELZ2 Is an IFN effector mediating suppression of dengue virus. *Front. Microbiol.* **8**, 240 (2017).
22. Carlton-Smith, C. & Elliott, R. M. Viperin, MTAP44, and protein kinase R contribute to the interferon-induced inhibition of Bunyamwera Orthobunyavirus replication. *J. Virol.* **86**, 11548–11557 (2012).
23. Atasheva, S., Frolova, E. I. & Frolov, I. Interferon-stimulated poly(ADP-Ribose) polymerases are potent inhibitors of cellular translation and virus replication. *J. Virol.* **88**, 2116–2130 (2014).
24. Cho, J. A. et al. The unfolded protein response element IRE1alpha senses bacterial proteins invading the ER to activate RIG-I and innate immune signaling. *Cell Host Microbe.* **13**, 558–569 (2013).
25. Eckard, S. C. et al. The SKIV2L RNA exosome limits activation of the RIG-I-like receptors. *Nat. Immunol.* **15**, 839–845 (2014).
26. Selinger, M. et al. Analysis of tick-borne encephalitis virus-induced host responses in human cells of neuronal origin and interferon-mediated protection. *J. Gen. Virol.* **98**, 2043–2060 (2017).
27. Yu, C., Achazi, K. & Niedrig, M. Tick-borne encephalitis virus triggers inositol-requiring enzyme 1 (IRE1) and transcription factor 6 (ATF6) pathways of unfolded protein response. *Virus Res.* **178**, 471–477 (2013).
28. Pena, J. & Harris, E. Dengue virus modulates the unfolded protein response in a time-dependent manner. *J. Biol. Chem.* **286**, 14226–14236 (2011).
29. Yu, C. Y., Hsu, Y. W., Liao, C. L. & Lin, Y. L. Flavivirus infection activates the XBP1 pathway of the unfolded protein response to cope with endoplasmic reticulum stress. *J. Virol.* **80**, 11868–11880 (2006).
30. Ambrose, R. L. & Mackenzie, J. M. West Nile virus differentially modulates the unfolded protein response to facilitate replication and immune evasion. *J. Virol.* **85**, 2723–2732 (2011).
31. Ambrose, R. L. & Mackenzie, J. M. ATF6 signaling is required for efficient West Nile virus replication by promoting cell survival and inhibition of innate immune responses. *J. Virol.* **87**, 2206–2214 (2013).
32. Medigeshi, G. R. et al. West Nile virus infection activates the unfolded protein response, leading to CHOP induction and apoptosis. *J. Virol.* **81**, 10849–10860 (2007).
33. Datan, E. et al. Dengue-induced autophagy, virus replication and protection from cell death require ER stress (PERK) pathway activation. *Cell Death Dis.* **7**, e2127 (2016).
34. Marceau, C. D. et al. Genetic dissection of Flaviviridae host factors through genome-scale CRISPR screens. *Nature* **535**, 159–163 (2016).
35. Zhang, R. et al. A CRISPR screen defines a signal peptide processing pathway required by flaviviruses. *Nature* **535**, 164–168 (2016).
36. Albornoz, A., Carletti, T., Corazza, G. & Marcello, A. The stress granule component TIA-1 binds tick-borne encephalitis virus RNA and is recruited to perinuclear sites of viral replication to inhibit viral translation. *J. Virol.* **88**, 6611–6622 (2014).
37. Cevik, R. E. et al. Hepatitis C virus NS5A targets nucleosome assembly protein NAP1L1 to control the innate cellular response. *J. Virol.* **91**, e00880–17. https://doi.org/10.1128/JVI.00880-17 (2017).
38. Dobin, A. & Gingeras, T. R. Mapping RNA-seq reads with STAR. *Curr. Protoc. Bioinform.* **51**, 11–19 (2015). 11 14.
39. Love, M. I., Huber, W. & Anders, S. Moderated estimation of fold change and dispersion for RNA-seq data with DESeq2. *Genome Biol.* **15**, 550 (2014).
40. Ignatiadis, N., Klaus, B., Zaugg, J. B. & Huber, W. Data-driven hypothesis weighting increases detection power in genome-scale multiple testing. *Nat. Methods* **13**, 577–580 (2016).
41. Love, M. I., Anders, S., Kim, V. & Huber, W. RNA-Seq workflow: gene-level exploratory analysis and differential expression. *F1000Res.* **4**, 1070 (2015).
42. Benjamini, Y. & Hochberg, Y. Controlling the false discovery rate: a practical and powerful approach to multiple testing. *J. R. Stat. Soc. Ser. B* **57**, 289–300 (1995).

Acknowledgements

Work on flaviviruses in A.M.'s laboratory is supported by the Beneficientia Stiftung, Vaduz Lichtenstein, and by the FLAVIPOC and SEVARE projects from the Regione FVG of Italy. We thank Tatjana Avšič – Županc for the Zika virus obtained through the European Virus Archive (EVAg).

Author contributions

T.C. and M.K.Z. performed experiments, analyzed the data, generated hypothesis, and contributed to the writing of the paper; V.F. contributed to virology experiments; L.R. contributed to the ATF6 data; Y.K. contributed to qPCR, virology, and protein analysis; D.L. performed the RNAseq and the analysis of data; A.M. conceived the work, analyzed the data, and wrote the paper.

Additional information

Supplementary Information accompanies this paper at https://doi.org/10.1038/s41467-019-11663-2.

Competing interests: The authors declare no competing interests.

Reprints and permission information is available online at http://npg.nature.com/reprintsandpermissions/

Peer review information: *Nature Communications* thanks Mariano Garcia-Blanco and Miguel Martin-Acebes for their contribution to the peer review of this work. Peer reviewer reports are available.

Publisher's note: Springer Nature remains neutral with regard to jurisdictional claims in published maps and institutional affiliations.

Open Access This article is licensed under a Creative Commons Attribution 4.0 International License, which permits use, sharing, adaptation, distribution and reproduction in any medium or format, as long as you give appropriate credit to the original author(s) and the source, provide a link to the Creative Commons license, and indicate if changes were made. The images or other third party material in this article are included in the article's Creative Commons license, unless indicated otherwise in a credit line to the material. If material is not included in the article's Creative Commons license and your intended use is not permitted by statutory regulation or exceeds the permitted use, you will need to obtain permission directly from the copyright holder. To view a copy of this license, visit http://creativecommons.org/licenses/by/4.0/.

© The Author(s) 2019

Appendix 2: Interferon-Stimulated Genes identified in the differential analysis from the Whole genome transcriptome analysis (Fig.13)

	ISG	Description	Characteristics	References
1	ISG15	ISG15 Ubiquitin-Like Modifier	• IFN-induced • Antiviral	Dai *et al*., 2011
2	IL22RA1	Interleukin 22 Receptor Subunit Alpha 1	IFN-induced	
3	IFI6	Interferon Alpha Inducible Protein 6	• IFN-induced • Antiviral	Richardson *et al*., 2018
4	IFI44L	Interferon Induced Protein 44 like	• IFN-induced • Antiviral	• Schoggins *et al*., 2011 • Metz *et al*., 2013
5	IFI44	Interferon Induced Protein 44	• IFN-induced • Antiviral • Alias: MTAP44	• Hallen *et al*., 2007 • Power *et al*., 2015 • Carlton-Smith and Elliot, 2012
6	RP5-968D22.1	ncRNA		
7	CREG2	Cellular Repressor Of E1A Stimulated Genes 2		
8	IFIH1	MDA5	• IFN-induced • Antiviral	Dias *et al*., 2019
9	ACKR3	Atypical Chemokine Receptor 3/ CXCR7	Acts as co-receptor with CXCR4 for a restricted number of HIV isolates	• nexprot.org • Chevingné *et al*., 2014
10	RP11-221J22.1	ncRNA		
11	ZPLD1	Zona Pellucida Like Domain Containing 1		
12	PARP9	Poly (ADP-Ribose) Polymerase Family Member 9	Involved in interferon signaling	
13	PDGFRA	Platelet Derived Growth Factor Receptor Alpha		
14	CXCL8	C-X-C Motif Chemokine Ligand 8, IL8	IFN-induced	
15	HERC6	HECT And RLD Domain Containing E3 Ubiquitin Protein		

		Ligase Family Member 6		
16	DDX60	DExD/H-Box Helicase 60	Antiviral	• Miyashita *et al*., 2011 • Schoggins *et al*., 2011 • Oshiumi *et al*., 2015
17	GFPT2	Glutamine-Fructose-6-Phosphate Transaminase 2		
18	SAMD9	SAM Domain-Containing Protein 9	• IFN-induced • Antiviral	• Liu and McFadden, 2015 • Meng *et al*., 2018
19	SAMD9L	SAM Domain-Containing Protein 9 like	• IFN-induced • Antiviral	Meng *et al*., 2018
20	ZC3HAV1	Zinc Finger CCCH-Type Containing, Antiviral 1	• Antiviral • Aliases: PARP13, ZAP	• Lee *et al*., 2013 • Ohainle *et al*., 2018
21	ZFPM2-AS1	ncRNA		
22	PARP10	Poly (ADP-Ribose) Polymerase Family Member 10	Antiviral	Atasheva *et al*., 2014
23	DDX58	RIG-I	• IFN-induced • Antiviral	Kato *et al*., 2006
24	BATF2	Basic Leucine Zipper ATF-Like Transcription Factor 2		
25	CXCL12	C-X-C Motif Chemokine Ligand 12, SDF1		
26	OASL	2'-5'-Oligoadenylate Synthetase Like	• IFN-induced • Antiviral	• Zhu *et al*., 2014 • Dhar *et al*., 2015
27	IRF9	Interferon Regulatory Factor 9	• Constitutive and IFN-inducible • Mostly acts as part of the ISGF3 complex	• Kimura *et al*., 1996 • Kraus *et al*., 2003 • Huber *et al*.,

				2017
28	TTC6	Tetratricopeptide Repeat Domain 6		
29	BCL2A1	BCL2 Related Protein A1		
30	RP11-401O9.4	ncRNA		
31	HELZ2	Helicase with Zinc Finger 2, Transcriptional Coactivator	• IFN-induced • Antiviral (DENV)	Fusco *et al*., 2017
32	S1PR5	Sphingosine-1-Phosphate Receptor 5		
33	USP18	Ubiquitin Specific Peptidase 18, ISG15-Specific-Processing Protease	• IFN-induced • Antiviral (some DNA viruses)	Zhang *et al*., 2016
34	USP41	Ubiquitin Specific Peptidase 41		
35	ZNRF3	E3 Ubiquitin-Protein Ligase ZNRF3		
36	CPSF1P1	Cleavage and Polyadenylation Specific Factor 1 Pseudogene 1		
37	FP671120.6	ncRNA		
38	FP236383.9	ncRNA		
39	FP236383.3	ncRNA		

6.REFERENCES

Aguirre, S., Maestre, A. M., Pagni, S., Patel, J. R., Savage, T., Gutman, D., and Fernandez-Sesma, A. 2012. DENV Inhibits Type I IFN Production in Infected Cells by Cleaving Human STING. *PLoS Pathogens*, *8*(10). https://doi.org/10.1371/journal.ppat.1002934

Aguirre, S., Luthra, P., Sanchez-Aparicio, M. T., Maestre, A. M., Patel, J., Lamothe, F., …and Fernandez-Sesma, A. 2017. Dengue virus NS2B protein targets cGAS for degradation and prevents mitochondrial DNA sensing during infection. *Nature Microbiology*, *2*(March), 1–11. https://doi.org/10.1038/nmicrobiol.2017.37

Akey D.L., Brown W.C., Dutta S., Konwerski J., Jose J, Jurkiw T.J., DelProposto J, Ogata C.M., Skiniotis, G., and Kuhn, R.J. 2014. Flavivirus NS1 structures reveal surfaces for associations with membranes and the immune system. *Science*, 343:881-885. 24.

Akira, S., Uematsu, S., and Takeuchi, O. 2006. Pathogen recognition and innate immunity. *Cell* 124, 783–801.

Alfano, C., Gladwyn-Ng, I., Couderc, T., Lecuit, M., and Nguyen, L. 2019. The unfolded protein response: A key player in zika virus-associated congenital microcephaly. *Frontiers in Cellular Neuroscience*, *13*(March), 1–9. https://doi.org/10.3389/fncel.2019.00094

Allison, S.L., Schalich, J., Stiasny, K., Mandl, C.W., Kunz, C., and Heinz, F.X. 1995a. Oligomeric rearrangement of tick-borne encephalitis virus envelope proteins induced by an acidic pH. *Journal of Virology*.69:695–700.

Ambrose, R. L., and Mackenzie, J. M. 2013b. Flaviviral regulation of the unfolded protein response: can stress be beneficial? *Future Virol*. 8 1095–1109 10.2217/fvl.13.1

Apte-Sengupta, S., Sirohi, D., and Kuhn, R. J. 2014. *Coupling of Replication and Assembly in Flaviviruses Swapna*. *100*(2), 130–134. https://doi.org/10.1016/j.pestbp.2011.02.012.Investigations

Asha, K., and Sharma-Walia, N. 2018. Virus and tumor microenvironment induced ER stress and unfolded protein response: from complexity to therapeutics. *Oncotarget*, *9*(61), 31920–31936. doi:10.18632/oncotarget.25886

Ashour, J., Laurent-Rolle, M., Shi, P.-Y., and García-Sastre, A. 2009. NS5 of dengue virus mediates STAT2 binding and degradation. *Journal of Virology*, *83*(11), 5408–18. https://doi.org/10.1128/JVI.02188-08

Asnis D.S., Conetta R., Teixeira A.A., Waldman G., and Sampson B.A. 2000. The West Nile Virus Outbreak of 1999 in New York: The Flushing Hospital Experience, *Clinical Infectious Diseases*, Volume 30, Issue 3, Pages 413–418, https://doi.org/10.1086/313737

Atasheva, S., Frolova, E. I., and Frolov, I. 2014. Interferon-stimulated poly (ADP-Ribose) polymerases are potent inhibitors of cellular translation and virus replication. *Journal of virology*, *88*(4), 2116–2130. doi:10.1128/JVI.03443-13

Avirutnan, P., Zhang, L., Punyadee, N., Manuyakorn, A., Puttikhunt, C., Kasinrerk, W., and Diamond, M.S. 2007. Secreted NS1 of dengue virus attaches to the surface of cells via interactions with heparan sulfate and chondroitin sulfate E. *PLoS Pathogens*, *3*(11), e183. https://doi.org/10.1371/journal.ppat.0030183

Barrera, M. J., Aguilera, S., Castro, I., González, S., Carvajal, P., Molina, C., … González, M. J. 2018. Endoplasmic reticulum stress in autoimmune diseases: Can altered protein quality control and/or unfolded protein response contribute to autoimmunity? A critical review on Sjögren's syndrome. *Autoimmunity Reviews*, *17*(8), 796–808. https://doi.org/10.1016/j.autrev.2018.02.009

Barrows, N. J., Campos, R. K., Liao, K.-C., Prasanth, K. R., Soto-Acosta, R., Yeh, S.-C., … Garcia-Blanco, M. A. 2018. Biochemistry and Molecular Biology of Flaviviruses. *Chemical Reviews*, acs.chemrev.7b00719. https://doi.org/10.1021/acs.chemrev.7b00719

Bergmann, T. J., Fregno, I., Fumagalli, F., Rinaldi, A., Bertoni, F., Boersema, P. J., … Molinari, M. 2018. Chemical stresses fail to mimic the unfolded protein response resulting from luminal load with unfolded polypeptides. *Journal of Biological Chemistry*, *293*(15), 5600–5612. https://doi.org/10.1074/jbc.RA117.001484

Best, S. M. 2017. The Many Faces of the Flavivirus NS5 Protein in Antagonism of Type I Interferon Signaling. *Journal of Virology*, *91*(3), e01970-16. https://doi.org/10.1128/JVI.01970-16

Bhatt, C., Gething, P. W., Brady, O. J., Messina, J. P., Farlow, A. W., Moyes, C. L., and Drake, J. M. 2013. The global distribution and burden of dengue. *Nature*, *496*(7446), 504–507. https://doi.org/10.1038/nature12060

Boehme, K. W., Guerrero, M., and Compton, T. 2006. Human Cytomegalovirus Envelope Glycoproteins B and H Are Necessary for TLR2 Activation in Permissive Cells. *The Journal of Immunology*, *177*(10), 7094–7102. https://doi.org/10.4049/jimmunol.177.10.7094

Blázquez, A. B., Escribano-Romero, E., Merino-Ramos, T., Saiz, J. C., and Martín-Acebes, M. A. 2014. Stress responses in flavivirus-infected cells: activation of unfolded protein response and autophagy. *Frontiers in microbiology*, *5*, 266. doi:10.3389/fmicb.2014.00266

Blitvich, B., and Firth, A. 2015. Insect-Specific Flaviviruses: A Systematic Review of Their Discovery, Host Range, Mode of Transmission, Superinfection Exclusion Potential and Genomic Organization. *Viruses*, *7*(4), 1927–1959. https://doi.org/10.3390/v7041927

Bolling, B. G., Weaver, S.C., Tesh, R. B., and Vasilakis, N. 2015. Insect-Specific Virus Discovery: Significance for the Arbovirus Community. *Viruses* 7, no. 9: 4911-4928.

Brunner, J.M., Plattet, P., Doucey, M.A., Rosso, L., Curie, T., Montagner, A., … Desvergne, B. 2012. Morbillivirus Glycoprotein Expression Induces ER Stress, Alters Ca2+ Homeostasis and Results in the Release of Vasostatin. *PLOS ONE*, *7*(3), e32803. Retrieved from https://doi.org/10.1371/journal.pone.0032803

Buchkovich, N. J., Yu, Y., Pierciey, F. J., and Alwine, J. C. 2010. Human Cytomegalovirus Induces the Endoplasmic Reticulum Chaperone BiP through Increased Transcription and Activation of Translation by Using the BiP Internal Ribosome Entry Site. *Journal of Virology*, *84*(21), 11479–11486. https://doi.org/10.1128/jvi.01330-10

Bussey, K.A., Lau, U., Schumann, S., Gallo, A., Osbelt, L., Stempel, M., et al. 2018 The interferon-stimulated gene product oligoadenylate synthetase-like protein enhances replication of Kaposi's sarcoma-associated herpesvirus (KSHV) and interacts with the KSHV ORF20 protein. PLoS Pathog 14(3): e1006937. https://doi.org/10.1371/journal.ppat.1006937

Cai, Y., Arikkath, J., Yang, L., Guo, M. L., Periyasamy, P., and Buch, S. 2016. Interplay of endoplasmic reticulum stress and autophagy in neurodegenerative disorders. *Autophagy*, *12*(2), 225–244. https://doi.org/10.1080/15548627.2015.1121360

Carletti, T., Zakaria, M. K., Faoro, V., Reale, L., Kazungu, Y., Licastro, D., and Marcello, A. 2019. Viral priming of cell intrinsic innate antiviral signaling by the unfolded protein response. *Nature Communications*, *10*(1), 3889. https://doi.org/10.1038/s41467-019-11663-2

Carlton-Smith, C., and Elliott, R. M. 2012. Viperin, MTAP44, and protein kinase R contribute to the interferon-induced inhibition of Bunyamwera Orthobunyavirus replication. *Journal of virology*, *86*(21), 11548–11557. doi:10.1128/JVI.01773-12

Carroll, T. P., Greene, C. M., O'Connor, C. A., Nolan, A. M., O'Neill, S. J., and McElvaney, N. G. 2010. Evidence for unfolded protein response activation in monocytes from individuals with alpha-1 antitrypsin deficiency. *J. Immunol.* 184, 4538–4546. doi: 10.4049/jimmunol.0802864

Chambers, T. J., Monath, T. P., Maramorosch, K., Shatkin, A. J., and Murphy-The, F. A. 2003. *Flaviviruses,Structure, Replication and Evolution*. p. 65

Chan, S.W. 2014. Unfolded protein response in Hepatitis C virus infection. *Frontiers in Microbiology*, *5*, 233. https://doi.org/10.3389/fmicb.2014.00233

Chang, Y.S, Liao, C.L, Tsao, C.H, Chen, M.C, Liu, C.I, et al. 1999. Membrane permeabilization by small hydrophobic nonstructural proteins of Japanese encephalitis virus. *J. Virol*. 73:6257–64

Chen, K., Liu, J., and Cao, X. 2017. Regulation of type I interferon signaling in immunity and inflammation: A comprehensive review. *Journal of Autoimmunity*, *83*, 1–11. https://doi.org/10.1016/j.jaut.2017.03.008

Chen, L., Borozan, I., Sun, J., Guindi, M., Fischer, S., Feld, J., et al. Cell-type specific gene expression signature in liver underlies response to interferon therapy in chronic hepatitis C infection. *Gastroenterology* (2010) 138(3): e1–3. doi: 10.1053/j.gastro.2009.10.046

Chen, S., Wu, Z., Wang, M., and Cheng, A. 2017. Innate Immune Evasion Mediated by Flaviviridae Non-Structural Proteins. *Viruses*, *9*(10), 291. https://doi.org/10.3390/v9100291

Cheng, G., Feng, Z., and He, B. 2005. Herpessimplexvirus1infection activates the endoplasmic reticulum resident kinase PERK and mediates eIF2α dephosphorylation by the γ134.5 protein. *Journal of Virology*. 79, 1379–1388.

Cheng, Y. L., Lin, Y. S., Chen, C. L., Tsai, T. T., Tsai, C. C., Wu, Y. W., … Lin, C. F. 2016. Activation of Nrf2 by the dengue virus causes an increase in CLEC5A, which enhances TNF-α production by mononuclear phagocytes. *Scientific reports*, *6*, 32000. doi:10.1038/srep32000

Chevigné, A., Fievez, V., Szpakowska, M., Fischer, A., Counson, M., Plesséria, J. M., … Deroo, S. 2014. Neutralising properties of peptides derived from CXCR4 extracellular loops towards CXCL12 binding and HIV-1 infection. *Biochimica et Biophysica Acta - Molecular Cell Research*, *1843*(5), 1031–1041. https://doi.org/10.1016/j.bbamcr.2014.01.017

Chipurupalli, S., Kannan, E., Tergaonkar, V., D'Andrea, R., and Robinson, N. 2019. Hypoxia Induced ER Stress Response as an Adaptive Mechanism in Cancer. *International journal of molecular sciences*, *20*(3), 749. doi:10.3390/ijms20030749

Clum, S., Ebner, K. E., and Padmanabhan, R. 1997. Co-translational membrane insertion of the serine proteinase precursor NS2B-NS3(Pro) of dengue virus type 2 is required for efficient in vitro processing and is mediated through the hydrophobic regions of NS2B. J Biol Chem 272, 30715–30723.

Cordero, J. G., Juárez, M. L., González-Y-Merchand, J. A., Barrón, L. C., and Castañeda, B. G. 2014. Caveolin-1 in lipid rafts interacts with dengue virus NS3 during polyprotein processing and replication in HMEC-1 cells. *PLoS ONE*, *9*(3), 1–10. https://doi.org/10.1371/journal.pone.0090704

Cormack, B. P., Valdivia, R. H., and Falkow, S. 1996. FACS-optimized mutants of the green fluorescent protein (GFP). *Gene*, *173*(1), 33–38. https://doi.org/10.1016/0378-1119(95)00685-0

Cox, J.S. and Walter, P. 1996. A novel mechanism for regulating activity of a transcription factor that controls the unfolded protein response. *Cell* 87, 391–404.

Cui, S., Eisenacher, K., Kirchhofer, A., Brzozka, K., Lammens, A., Lammens, K., Fujita, T., Conzelmann, K.K., Krug, A., and Hopfner, K.P. 2008. The C-terminal regulatory domain is the RNA 5'-triphosphate sensor of RIG-I. *Mol. Cell* 29 (2), 169–179.

Cumberworth, S. L., Clark, J. J., Kohl, A., and Donald, C. L. 2017. Inhibition of type I interferon induction and signalling by mosquito-borne flaviviruses. *Cellular Microbiology*, *19*(5), e12737. https://doi.org/10.1111/cmi.12737

Cybulsky, A. V. 2017. Endoplasmic reticulum stress, the unfolded protein response and autophagy in kidney diseases. *Nature Reviews Nephrology*, *13*(11), 681–696. https://doi.org/10.1038/nrneph.2017.129

Daffis, S., Szretter, K.J., Schriewer, J., Li, J., Youn, S., Errett, J. 2010. 2'-O methylation of the viral mRNA cap evades host restriction by IFIT family members. Nature; 2468(7322):452–6.

Dai, J., Pan, W., and Wang, P. 2011. ISG15 facilitates cellular antiviral response to dengue and west nile virus infection in vitro. *Virology journal*, *8*, 468. doi:10.1186/1743-422X-8-468

Dalrymple, N.A., Cimica, V., and Mackow, E.R. 2015. Dengue Virus NS Proteins Inhibit RIG-I/MAVS Signaling by Blocking TBK1/IRF3 Phosphorylation: Dengue Virus Serotype 1 NS4A Is a Unique Interferon-Regulating Virulence Determinant. *MBio.*, 6, e00553-15.

Dash, S., Chava, S., Aydin, Y., Chandra, P. K., Ferraris, P., Chen, W., Balart, L. A., Wu, T., and Garry, R. F. 2016. Hepatitis C virus infection induces autophagy as a prosurvival mechanism to alleviate hepatic ER-stress response. *Viruses*, *8*(5). https://doi.org/10.3390/v8050150

de Weerd N.A., Vivian J.P., Nguyen T.K., Mangan N.E.,Gould J.A., Braniff S.J, Zaker-Tabrizi L.,Fung K.Y., Forster S. C, Beddoe T,et al. 2013. Structural basis of a unique interferon-beta signaling axis mediated via the receptor IFNAR1.*Nat Immunol*.;14:901907

Dhar, J., Cuevas, R. A., Goswami, R., Zhu, J., Sarkar, S. N., and Barik, S. 2015. 2'-5'-Oligoadenylate Synthetase-Like Protein Inhibits Respiratory Syncytial Virus Replication and Is Targeted by the Viral Nonstructural Protein 1. *Journal of virology*, *89*(19), 10115–10119. doi:10.1128/JVI.01076-15

Dias Junior, A. G., Sampaio, N. G., and Rehwinkel, J. 2019. A Balancing Act: MDA5 in Antiviral Immunity and Autoinflammation. *Trends in Microbiology*, *27*(1), 75–85. https://doi.org/10.1016/j.tim.2018.08.007

Druelle, C., Drullion, C., Deslé, J., Martin, N., Saas, L., Cormenier, J., Malaquin, N., Huot, L., Slomianny, C., Bouali, F., Vercamer, C., Hot, D., Pourtier, A., Chevet, E., Abbadie, C., and Pluquet, O. ATF6α regulates morphological changes associated with senescence in human fibroblasts. Oncotarget 2016 Aug 22;7(42):67699-67715

Duan, X., Lu, X., Li, J., and Liu, Y. 2008. Novel binding between pre-membrane protein and vacuolar ATPase is required for efficient dengue virus secretion. *Biochemical and Biophysical Research Communications*, *373*(2), 319–324. https://doi.org/10.1016/j.bbrc.2008.06.041

DuRose, J.B., Tam, A.B., Niwa, M. 2006. Intrinsic capacities of molecular sensors of the unfolded protein response to sense alternate forms of endoplasmic reticulum stress. *Mol Biol Cell*;17(7):3095-107.

Edgil, D., Diamond, M. S., Holden, K. L., Paranjape, S. M., and Harris, E. 2003. Translation efficiency determines differences in cellular infection among dengue virus type 2 strains. *Virology*, *317*(2), 275–290. https://doi.org/10.1016/J.VIROL.2003.08.012

Eyer, L., Valdés, J. J., Gil, V. A., Nencka, R., Hřebabecký, H., Šála, M., Salát, J., Černý, J., Palus, M., De Clercq, E., and Růžek, D. 2015. Nucleoside inhibitors of tick-borne encephalitis virus. Antimicrobial Agents and Chemotherapy, 59(9), 5483–5493. https://doi.org/10.1128/AAC.00807-15

Fauci, A. S., and Morens, D. M. 2016. Zika Virus in the Americas — Yet Another Arbovirus Threat. *New England Journal of Medicine*, *374*(7), 601–604. https://doi.org/10.1056/NEJMp1600297

Fernandez-Garcia, M. D., Mazzon, M., Jacobs, M., and Amara, A. 2009. Pathogenesis of Flavivirus Infections: Using and Abusing the Host Cell. *Cell Host & Microbe*, *5*(4), 318–328. https://doi.org/10.1016/J.CHOM.2009.04.001

Fernandez-Garcia, M. D., Meertens, L., Chazal, M., Hafirassou, M. L., Dejarnac, O., Zamborlini, A., Amara, A. 2016. Vaccine and Wild-Type Strains of Yellow Fever Virus Engage Distinct Entry Mechanisms and Differentially Stimulate Antiviral Immune Responses. *MBio*,*7*(1), e01956-15. https://doi.org/10.1128/mBio.01956-15

Ferris, S. P., Jaber, N. S., Molinari, M., Arvan, P., and Kaufman, R. J. 2013. UDP-glucose: glycoprotein glucosyltransferase (UGGT1) promotes substrate solubility in the endoplasmic reticulum. *Molecular Biology of the Cell*, *24*(17), 2597–2608. http://doi.org/10.1091/mbc. E13-02-0101

Foufelle, F., and Fromenty, B. 2016. Role of endoplasmic reticulum stress in drug-induced toxicity. *Pharmacology research & perspectives*, *4*(1), e00211. doi:10.1002/prp2.211

Frabutt, D.A., and Zheng, Y.H. 2016. Arms race between enveloped viruses and the host ERAD machinery. *Viruses*, *8*(9). https://doi.org/10.3390/v8090255

Frabutt D.A., Wang B., Riaz S., Schwartz R.C., and Zheng Y-H. 2018. Innate sensing of influenza A virus hemagglutinin glycoproteins by the host endoplasmic reticulum (ER) stress pathway triggers a potent antiviral response via ER-associated protein degradation. *J Virol* 92: e01690-17. https://doi.org/10.1128/JVI.01690-17

Fredericksen B.L and Gale Jr M. 2006. West Nile virus evades activation of interferon regulatory factor 3 through RIG-I-dependent and -independent pathways without antagonizing host defense signaling. *J Virol*; 80:2913–23.

Fregonese, L., and Stolk, J. 2008. Hereditary alpha-1-antitrypsin deficiency and its clinical consequences. *Orphanet Journal of Rare Diseases*, *3*, 16. http://doi.org/10.1186/1750-1172-3-16

Fung, T. S., Torres, J., and Liu, D. X. 2015. The emerging roles of viroporins in ER stress response and autophagy induction during virus infection. *Viruses*, *7*(6), 2834–2857. https://doi.org/10.3390/v7062749

Fusco, D. N., Pratt, H., Kandilas, S., Cheon, S. S., Lin, W., Cronkite, D. A., … Chung, R. T. 2017. HELZ2 Is an IFN Effector Mediating Suppression of Dengue Virus. *Frontiers in microbiology*, *8*, 240. doi:10.3389/fmicb.2017.00240

Ghosh, A., Shao, L., Sampath, P., Patel, N., Zhu, J., Hornung, V., … Sarkar, S. N. 2017. 2′-5′ Oligoadenylate like (OASL) inhibits interferon induction by inhibiting cGAS activity during DNA virus infection. *The Journal of Immunology*, *198*(1 Supplement), 129.9 LP-129.9. Retrieved from http://www.jimmunol.org/content/198/1_Supplement/129.9.abstract

Gladwyn-Ng, I., Cordón-Barris, L., Alfano, C., Creppe, C., Couderc, T., Morelli, G., … Nguyen, L. 2018. Stress-induced unfolded protein response contributes to Zika virus-associated microcephaly. *Nature Neuroscience*, *21*(1), 63–73. https://doi.org/10.1038/s41593-017-0038-4

Gopala Reddy, S. B., Chin, W. X., and Shivananju, N. S. 2018. Dengue virus NS2 and NS4: Minor proteins, mammoth roles. *Biochemical Pharmacology*. https://doi.org/10.1016/j.bcp.2018.04.008

Goubau, D., Schlee, M., Deddouche, S., Pruijssers, A. J., Zillinger, T., Goldeck, M., … Reis e Sousa, C. 2014. Antiviral immunity via RIG-I-mediated recognition of RNA bearing 5'-diphosphates. *Nature*, *514*(7522), 372–375. doi:10.1038/nature13590

Green, A.M., Beatty, P.R., Hadjilaou,A., and Harris, E. 2014.Innate immunity To dengue virus infection and subversion of antiviral responses. J*. Mol.Biol*. 426, 1148–1160. doi: 10.1016/j.jmb.2013.11.023

Grootjans, J., Kaser, A., Kaufman, R. J., and Blumberg, R. S. 2016. The unfolded protein response in immunity and inflammation. *Nature Reviews. Immunology*, *16*(8), 469–84. https://doi.org/10.1038/nri.2016.62

Gubler D.J. 1998. Dengue and dengue hemorrhagic fever. *Clin Microbiol Rev*; 11:480–96.

Gubler, D.J. 2002.Epidemic dengue/dengue hemorrhagic fever as a public health, social and economic problem in the 21st century.*Trends Microbiol*;10:100-3.

Halbleib, K., Pesek, K., Covino, R., Hofbauer, H. F., Wunnicke, D., Hänelt, I., Hummer, G., and Ernst, R. 2017. Activation of the Unfolded Protein Response by Lipid Bilayer Stress. *Molecular Cell*, *67*(4), 673-684.e8. https://doi.org/10.1016/j.molcel.2017.06.012

Hallen, L. C., Burki, Y., Ebeling, M., Broger, C., Siegrist, F., Oroszlan-Szovik, K., … Foser, S. 2007. Antiproliferative activity of the human IFN-α inducible protein IFI44. *Journal of Interferon and Cytokine Research*, *27*(8), 675–680. https://doi.org/10.1089/jir.2007.0021

Hammadi, M., Oulidi, A., Gackière, F., Katsogiannou, M., Slomianny, C., Roudbaraki, M., … Van Coppenolle, F. 2013. Modulation of ER stress and apoptosis by endoplasmic reticulum calcium leak *via* translocon during unfolded protein response: involvement of GRP78. *The FASEB Journal*, *27*(4), 1600–1609. https://doi.org/10.1096/fj.12-218875

Haze, K., Yoshida, H., Yanagi, H, Yura, T and Mori, K. 1999. Mammalian transcription factor ATF6 is synthesized as a transmembrane protein and activated by proteolysis in response to endoplasmic reticulum stress. *Mol Biol Cell*; 10(11):3787–3799.

He, B. 2006. Viruses, endoplasmic reticulum stress, and interferon responses. *Cell Death Differ*. 13, 393–403

Helbig, K. J., and Beard, M. R. 2014. The role of viperin in the innate antiviral response. *Journal of Molecular Biology*, *426*(6), 1210–1219. https://doi.org/10.1016/j.jmb.2013.10.019

Heinz, F. X., Mandl, C. W., Holzmann, H., Kunz, C., Harris, B. A., Rey, F., and Harrison, S. C. 1991. The flavivirus envelope protein E: isolation of a soluble form from tick-borne encephalitis virus and its crystallization. *Journal of Virology*, *65*(10), 5579–5583. Retrieved from http://jvi.asm.org/cgi/content/short/65/10/5579

Heinz, F. X., and Allison, S. 2003. Flavivirus Structure and Membrane Fusion. *Advances in virus research*. 59. 63-97. 10.1016/S0065-3527(03)59003-0.

Hendershot, L., Wei, J., Gaut, J., Melnick, J., Aviel, S., and Argon, Y. 1996. Inhibition of immunoglobulin folding and secretion by dominant negative BiP ATPase mutants. Proceedings of the National Academy of Sciences of the United States of America, *93*(11), 5269–5274.

Hetz, C., Bernasconi, P., Fisher, J.,Lee, A. H., Bassik, M.C., Antonsson, B., et al. 2006. Pro apoptotic BAX and BAK modulate the unfolded protein response by a direct interaction with IRE1α. *Science* 312, 572.

Hetz, C., Martinon, F., Rodriguez, D., and Glimcher, L.H. 2011. The unfolded protein response: integrating stress signals through the stress sensor IRE1α. *Physiol.Rev*.91, 1219–1243.

Hetz, C., Chevet, E., and Oakes, S. A. 2015. Proteostasis control by the unfolded protein response. *Nature Cell Biology*, *17*(7), 829–838. https://doi.org/10.1038/ncb3184

Hetz, C., and Papa, F. R. 2018. The Unfolded Protein Response and Cell Fate Control. *Molecular Cell*, *69*(2), 169–181. https://doi.org/10.1016/j.molcel.2017.06.017

Hightower, L. E. 1980. Cultured animal cells exposed to amino acid analogues or puromycin rapidly synthesize several polypeptides. *Journal of Cellular Physiology*, *102*(3), 407–427. https://doi.org/10.1002/jcp.1041020315

Hosoi, T., Nomura, J., Tanaka, K., et al. 2017. Link between endoplasmic reticulum stress and autophagy in neurodegenerative diseases. *Endoplasmic Reticulum Stress in Diseases*, 4(1), pp. 37-45. http://doi:10.1515/ersc-2017-0004

Hou, F., Sun, L., Zheng, H., Skaug, B., Jiang, Q. X., & Chen, Z. J. (2011). MAVS forms functional prion-like aggregates to activate and propagate antiviral innate immune response. *Cell*, *146*(3), 448–461. doi:10.1016/j.cell.2011.06.041

Hrincius, E. R., Liedmann, S., Finkelstein, D., Vogel, P., Gansebom, S., Samarasinghe, A. E., … McCullers, J. A. 2015. Acute Lung Injury Results from Innate Sensing of Viruses by an ER Stress Pathway. *Cell Reports*, *11*(10), 1591–1603. https://doi.org/10.1016/j.celrep.2015.05.012

Hornung, V., Ellegast, J., Kim, S., Brzozka, K., Jung, A., Kato, H., Poeck, H., Akira, S., Conzelmann, K.K., Schlee, M., Endres, S.,and Hartmann, G., 2006. 5'-Triphosphate RNA is the ligand for RIG-I. *Science* 314 (5801), 994–997.

Hosokawa, N., Wada, I., Hasegawa, K., Yorihuzi, T., Tremblay, L. O., Herscovics, A., and Nagata, K. 2001. A novel ER α-mannosidase-like protein accelerates ER-associated degradation. *EMBO Reports*, *2*(5), 415–422. https://doi.org/10.1093/embo-reports/kve084

Hu, F., Yu, X., Wang, H., Zuo, D., Guo, C., Yi, H., Tirosh, B. et al. 2011. ER stress and its regulator X-box binding protein-1 enhance polyIC induced innate immune response in dendritic cells. *Eur. J. Immunol*. 41: 1086–1097

Huber, M., Suprunenko, T., Ashhurst, T., Marbach, F., Raifer, H., Wolff, S., Strecker, T., Viengkhou, B., Jung, S.R., Obermann, H-L., Bauer, S., Xu, H.C., Lang, P.A., Tom, A., Lang, K.S., King, N.J.C., Campbell, I.L., and Hofer, M.J. 2017. IRF9 prevents $CD8^+$ T cell exhaustion in an extrinsic manner during acute lymphocytic choriomeningitis virus infection. J Virol 91: e01219-17. https://doi .org/10.1128/JVI.01219-17.

Ivashkiv, L. B., and Donlin, L. T. 2014. Regulation of type I interferon responses. *Nature Reviews. Immunology*, *14*(1), 36–49. http://doi.org/10.1038/nri3581

Jang, B. Y., Ryoo, H. D., Son, J., Choi, K. C., Shin, D. M., Kang, S. W., and Kang, M. J. 2015. Role of Drosophila EDEMs in the degradation of the alpha-1-antitrypsin Z variant. *International journal of molecular medicine*, *35*(4), 870–876. doi:10.3892/ijmm.2015.2109

Janssens, S., Pulendran, B., and Lambrecht, B. N. 2014. Emerging functions of the unfolded protein response in immunity. *Nature Immunology*, *15*(10), 910–9. https://doi.org/10.1038/ni.2991

Jheng, J. R., Ho, J. Y., and Horng, J. T. 2014. ER stress, autophagy, and RNA viruses. *Frontiers in Microbiology*, *5*(AUG), 1–13. https://doi.org/10.3389/fmicb.2014.00388

Jiang, X., Kanda, T., Haga, Y., Sasaki, R., Nakamura, M., Wu, S., … Yokosuka, O. 2017. Glucose-regulated protein 78 is an antiviral against hepatitis a virus replication. *Experimental and Therapeutic Medicine*, *13*(6), 3305–3308. https://doi.org/10.3892/etm.2017.4407

Jonathan, H., Lin, P., Walter, T.S., and Benedict, Y. 2008. Endoplasmic Reticulum Stress in Disease Pathogenesis. *Annual Review of Pathology: Mechanisms of Disease* 3:1, 399-425

Kabir, M.F., Kim H., and Chae, H. 2018. Endoplasmic Reticulum Stress and Autophagy, Endoplasmic Reticulum. Angel Català (Ed), IntechOpen. DOI: 10.5772/intechopen.81381. https://www.intechopen.com/books/endoplasmic-reticulum/endoplasmic-reticulum-stress-and-autophagy

Kane, M., Zang, T. M., Rihn, S. J., Zhang, F., Kueck, T., Alim, M., … Bieniasz, P. D. 2016. Identification of Interferon-Stimulated Genes with Antiretroviral Activity. *Cell Host and Microbe*, *20*(3), 392–405. https://doi.org/10.1016/j.chom.2016.08.005

Kato, H., Takeuchi, O., Sato, S., Yoneyama, M., Yamamoto, M., Matsui, K., … Akira, S. 2006. Differential roles of MDA5 and RIG-I helicases in the recognition of RNA viruses. *Nature*, *441*(1), 101–105. https://doi.org/10.1038/nature04734

Kato, H., Takeuchi, O., Mikamo-Satoh, E., Hirai, R., Kawai, T., Matsushita, K., Hiiragi, A., Dermody, T.S., Fujita, T., and Akira, S., 2008. Length-dependent recognition of double- stranded ribonucleic acids by retinoic acid-inducible gene-I and melanoma differentiation-associated gene 5. *J. Exp. Med*. 205 (7), 1601–1610.

Kato, H., and Fujita, T. 2015. RIG-I-like receptors and autoimmune diseases. *Current Opinion in Immunology*, *37*, 40–45. https://doi.org/10.1016/J.COI.2015.10.002

Kaufusi, P. H., Kelley, J. F., Yanagihara, R., Nerurkar, V. R. 2014. Induction of Endoplasmic Reticulum-Derived Replication-Competent Membrane Structures by West Nile Virus Non-Structural Protein 4B. *PLoS One*, 9, e84040.

Kaukinen, P., Sillanpaa, M., Nousiainen, L., Melen, K., and Julkunen, I. 2013. Hepatitis C virus NS2 protease inhibits host cell antiviral response by inhibiting IKK epsilon and TBK1 functions. *J. Med. Virol*., 85, 71–82.

Kawai, T., and Akira, S. 2010. The role of pattern-recognition receptors in innate immunity: update on Toll-like receptors. *Nature Immunology*, *11*, 373. Retrieved from http://dx.doi.org/10.1038/ni.1863

Kenney, J. L., Solberg, O. D., Langevin, S. A., and Brault, A. C. 2014. Characterization of a novel insect-specific flavivirus from Brazil: potential for inhibition of infection of arthropod cells with medically important flaviviruses HHS Public Access. *Journal of General Virology*, *95*, 2796–2808. https://doi.org/10.1099/vir.0.068031-0

Khromykh, A.A., Varnavski, A.N., Sedlak, P.L., and Westaway, E.G. 2001. Coupling between replication and packaging of flavivirus RNA: evidence derived from the use of DNA-based full-length cDNA clones of Kunjin virus. *J Virol*, 75:4633-4640.

Kim, I., Xu, W., and Reed, J.C. 2008. Cell death and endoplasmic reticulum stress: disease relevance and therapeutic opportunities. *Nat.Rev.Drug Discov*. 7, 1013–1030.

Kimura, T., Kadokawa, Y., Harada, H., Matsumoto, M., Sato, M., Kashiwazaki, Y., … Taniguchi, T. 1996. Essential and non-redundant roles of p48 (ISGF3γ) and IRF-1 in both type I and type II interferon responses, as revealed by gene targeting studies. *Genes to Cells*, *1*(1), 115–124. https://doi.org/10.1046/j.1365-2443.1996.08008.x

Kraus, T. A., Lau, J. F., Parisien, J. P., and Horvath, C. M. 2003. A hybrid IRF9-STAT2 protein recapitulates interferon-stimulated gene expression and antiviral response. *Journal of Biological Chemistry*, *278*(15), 13033–13038. https://doi.org/10.1074/jbc.M212972200

Kumar, K. G. S., Tang, W., Ravindranath, A. K., Clark, W. A., Croze, E., Fuchs, S. Y., … Zhang, D. 2003. SCF(HOS) ubiquitin ligase mediates the ligand-induced down-regulation of the interferon-alpha receptor. *The EMBO Journal*, *22*(20), 5480–90. https://doi.org/10.1093/emboj/cdg524

Kummerer, B.M., and Rice, C.M. 2002. Mutations in the yellow fever virus nonstructural protein NS2A selectively block production of infectious particles. *J Virol*, 76:4773-4784. 6.

Lajoie, P., Fazio, E. N., and Snapp, E. L. 2014. Approaches to imaging unfolded secretory protein stress in living cells. *Endoplasmic reticulum stress in diseases*, *1*(1), 27–39. doi:10.2478/ersc-2014-0002

Laureti, M., Narayanan, D., Rodriguez-Andres, J., Fazakerley, J. K., and Kedzierski, L. 2018. Flavivirus Receptors: Diversity, Identity, and Cell Entry. *Frontiers in immunology*, *9*, 2180. doi:10.3389/fimmu.2018.02180

Lee, A. S. 2005. The ER chaperone and signaling regulator GRP78/BiP as a monitor of endoplasmic reticulum stress. *Methods*, *35*(4), 373–381. https://doi.org/https://doi.org/10.1016/j.ymeth.2004.10.010

Lee, C.J., Liao, C.L and Lin, Y.L. 2005. Flavivirus activates phosphatidylinositol 3-kinase signaling to block caspase-dependent apoptotic cell death at the early stage of virus infection. *J Virol*. ;79(13):8388–99.

Lee, H., Komano, J., Saitoh, Y., Yamaoka, S., Kozaki, T., Misawa, T., … Akira, S. 2013. Zinc-finger antiviral protein mediates retinoic acid inducible gene I-like receptor-independent antiviral response to murine leukemia virus. *Proceedings of the National Academy of Sciences of the United States of America*, *110*(30), 12379–12384. https://doi.org/10.1073/pnas.1310604110

Lee, K., Tirasophon,W., Shen,X., Michalak,M., Prywes,R., Okada, T.,et al. 2002. IRE1-mediated unconventional mRNA splicing and S2P-mediated ATF6 cleavage merge to regulate XBP1in signaling the unfolded protein response. *Genes Dev*. 16, 452–466.

Lenz, N., Engler, O., Grandgirard, D., Leib, S. L., and Ackermann-Gäumann, R. 2018. Evaluation of antivirals against tick-borne encephalitis virus in organotypic brain slices of rat cerebellum. *PLoS ONE*, *13*(10), 1–13. https://doi.org/10.1371/journal.pone.0205294

León-Juárez, M., Martínez-Castillo, M., Shrivastava, G., García-Cordero, J., Villegas-Sepulveda, N., Mondragón-Castelán, M., … Cedillo-Barrón, L. 2016. Recombinant Dengue virus protein NS2B alters membrane permeability in different membrane models. *Virology Journal*, *13*(1), 1–11. https://doi.org/10.1186/s12985-015-0456-4

Leung, J. Y., Pijlman, G. P., Kondratieva, N., Hyde, J., Mackenzie, J. M., and Khromykh, A. A. 2008. Role of Nonstructural Protein NS2A in Flavivirus Assembly. *Journal of Virology*, *82*(10), 4731–4741. https://doi.org/10.1128/jvi.00002-08

Li, K., Phoo, W. W., and Luo, D. 2014. Functional interplay among the flavivirus NS3 protease, helicase, and cofactors. *Virologica Sinica*, *29*(2), 74–85. https://doi.org/10.1007/s12250-014-3438-6

Li, S., Kong, L., and Yu, X. 2013. The expanding roles of endoplasmic reticulum stress in virus replication and pathogenesis. *Critical Reviews in Microbiology*, *41*(2), 150–164. https://doi.org/10.3109/1040841X.2013.813899

Li, X., Deng, C., Ye, H., Zhang, H., Zhang, Q., Chen, D., and Zhang, P. 2016. Transmembrane Domains of NS2B Contribute to both Viral RNA. *J Virol*, *90*(12), 5735–5749. https://doi.org/10.1128/JVI.00340-16

Liberman, E., Fong, Y.L., Selby, M.J., Choo, Q.L., Cousens, L., Houghton, M .1999.Activation of the grp78 and grp94 Promoters by Hepatitis C Virus E2 Envelope Protein. *Journal of Virology*. 73, 3718–3722.

Lin, R., Genin, P., Mamane, Y., and Hiscott, J. 2000. Selective DNA Binding and Association with the CREB Binding Protein Coactivator Contribute to Differential Activation of Alpha/Beta Interferon Genes by Interferon Regulatory Factors 3 and 7. *Molecular and Cellular Biology*, *20*(17), 6342–6353. https://doi.org/10.1128/mcb.20.17.6342-6353.2000

Lindenbach, B.D., and Rice, C.M. 1999. Genetic interaction of flavivirus nonstructural proteinsNS1 andNS4A as a determinant of replicase function. *J. Virol*. 73:4611–21

Lindenbach, B.D., Thiel, H.J., Rice, C.M. 2007. Flaviviridae: The viruses and their replication. *In Fields Virology*, 5th ed.; Knipe, D.M., Howley, P.M., Eds.; Lippincott Williams and Wilkins: Philadelphia, PA, USA; pp. 1101–1152

Lindqvist, R., Kurhade, C., Gilthorpe, J. D., and Överby, A. K. 2018. Cell-type- and region-specific restriction of neurotropic flavivirus infection by viperin. *Journal of neuroinflammation*, *15*(1), 80. doi:10.1186/s12974-018-1119-3

Liu, H. M., Loo, Y. M., Horner, S. M., Zornetzer, G. A., Katze, M. G., and Gale, M., Jr. 2012. The mitochondrial targeting chaperone 14-3-3ε regulates a RIG-I translocon that mediates membrane association and innate antiviral immunity. *Cell host & microbe*, *11*(5), 528–537. doi:10.1016/j.chom.2012.04.006

Liu, W.J., Chen, H.B., Wang, X.J., Huang, H., and Khromykh, A.A. 2004. Analysis of adaptive mutations in Kunjin virus replicon RNA reveals a novel role for the flavivirus nonstructural protein NS2A in inhibition of β interferon promoter-driven transcription. *J. Virol*., 78, 12225–12235.

Liu, W.J., Wang, X.J., Mokhonov, V.V., Shi, P.Y., Randall, R., Khromykh, A.A. 2005. Inhibition of interferon signaling by the New York 99 strain and Kunjin subtype of West Nile virus involves blockage of STAT1 and STAT2 activation by nonstructural proteins. *J. Virol*. 79, 1934.

Livak, K. J., and Schmittgen, T. D. 2001. Analysis of relative gene expression data using real-time quantitative PCR and the 2-ΔΔCT method. *Methods*, *25*(4), 402–408. https://doi.org/10.1006/meth.2001.1262

Lu, P.D., Harding, H.P., and Ron, D. 2004.Translation reinitiation at alternative open reading frames regulates gene expression in an integrated stress response. J*. Cell Biol*. 167, 27–33.

Luo, S., Mao, C., Lee, B., and Lee, A. S. 2006. GRP78/BiP is required for cell proliferation and protecting the inner cell mass from apoptosis during early mouse embryonic development. *Molecular and cellular biology*, *26*(15), 5688–5697. doi:10.1128/MCB.00779-06

Ma, Y., Yu, J., Chan, H. L. Y., Chen, Y. C., Wang, H., Chen, Y., … He, M. L. 2009. Glucose-regulated protein 78 is an intracellular antiviral factor against hepatitis B virus. *Molecular and Cellular Proteomics*, *8*(11), 2582–2594. https://doi.org/10.1074/mcp.M900180-MCP200

Mackenzie, J. M., Khromykh, A. A., Jones, M. K., and Westaway, E. G. 1998. Subcellular Localization and Some Biochemical Properties of the Flavivirus Kunjin Nonstructural Proteins Ns2a and Ns4a. *Virology*, 245, 203−15.

Mackenzie, J.M., Jones, M.K., and Westaway, E.G. 1999. Markers for trans-Golgi membranes and the intermediate compartment localize to induced membranes with distinct replication functions in flavivirus-infected cells. *J. Virol*.; 73:9555–9567.

Mackenzie, J. 2005. Wrapping Things up about Virus RNA Replication, 967–977. https://doi.org/10.1111/j.1600-0854.2005.00339.x

Mackenzie, J. S., Gubler, D. J., and Petersen, L. R. 2004. Emerging flaviviruses: the spread and resurgence of Japanese encephalitis, West Nile and dengue viruses. *Nature Medicine*, *10*(12s), S98–S109. https://doi.org/10.1038/nm1144

Madden, E., Logue, S. E., Healy, S. J., Manie, S., and Samali, A. 2019. The role of the unfolded protein response in cancer progression: From oncogenesis to chemoresistance. *Biology of the Cell*, *111*(1), 1–17. https://doi.org/10.1111/boc.201800050

Mandl, C. W. 2005. Steps of the tick-borne encephalitis virus replication cycle that affect neuropathogenesis. *Virus Research*, *111*(2 SPEC. ISS.), 161–174. https://doi.org/10.1016/j.virusres.2005.04.007

Mateus, D., Marini, E. S., Progida, C., and Bakke, O. 2018. Rab7a modulates ER stress and ER morphology. *Biochimica et Biophysica Acta - Molecular Cell Research*, *1865*(5), 781–793. https://doi.org/10.1016/j.bbamcr.2018.02.011

Maurel, M., Chevet, E., Tavernier, J., and Gerlo, S. 2014. Getting RIDD of RNA: IRE1 in cell fate regulation. *Trends in Biochemical Sciences*, *39*(5), 245–254. https://doi.org/10.1016/j.tibs.2014.02.008

Mayer, M.P., and Bukau, B. 2005. Hsp70 chaperones: Cellular functions and molecular mechanism. *CMLS, Cell. Mol. Life Sci*.62:670. https://doi.org/10.1007/s00018-004-4464-6

Mazzon, M., Jones, M., Davidson, A., Chain, B., and Jacobs, M. 2009. Dengue Virus NS5 Inhibits Interferon‐α Signaling by Blocking Signal Transducer and Activator of Transcription 2 Phosphorylation. *The Journal of Infectious Diseases*, *200*(8), 1261–1270. https://doi.org/10.1086/605847

McMahon, H.T., and Gallop, J.L. 2005. Membrane curvature and mechanisms of dynamic cell membrane remodelling. *Nature*, 438:590-596. 18.

Meertens, L., Carnec, X., Lecoin, M. P., Ramdasi, R., Guivel-Benhassine, F., Lew, E., … Amara, A. 2012. The TIM and TAM families of phosphatidylserine receptors mediate dengue virus entry. *Cell host & microbe*, *12*(4), 544–557. doi: 10.1016/j.chom.2012.08.009

Meng, X., Zhang, F., Yan, B., Si, C., Honda, H., Nagamachi, A., … Xiang, Y. 2018. A paralogous pair of mammalian host restriction factors form a critical host barrier against poxvirus infection. *PLoS pathogens*, *14*(2), e1006884. doi: 10.1371/journal.ppat.1006884

Merquiol, E., Uzi, D., Mueller, T., Goldenberg, D., Nahmias, Y., Xavier, R. J., Tirosh, B., and Shibolet, O. 2011. HCV causes chronic endoplasmic reticulum stress leading to adaptation and interference with the unfolded protein response. *PLoS ONE*, *6*(9), 1–12. https://doi.org/10.1371/journal.pone.0024660

Metz, P., Reuter, A., Bender, S., and Bartenschlager, R. 2013. Interferon-stimulated genes and their role in controlling hepatitis C virus. *Journal of Hepatology*, *59*(6), 1331–1341. https://doi.org/10.1016/j.jhep.2013.07.033

Miller, S., Sparacio, S., and Bartenschlager, R. 2006. Subcellular localization and membrane topology of the dengue virus type 2 non-structural protein 4B. *J. Biol. Chem*. 281:8854–63

Miller, S., Kastner, S., Krijnse-Locker,J., Buhler, S.,and Bartenschlager, R. 2007. The non-structural protein 4A of dengue virus is an integral membrane protein inducing membrane alterations in a 2K-regulated manner. *J Biol Chem* 282:8873–8882. 10.1074/jbc.M609919200

Miorin, L., Albornoz, A., Baba, M.M., D'Agaro, P., and Marcello, A. 2012. Formation of membrane-defined compartments by tick-borne encephalitis virus contributes to the early delay in interferon signaling. *Virus Res*. 163:660–666

Miorin, L., Romero-Brey, I., Maiuri, P., Hoppe, S., Krijnse-Locker, J., Bartenschlager, R., and Marcello, A. 2013. Three-dimensional architecture of tick-borne encephalitis virus replication sites and trafficking of the replicated RNA. *Journal of Virology*, *87*(11), 6469–81. https://doi.org/10.1128/JVI.03456-12

Miyashita, M., Oshiumi, H., Matsumoto, M., and Seya, T. 2011. DDX60, a DEXD/H box helicase, is a novel antiviral factor promoting RIG-I-like receptor-mediated signaling. *Molecular and cellular biology*, *31*(18), 3802–3819. doi:10.1128/MCB.01368-10

Mogensen, T. H., and Paludan, S. R. 2001. Molecular pathways in virus-induced cytokine production. *Microbiology and molecular biology reviews: MMBR*, *65*(1), 131–150. doi:10.1128/MMBR.65.1.131-150.2001

Morito, D., and Nagata, K. 2012. ER Stress Proteins in Autoimmune and Inflammatory Diseases. *Frontiers in immunology*, *3*, 48. doi:10.3389/fimmu.2012.00048

Munoz‐Jordan, J. L., and Fredericksen, B. L. 2010. How flaviviruses activate and suppress the interferon response. *Virus*, 2, 676–691.

Nain, M., Mukherjee, S., Karmakar, S. P., Paton, A. W., Paton, J. C., Abdin, M. Z., and Vrati, S. 2017. GRP78 Is an Important Host Factor for Japanese Encephalitis Virus Entry and Replication in Mammalian Cells. *Journal of Virology*, *91*(6), e02274-16. https://doi.org/10.1128/JVI.02274-16

Nash, D., Mostashari, F., Fine, A., et al. 2001. The outbreak of West Nile virus infection in the New York City area in 1999. *N. Engl. J. Med*. **344**, 1807–1814

Nazmi, A., Dutta, K., Hazra, B., and Basu, A. 2014. Role of pattern recognition receptors in flavivirus infections. *Virus Research*, *185*, 32–40. https://doi.org/10.1016/j.virusres.2014.03.013

Ng, L. F. P.,and Hiscox, J. A. 2018. Viperin Poisons Viral Replication. *Cell Host and Microbe*, *24*(2), 181–183. https://doi.org/10.1016/j.chom.2018.07.014

Novoa, I., Zeng, H., Harding, H. P., and Ron, D. 2001. Feedback inhibition of the unfolded protein response by GADD34-mediated dephosphorylation of eIF2α. *Journal of Cell Biology*, *153*(5), 1011–1021. https://doi.org/10.1083/jcb.153.5.1011

Offerdahl D.K., Dorward D.W., Hansen, B.T and Bloom, M.E. 2012. A three-dimensional comparison of tick-borne flavivirus infection in mammalian and tick cell lines. *PLoS ONE*, 7: e47912.

Ohainle, M., Helms, L., Vermeire, J., Roesch, F., Humes, D., Basom, R., … Emerman, M. 2018. A virus-packageable CRISPR screen identifies host factors mediating interferon inhibition of HIV. *ELife*, *7*, 1–32. https://doi.org/10.7554/eLife.39823

Ordóñez, A., Snapp, E. L., Tan, L., Miranda, E., Marciniak, S. J., and Lomas, D. A. 2013. Endoplasmic reticulum polymers impair luminal protein mobility and sensitise to cellular stress in α_1-antitrypsin deficiency. Hepatology (Baltimore, Md.*)*, *57*(5), 10.1002/hep.26173. http://doi.org/10.1002/hep.26173

Oshiumi, H., Miyashita, M., Okamoto, M., Morioka, Y., Okabe, M., Matsumoto, M., and Seya, T. 2015. DDX60 Is Involved in RIG-I-Dependent and Independent Antiviral Responses, and Its Function Is Attenuated by Virus-Induced EGFR Activation. *Cell Reports*, *11*(8), 1193–1207. https://doi.org/10.1016/j.celrep.2015.04.047

Oslowski, C. M., and Urano, F. 2011. Measuring ER stress and the unfolded protein response using mammalian tissue culture system. *Methods in Enzymology*, *490*, 71–92. https://doi.org/10.1016/B978-0-12-385114-7.00004-0

Overby, A. K., Popov, V. L., Niedrig, M., and Weber, F. 2010. Tick-Borne Encephalitis Virus Delays Interferon Induction and Hides Its Double-Stranded RNA in Intracellular Membrane Vesicles. *Journal of Virology*, *84*(17), 8470–8483. https://doi.org/10.1128/jvi.00176-10

Paul, D., and Bartenschlager, R. 2015. Flaviviridae Replication Organelles: Oh, what a Tangled Web We Weave. *Annual Review of Virology*, *2*(1), 289–310. https://doi.org/10.1146/annurev-virology-100114-055007

Perera, N., Miller, J. L., and Zitzmann, N. 2017. The role of the unfolded protein response in dengue virus pathogenesis. *Cellular Microbiology*, *19*(5), 1–9. https://doi.org/10.1111/cmi.12734

Perri, E. R., Thomas, C. J., Parakh, S., Spencer, D. M., and Atkin, J. D. 2015. The Unfolded Protein Response and the Role of Protein Disulfide Isomerase in Neurodegeneration. *Frontiers in Cell and Developmental Biology*, *3*, 80. http://doi.org/10.3389/fcell.2015.00080

Petersen, L. R., Jamieson, D. J., Powers, A. M., and Honein, M. A. 2016. Zika Virus. *New England Journal of Medicine*, *374*(16), 1552–1563. https://doi.org/10.1056/NEJMra1602113

Pichlmair, A., Schulz, O., Tan, C.P., Naslund, T.I., Liljestrom, P., Weber, F., Reis e, S. 2006. RIG-I-mediated antiviral responses to single-stranded RNA bearing 5'-phosphates. Science 314, 997–1001

Pichlmair, A., and Reis e Sousa, C. 2007. Innate recognition of viruses. *Immunity*, *27*(3), 370–83. https://doi.org/10.1016/j.immuni.2007.08.012

Power, D., Santoso, N., Dieringer, M., Yu, J., Huang, H., Simpson, S., … Zhu, J. 2015. IFI44 suppresses HIV-1 LTR promoter activity and facilitates its latency. *Virology*, *481*, 142–150. doi: 10.1016/j.virol.2015.02.046

Promlek, T., Ishiwata-Kimata, Y., Shido, M., Sakuramoto, M., Kohno, K., and Kimata, Y. 2011. Membrane aberrancy and unfolded proteins activate the endoplasmic reticulum stress sensor Ire1 in different ways. *Molecular Biology of the Cell*, *22*(18), 3520–3532. https://doi.org/10.1091/mbc.E11-04-0295

Pulkkinen, L., Butcher, S., and Anastasina, M. 2018. Tick-Borne Encephalitis Virus: A Structural View. *Viruses*, *10*(7), 350. https://doi.org/10.3390/v10070350

Randall, G., Chen, L., Panis, M., Fischer, A.K., Lindenbach, B.D., Sun, J., et al. 2006. Silencing of USP18 potentiates the antiviral activity of interferon against hepatitis C virus infection. *Gastroenterology* 131(5):1584–91.doi: 10.1053/j.gastro.2006.08.043

Ravindran, M. S., Bagchi, P., Cunningham, C. N., Tsai, B., Place, P., and Arbor, A. 2016. Opportunistic intruders: how viruses orchestrate ER functions to infect cells. *Nat Rev Microbiol*, *14*(7), 407–420. https://doi.org/10.1038/nrmicro.2016.60.

Reis e Sousa, C. 2017. Sensing infection and tissue damage. *EMBO Molecular Medicine*, *9*(3), 285–288. https://doi.org/10.15252/emmm.201607227

Rehwinkel, J., and Reis e Sousa, C. 2010. RIGorous Detection: Exposing Virus Through RNA Sensing. *Science*, *327*(5963), 284 LP – 286. https://doi.org/10.1126/science.1185068

Richard Lindqvist and Anna K. Överby. DNA and Cell Biology. Sep 2018.ahead of print http://doi.org/10.1089/dna.2018.4328

Richardson, R. B., Ohlson, M. B., Eitson, J. L., Kumar, A., McDougal, M. B., Boys, I. N., … Schoggins, J. W. 2018. A CRISPR screen identifies IFI6 as an ER-resident interferon effector that blocks flavivirus replication. *Nature microbiology*, *3*(11), 1214–1223. https://doi:10.1038/s41564-018-0244-1

Roby, J.A., Funk, A., and Khromykh, A.A. 2012. *from:* Molecular Virology and Control of Flaviviruses (Edited by: Pei-Yong Shi). Caister Academic Press, U.K.

Romero-Brey, I., and Bartenschlager, R. 2014. Membranous replication factories induced by plus-strand RNA viruses. In *Viruses* (Vol. 6, Issue 7). https://doi.org/10.3390/v6072826

Romero-Brey, I., and Bartenschlager, R. 2016. Endoplasmic Reticulum: The Favorite Intracellular Niche for Viral Replication and Assembly. *Viruses*, *8*(6), 160. doi:10.3390/v8060160

Rothan, H. A., and Kumar, M. 2019. Role of Endoplasmic Reticulum-Associated Proteins in Flavivirus Replication and Assembly Complexes. *Pathogens*, *8*(3), 148. https://doi.org/10.3390/pathogens8030148

Saito, T., Hirai, R., Loo, Y. M., Owen, D., Johnson, C. L., Sinha, S. C., … Gale, M., Jr 2007. Regulation of innate antiviral defenses through a shared repressor domain in RIG-I and LGP2. *Proceedings of the National Academy of Sciences of the United States of America*, *104*(2), 582–587. doi:10.1073/pnas.0606699104

Sasset, L., Petris, G., Cesaratto, F., and Burrone, O. R. 2015. The VCP/p97 and YOD1 proteins have different substratedependent activities in endoplasmic reticulum-associated degradation (ERAD). *Journal of Biological Chemistry*, *290*(47), 28175–28188. https://doi.org/10.1074/jbc.M115.656660

Satoh, T., Kato, H., Kumagai, Y., Yoneyama, M., Sato, S., et al. 2010. LGP2 is a positive regulator of RIG-I- and MDA5-mediated antiviral responses. *PNAS* 107:1512–17

Schmitz, M. L., Shaban, M. S., Albert, B. V., Gökçen, A., and Kracht, M. 2018. The crosstalk of Endoplasmic Reticulum (ER) stress pathways with NF-κB: Complex mechanisms relevant for cancer, inflammation and infection. *Biomedicines*, *6*(2), 1–18. https://doi.org/10.3390/biomedicines6020058

Schoggins, J. W., Wilson, S. J., Panis, M., Murphy, M. Y., Jones, C. T., Bieniasz, P., and Rice, C. M. 2011. A diverse range of gene products are effectors of the type I interferon antiviral response. *Nature*, *472*(7344), 481–485. doi:10.1038/nature09907

Schoggins, J. W. 2019. Interferon-Stimulated Genes: What Do They All Do? *Annual Review of Virology*. https://doi.org/10.1146/annurev-virology-092818-015756

Schröder,M.,and Kaufman,R.J. 2005. The mammalian unfolded protein response. *Annu.Rev. Biochem*. 74, 739–789.

Schwenzer, H., Jühling, F., Chu, A., Pallett, L. J., Baumert, T. F., Maini, M., and Fassati, A. 2019. Oxidative Stress Triggers Selective tRNA Retrograde Transport in Human Cells during the Integrated Stress Response. *Cell Reports*. https://doi.org/10.1016/j.celrep.2019.02.077

Senft, D., and Ronai, Z. A. 2015. UPR, autophagy, and mitochondria crosstalk underlies the ER stress response. *Trends in biochemical sciences*, *40*(3), 141–148. https://doi:10.1016/j.tibs.2015.01.002

Siddiquey, M. N. A., Zhang, H., Nguyen, C. C., Domma, A. J., and Kamil, J. P. 2018. The Human Cytomegalovirus Endoplasmic Reticulum-Resident Glycoprotein UL148 Activates the Unfolded Protein Response. *Journal of Virology*, *92*(20), 1–42. https://doi.org/10.1128/jvi.00896-18

Simmonds, P., Becher, B., Bukh, J., Gould, E.A., Meyers, G., Monath, T., Muerhoff, S., Pletnev, A., Rico-Hesse, R., Smith, D.B., Stapleton, J.T., and ICTV Report Consortium. 2017. ICTV Virus Taxonomy Profile: *Flaviviridae*, *Journal of General Virology*, 98:2–3.

Smit, J. M., Moesker, B., Rodenhuis-Zybert, I., and Wilschut, J. 2011. Flavivirus Cell Entry and Membrane Fusion. *Viruses*, *3*, 160–171. https://doi.org/10.3390/v3020160

Smith, J. A. 2014. A new paradigm: Innate immune sensing of viruses via the unfolded protein response. *Frontiers in Microbiology*, *5*(MAY), 1–10. https://doi.org/10.3389/fmicb.2014.0022

Smith, J. A. 2018. Regulation of cytokine production by the unfolded protein response; Implications for infection and autoimmunity. *Frontiers in Immunology*, *9*(MAR), 1–21. https://doi.org/10.3389/fimmu.2018.00422

Smith, J. A., Turner, M. J., Delay, M. L., Klenk, E. I., Sowders, D. P., and Colbert, R. A. 2008. Endoplasmic reticulum stress and the unfolded protein response are linked to synergistic IFN-beta induction via X-box binding protein 1. *Eur. J. Immunol.* 38, 1194–1203. doi: 10.1002/eji.200737882

Smith, D. B., Meyers, G., Bukh, J., Gould, E. A., Monath, T., Muerhoff, A. S., … Becher, P. 2017. Proposed revision to the taxonomy of the genus Pestivirus, family Flaviviridae. *Journal of General Virology*, *98*, 2106–2112. https://doi.org/10.1099/jgv.0.000873

So, J. S. 2018. Roles of endoplasmic reticulum stress in immune responses. *Molecules and Cells*, *41*(8), 705–716. https://doi.org/10.14348/molcells.2018.0241

Sommereyns, C., Paul, S., Staeheli, P., and Michiels, T. 2008. IFN-Lambda (IFN- λ) Is Expressed in a Tissue-Dependent Fashion and Primarily Acts on Epithelial Cells In Vivo. *PLoS Pathogens*, *4*(3), e1000017. https://doi.org/10.1371/journal.ppat.1000017

Spiegel, M., Pichlmair, A., Martinez-Sobrido, L., Cros, J., Garcia-Sastre, A., Haller, O., Weber, F. 2005. Inhibition of beta interferon induction by severe acute respiratory syndrome coronavirus suggests a two-step model for activation of interferon regulatory factor 3. *J. Virol*. 79 (4), 2079–2086.

Stark, G. R and Darnell, J. E Jr. 2012.The JAK-STAT pathway at twenty. Immunity; 36:503–514.

Stern, O., Hung, Y.F., Valdau, O., Yaffe, Y., Harris, E., et al. 2013. An N-terminal amphipathic helix in dengue virus nonstructural protein 4A mediates oligomerization and is essential for replication. *J. Virol*. 87:4080–85

Stock, N. K., Laraway, H., Faye, O., Diallo, M., Niedrig, M., and Sall, A. A. 2013. Biological and phylogenetic characteristics of yellow fever virus lineages from West Africa. *Journal of Virology*, *87*(5), 2895–907. https://doi.org/10.1128/JVI.01116-12

Strode G.K. Yellow fever. New York: McGraw-Hill Book Company, 1951.

Su,H.L., Liao,C.L., and Lin,Y.L. 2002. Japanese encephalitis virus infection initiates endoplasmic reticulum stress and an unfolded protein response. *J. Virol*.76, 4162–4171.

Suthar, M. S., Aguirre, S., and Fernandez-Sesma, A. 2013. Innate immune sensing of flaviviruses. *PLoS Pathogens*, 9, e1003541.

Suzuki, T., Lu, J., Zahed, M., Kita, K., and Suzuki, N. 2007. Reduction of GRP78 expression with siRNA activates unfolded protein response leading to apoptosis in HeLa cells. Arch Biochem Biophys; 468:1– 14.

Szretter, K.J., Daniels, B.P., Cho, H., Gainey, M.D., Yokoyama, W.M., and Gale Jr, M. 2012. 2'-O methylation of the viral mRNA cap by West Nile virus evades IFIT1-dependent and independent mechanisms of host restriction in vivo. *PLoS Pathog*: e1002698.

Takahasi, K., Yoneyama, M., Nishihori, T., Hirai, R., Kumeta, H., Narita, R., Gale Jr., M., Inagaki, F., Fujita, T. 2008. Nonself RNA-sensing mechanism of RIG-I helicase and activation of antiviral immune responses. *Mol. Cell* 29 (4), 428–440.

Takeuchi, O., and Akira, S. 2010. Pattern recognition receptors and inflammation. *Cell*, *140*(6), 805–20. https://doi.org/10.1016/j.cell.2010.01.022

Tan, Z., Zhang, W., Sun, J., Fu, Z., Ke, X., Zheng, C., … Zheng, Z. 2018. ZIKV infection activates the IRE1-XBP1 and ATF6 pathways of unfolded protein response in neural cells. *Journal of Neuroinflammation*, *15*(1), 1–16. https://doi.org/10.1186/s12974-018-1311-5

Tanguy, M., Véron, L., Stempor, P., Ahringer, J., Sarkies, P., and Miska, E. A. 2017. An Alternative STAT Signaling Pathway Acts in Viral Immunity in **Viral Immunity in *Caenorhabditis elegans*** *MBio*, *8*(5), e00924-17. https://doi.org/10.1128/mBio.00924-17

Tardif, K.D., Mori, K., and Siddiqui, A. 2002. Hepatitis C virus subgenomic replicons induce endoplasmic reticulum stress activating an intracellular signaling pathway.J*. Virol*. 76, 7453–7459.

Tardif, K.D., Waris, G., and Siddiqui, A. 2005.Hepatitis C virus, ER stress, and oxidative stress. *Trends in Microbiology*. 13, 159–163.

Tarpey, I., and Greenwood, N. 2001. Canine parvovirus DNA vaccination. US Patent 6187759B1

van Anken E., Romijn E.P., Maggioni C., Mezghrani A., Sitia R., Braakman I., Heck A.J. 2003. Sequential waves of functionally related proteins are expressed when B cells prepare for antibody secretion. Immunity. 18:243–253 10.1016/S1074-7613(03)00024-4

Verfaillie, T., Salazar, M., Velasco, G., & Agostinis, P. (2010). Linking ER Stress to Autophagy: Potential Implications for Cancer Therapy. *International Journal of Cell Biology*, *2010*, 930509. https://doi.org/10.1155/2010/930509

Volmer, R., Van Der Ploeg, K., and Ron, D. 2013. Membrane lipid saturation activates endoplasmic reticulum unfolded protein response transducers through their transmembrane domains. *Proceedings of the National Academy of Sciences of the United States of America*, *110*(12), 4628–4633. https://doi.org/10.1073/pnas.1217611110

Vonderstein, K., Nilsson, E., Hubel, P., Nygård Skalman, L., Upadhyay, A., Pasto, J., … Överby, A. K. 2017. Viperin Targets Flavivirus Virulence by Inducing Assembly of Non-infectious Capsid Particles. *Journal of virology*, *92*(1), e01751-17. doi:10.1128/JVI.01751-17

Wacher, C., Müller, M., Hofer, M. J., Getts, D. R., Zabaras, R., Ousman, S. S., … Campbell, I. L. 2007. Coordinated regulation and widespread cellular expression of interferon-stimulated genes (ISG) ISG-49, ISG-54, and ISG-56 in the central nervous system after infection with distinct viruses. *Journal of virology*, *81*(2), 860–871. doi:10.1128/JVI.01167-06

Walczak, A., Gradzik, K., Kabzinski, J., Przybylowska-Sygut, K., and Majsterek, I. 2019. The role of the ER-induced UPR pathway and the efficacy of its inhibitors and inducers in the inhibition of tumor progression. *Oxidative Medicine and Cellular Longevity*, *2019*. https://doi.org/10.1155/2019/5729710

Walter, P., and Ron, D. 2011. The unfolded protein response: From stress pathway to homeostatic regulation. *Science*, *334*(6059), 1081–1086. https://doi.org/10.1126/science.1209038

Welsch, S., Miller, S., Romero-Brey, I., Merz, A., Bleck, C. K. E., Walther, P., … Bartenschlager, R. 2009. Composition and three-dimensional architecture of the dengue virus replication and assembly sites. *Cell Host & Microbe*, *5*(4), 365–75. https://doi.org/10.1016/j.chom.2009.03.007

Wengler, G., and Gross, H.J. 1978. Studies on virus-specific nucleic acids synthesized in vertebrate and mosquito cells infected with flaviviruses. *Virology*; 89:423–437.

Xie, X., Gayen, S., Kang, C., Yuan, Z., and Shi, P.Y. 2013. Membrane topology and function of dengue virus NS2A protein. *J. Virol*. 87:4609–22

Xie, X., Zou, J., Puttikhunt, C., Yuan, Z., and Shi, P. Y. 2015. Two Distinct Sets of NS2A Molecules Are Responsible for Dengue Virus Rna Synthesis and Virion Assembly. *J. Virol*. 2015, 89, 1298−313

Yamamoto, K., Sato, T., Matsui, T., Sato, M., Okada, T., Yoshida,H., et al. 2007. Transcriptional induction of mammalian ER quality control proteins is mediated by single or combined action of ATF6α and XBP1. *Dev.Cell* 13, 365–376

Yau, W. L., Nguyen-Dinh, V., Larsson, E., Lindqvist, R., Överby, A. K., and Lundmark, R. 2019. Model System for the Formation of Tick-Borne Encephalitis Virus Replication Compartments without Viral RNA Replication. *Journal of virology*, *93*(18), e00292-19. doi:10.1128/JVI.00292-19

Yoneyama, M., Kikuchi, M., Natsukawa, T., Shinobu, N., Imaizumi, T., Miyagishi, M., and Fujita, T. 2004. The RNA helicase RIG-I has an essential function in double-stranded RNA-induced innate antiviral responses. *Nature Immunology*, *5*(7), 730–737. https://doi.org/10.1038/ni1087

Yoshida, H., Haze, K., Yanagi, H., Yura, T., and Mori, K. 1998. Identification of the cis-acting endoplasmic reticulum stress response element responsible for transcriptional induction of mammalian glucose- regulated proteins. Involvement of basic leucine zipper transcription factors. *J Biol Chem*.; 273(50):33741–33749

Yoshida, H., Matsui, T., Yamamoto, A., Okada, T. and Mori, K. 2001. XBP1 mRNA is induced by ATF6 and spliced by IRE1 in response to ER stress to produce a highly active transcription factor. *Cell* 107, 881–891

Youn, S., Li, T., McCune, B.T., Edeling, M.A., Fremont, D.H., et al. 2012. Evidence for a genetic and physical interaction between nonstructural proteins NS1 and NS4B that modulates replication of West Nile virus. *J. Virol*. 86:7360–71

Yu, C.Y., Hsu, Y.W., Liao, C.L., and Lin, Y.L. 2006. Flavivirus Infection Activates the XBP1 Pathway of the Unfolded Protein Response to Cope with Endoplasmic Reticulum Stress. *Journal of Virology*, *80*(23), 11868–11880. https://doi.org/10.1128/jvi.00879-06

Yu, C., Achazi, K., and Niedrig, M. 2013. Tick-borne encephalitis virus triggers inositol-requiring enzyme 1 (IRE1) and transcription factor 6 (ATF6) pathways of unfolded protein response. *Virus Research*, *178*(2), 471–477. https://doi.org/10.1016/j.virusres.2013.10.012

Yu, I.M., Zhang, W., Holdaway, H. A., Li, L., Kostyuchenko, V. A., Chipman, P. R., … Chen, J. 2008. Structure of the Immature Dengue Virus at Low pH Primes Proteolytic Maturation. *Science*, *319*(5871), 1834 LP-1837. Retrieved from http://science.sciencemag.org/content/319/5871/1834.abstract

Zhang, H.L., Ye, H.Q., Liu, S.Q., Deng, C.L., Li, X.D., Shi, P.Y., and Zhang, B. 2017. West Nile virus NS1 antagonizes interferon-beta production by targeting RIG-I and MDA5. *Journal of Virology*, (June), JVI.02396-16. https://doi.org/10.1128/JVI.02396-16

Zhang, L., and Wang, A. 2012. Virus-induced ER stress and the unfolded protein response. *Frontiers in Plant Science*, *3*, 293 http://doi.org/10.3389/fpls.2012.00293

Zhang, L., Zhang, C., and Wang, A. 2016. Divergence and Conservation of the Major UPR Branch IRE1-bZIP Signaling Pathway across Eukaryotes. *Scientific reports*, *6*, 27362. doi:10.1038/srep27362

Zhang, M., Zhang, M. X., Zhang, Q., Zhu, G. F., Yuan, L., Zhang, D. E., … Zhong, B. 2016. USP18 recruits USP20 to promote innate antiviral response through deubiquitinating STING/MITA. *Cell research*, *26*(12), 1302–1319. doi:10.1038/cr.2016.125

Zhang, W., Chipman, P. R., Corver, J., Johnson, P. R., Zhang, Y., Mukhopadhyay, S., … Kuhn, R. J. 2003. Visualization of membrane protein domains by cryo-electron microscopy of dengue virus. *Nature Structural Biology*, *10*, 907. Retrieved from http://dx.doi.org/10.1038/nsb990

Zhao, D., Yang, J., Han, K., Liu, Q., Wang, H., Liu, Y., … Li, Y. 2019. The unfolded protein response induced by Tembusu virus infection. *BMC veterinary research*, *15*(1), 34. doi:10.1186/s12917-019-1781-4

Zheng, N. Q., Zheng, Z. H., Xu, H. X., Huang, M. X., and Peng, X. M. 2017. Glucose-regulated protein 78 demonstrates antiviral effects but is more suitable for hepatocellular carcinoma prevention in hepatitis B. *Virology Journal*, *14*(1), 77. https://doi.org/10.1186/s12985-017-0747-z

Zhu, G., and Lee, A. S. 2015. Role of the Unfolded Protein Response, GRP78 and GRP94 in Organ Homeostasis. Journal of Cellular Physiology, *230*(7), 1413–1420. http://doi.org/10.1002/jcp.24923

Zhu, J., Zhang, Y., Ghosh, A., Cuevas, R. A., Forero, A., Dhar, J., … Sarkar, S. N. 2014. Antiviral activity of human OASL protein is mediated by enhancing signaling of the RIG-I RNA sensor. *Immunity*, *40*(6), 936–948. doi: 10.1016/j.immuni.2014.05.007

Zhu, J., Ghosh, A., and Sarkar, S. N. 2015. OASL-a new player in controlling antiviral innate immunity. *Current opinion in virology*, *12*, 15–19. doi:10.1016/j.coviro.2015.01.010

Zou, J., Xie. X., Wang, Q.Y., Dong, H., Lee, M.Y., et al. 2015. Characterization of dengue virus NS4A and NS4B protein interaction. *J. Virol*. 89:3455–70